The desert ant's celestial compass system

Evaluating the role of the polarization compass of *Cataglyphis fortis*

D I S S E R T A T I O N

zur Erlangung des akademischen Grades

d o c t o r r e r u m n a t u r a l i u m
(Dr. rer. nat.)
im Fach Biologie

eingereicht an der
Lebenswissenschaftlichen Fakultät
Humboldt-Universität zu Berlin

von
M.Sc. Fleur Lebhardt

Präsident der Humboldt-Universität zu Berlin:
Prof. Dr. Jan-Hendrik Olbertz

Dekan der Lebenswissenschaftlichen Fakultät:
Prof. Dr. Richard Lucius

Gutachter/innen:
1. Prof. Dr. Bernhard Ronacher
2. Prof. Dr. Rüdiger Wehner
3. Prof. Dr. Harald Wolf

eingereicht am: 21.07.2015
Tag der mündlichen Prüfung: 05.11.2015

Abstract

Desert ants of the genus *Cataglyphis* navigate predominantly by means of path integration. During foraging, the ant is constantly informed about its current position relative to the nest. The information about the distance and direction of individual path segments is integrated into a home vector, which allows the ant to return to the starting point (the nest) on the shortest way. The distances covered are determined by a stride integrator (pedometer). The heading direction is inferred mainly via celestial cues, i.e., the sky's polarization pattern, the position of the sun, and the spectral and intensity gradient. This thesis studies the orientation ability of *Cataglyphis fortis* and focuses on the role of the polarization compass to determine the heading direction.

In the experiments, the ant's polarization compass was selectively manipulated by providing linearly polarized light with a defined orientation, as opposed to natural light. The idiothetic information about the heading direction towards a feeding site was provided by the geometrical arrangement of the training channels. In the first series of experiments it was shown that if only idiothetic information and information from the polarization compass are available, the ants rely exclusively on the polarization compass to determine their heading direction.

In a second series of experiments, the ants additionally had the sun compass at their disposal. When the ants experienced contradicting information detected via the sun and the polarization compass systems, an intermediate homing direction was calculated, influenced equally strongly by both compass systems. Note that although these two compass cues are closely related in the natural sky, the ant perceives the respective signals via different regions within its eye and thus interprets them via separate compass systems.

The determination of an intermediate homing direction can be explained by the combined neural processing of both signals. This statement is supported by the transfer experiments in a third series of experiments. If the animals were trained to walk with only one of both compass signals (the position of the sun or the polarization pattern), they headed towards the expected direction in the test situation when they had only the other signal at their disposal. Hence, the information provided by the sun compass can also be recalled by the polarization compass and vice versa.

In the fourth series of experiments the input part of the polarization compass was manipulated. Instead of using the polarization filter, particular regions (DRA) of the ant's eye which are specialized to detect polarized light were occluded. By covering the eyes except for specific parts of the DRAs, their role for the polarization compass could be investigated. Being able to use only the frontal or caudal parts of the DRA, the ant became disoriented. The entire DRA of one eye enables the ant to perform more precise paths, although the heading course deviates from the expected direction.

The present thesis suggests that the polarization compass provides the most accurate directional information and dominates the celestial compass system of the desert ant. Moreover, the different experiments show that *Cataglyphis fortis* considers also the inferior compass cues and thus is able to navigate virtually without errors in the featureless desert.

Keywords: insect navigation, path integration, sky compass, polarization compass, Cataglyphis fortis

Zusammenfassung

Wüstenameisen der Gattung *Cataglyphis* orientieren sich vor allem mittels Wegintegration. Auf diese Weise sind sie während der Futtersuche fortlaufend über ihre aktuelle Position relativ zum Nest informiert. Über einen Heimvektor, den sie aus Distanz und Richtung einzelner Teilstücke ihres Weges berechnen, können sie auf dem kürzesten Weg zu ihrem Ausgangspunkt (Nest) zurückkehren. Zur Bestimmung der zurückgelegten Strecken verwenden sie einen Schrittintegrator (Schrittzähler). Die Laufrichtung wird hauptsächlich über Himmelsinformation wahrgenommen, diese setzt sich zusammen aus dem Polarisationsmuster am Himmel, der Position der Sonne, sowie dem Spektral- und Intensitätsgradienten. In dieser Arbeit über die Orientierungsfähigkeit von *Cataglyphis fortis* soll die Rolle des Polarisationskompasses bei der Bestimmung der Laufrichtung untersucht werden.

Für die Versuche wurde das natürliche Licht mit Hilfe eines Polarisationsfilters auf einen linear polarisierten Anteil definierter Ausrichtung reduziert und damit der Polarisationskompass der Ameise gezielt manipuliert. Die idiothetische Richtungswahrnehmung wurde beim Training zu einer Futterstelle durch die Geometrie der Dressurkanäle vorgegeben. In der ersten Versuchsreihe wurde gezeigt, dass die Richtungsbestimmung vom Polarisationskompass dominiert wird, wenn allein die Information des Polarisationskompass und idiothetische Richtungsinformation zur Verfügung stehen.

In einer zweiten Versuchsreihe konnten die Ameisen zusätzlich die Richtungsinformation ihres Sonnenkompasses nutzen. Erfährt die Ameise widersprüchliche Informationen von Sonnen- und Polarisationskompass, berechnet sie eine mittlere Heimlaufrichtung, die von beiden Kompasssystemen in gleichem Maße beeinflusst wird. Beachtenswert ist, dass trotz der physikalischen Abhängigkeit dieser beiden Kompassinformationen am natürlichen Himmel diese von der Ameise als separate Richtungsinformationen über unterschiedliche Bereiche im Auge wahrgenommen werden. Es handelt sich demnach um getrennte Kompasssysteme.

Erstaunlicherweise scheint die Berechnung einer mittleren Heimlaufrichtung durch eine gemeinsame neuronale Verarbeitung der beiden Signale zu erfolgen. Diese These wird gestützt durch die Transferexperimente der dritten Versuchsreihe. Wurden die Testtiere unter Einfluss nur eines der beiden Kompasssignale (Sonnenstand bzw. Polarisationsmuster) trainiert, liefen sie im Test in die erwartete Richtung, wenn ihnen nur das andere Signal zur Verfügung stand. Die Information aus dem Sonnenkompass kann also auch für den Polarisationskompass genutzt werden und umgekehrt.

In der vierten Versuchsreihe wurde die Wahrnehmung des Polarisationsmusters durch direkte Manipulation der entsprechenden Regionen in den Ameisenaugen (DRA) untersucht. Das gezielte Übermalen der Augen bis auf definierte Bereiche der DRAs sollte deren Einfluss auf den Polarisationskompass ermitteln. Stehen der Ameise in beiden Augen (binokular) entweder nur der frontale oder caudale Bereich der DRA zur Verfügung führt dies zu einem deutlichen Orientierungsverlust. Die vollständige DRA eines Auges erlaubt ihr zwar eine zielgerichtete Fortbewegung, der eingeschlagene Kurs weicht jedoch von der Erwartungsrichtung ab.

Die Ergebnisse der vorliegenden Studie zeigen, dass der Polarisationskompass der Ameise (*Cataglyphis fortis*) die präziseste Richtungsinformation liefert und ihren Himmelskompass dominiert. Die durchgeführten Versuchsreihen veranschaulichen zudem, dass *C. fortis* durch das Zusammenspiel mit den untergeordneten Kompasssignalen in der Lage ist, praktisch fehlerfrei in der kargen, landmarkenarmen Wüstenlandschaft zu navigieren.

Schlüsselwörter: Insektennavigation, Wegintegration, Himmelskompass, Polarisationskompass, Cataglyphis fortis

Contents

1. Introduction **1**
- 1.1. Insect navigation . . . 1
- 1.2. Path integration . . . 2
- 1.3. The desert ant's celestial compass system . . . 3
  - 1.3.1. The sun compass system . . . 4
  - 1.3.2. The polarization compass system . . . 4
- 1.4. Scope of the thesis . . . 6

2. Methodological approach and technical details **7**
- 2.1. Summary . . . 7
- 2.2. Animals and location . . . 7
- 2.3. Vector navigation and displacement experiments . . . 7
- 2.4. Channel system . . . 8
- 2.5. Manipulating the celestial compass cues . . . 9
- 2.6. Data evaluation and statistical analysis . . . 10

3. The dominance of the polarization compass over idiothetic cues in path integration of desert ants **13**
- 3.1. Summary . . . 13
- 3.2. Introduction . . . 13
- 3.3. Materials and methods . . . 15
  - 3.3.1. Data analysis and statistics . . . 17
- 3.4. Results . . . 18
  - 3.4.1. Training with a single e-vector orientation . . . 18
  - 3.4.2. Cue conflict experiments . . . 20
  - 3.4.3. Length of home vectors . . . 25
  - 3.4.4. Bayesian interpretation of the cue conflict? . . . 26
  - 3.4.5. Multiple visual bends influence the ant's homing performance . . . 28
- 3.5. Discussion . . . 31
  - 3.5.1. Training with a single e-vector direction . . . 31
  - 3.5.2. Additional evidence for a simplified internal template . . . 32
  - 3.5.3. Cue conflict experiments . . . 33

4. Interactions of the polarization and the sun compass in path integration of desert ants **37**
- 4.1. Summary . . . 37
- 4.2. Introduction . . . 37
- 4.3. Materials and methods . . . 38
  - 4.3.1. Manipulation of compass cues . . . 38
  - 4.3.2. Data evaluation and statistical analysis . . . 40

4.4. Results . . . 40
4.4.1. Interactions of sun and polarization compasses in the first cue conflict paradigm . . . 40
4.4.2. Manipulating the reliability of compass cues in the second cue conflict paradigm . . . 44
4.5. Discussion . . . 46

5. Transfer of directional information between the polarization compass and the sun compass in desert ants 49
5.1. Summary . . . 49
5.2. Introduction . . . 49
5.3. Materials and methods . . . 50
5.3.1. Training and test procedure . . . 50
5.3.2. Paradigm I: Training with sun compass information while excluding the POL compass cue . . . 51
5.3.3. Paradigm II and III: Excluding the sun compass cue while providing POL compass information during training . . . 52
5.3.4. Data evaluation and statistical analysis . . . 52
5.4. Results . . . 53
5.4.1. Recall with the POL compass after sun compass training? . . . 53
5.4.2. Recall with the sun compass after training with the POL compass? . . . 54
5.5. Discussion . . . 56
5.5.1. Salience of different orientation cues . . . 56
5.5.2. The long-wavelength filter induces an additional phototaxis effect . . . 57
5.5.3. Dominance of the POL compass? . . . 58
5.5.4. The main findings suggest a common final stage of compass direction processing . . . 59

6. The significance of different parts of the dorsal rim areas in the desert ant compound eyes 61
6.1. Summary . . . 61
6.2. Introduction . . . 61
6.3. Materials and methods . . . 62
6.3.1. Training and testing procedure . . . 62
6.3.2. Analysis of the compound eyes . . . 64
6.3.3. Analysis of the trajectories . . . 64
6.3.4. Data evaluation and statistics . . . 64
6.4. Results . . . 65
6.4.1. Paradigm I: The impact of the asymmetric shape of the DRA . . . 65
6.4.2. Paradigm II: Desert ant's orientation ability with a single DRA . . . 69
6.4.3. Comparing homing performances of ants with partially covered DRAs and one-sided DRAs . . . 72
6.5. Discussion . . . 75
6.5.1. Desert ants' orientation abilities with a reduced number of free DRA-ommatidia . . . 75
6.5.2. A potential impact of spectral cues (detected via free nonDRA-ommatidia) 77

7. Conclusion **81**
7.1. Manipulation of polarization compass information using a polarizing filter . . 81
7.2. Polarization compass information dominates over idiothetic information . . . 82
7.3. Polarization compass and sun compass information is processed jointly . . . 82
7.4. Number and combination of e-vector analyzers determine the functionality of the polarization compass 83
7.5. Closing remarks 84

A. Appendix **85**
A.1. Trajectories observed in the experiments presented in Chapter 5 85
A.2. Defining the role of nonDRA-ommatidia via multiple regression analyses (Chapter 6) 86

1. Introduction

1.1. Insect navigation

Navigation is an essential skill for moving animals. Their survival depends on how efficiently they are able to locate resources and return home safely. The journeys can be classified according to motivation (e.g., finding food, shelter, mating partners) and differ in strategies likely depending on the range (from very small distances up to over 1000 km). Insects have proven to be outstanding navigators despite their tiny brains, as compared to vertebrates. Monarch butterflies, for example, migrate seasonally over comparable large distances as vertebrates (e.g., birds or sea turtles) from North-America to Mexico to find overwintering grounds (Brower, 1996).

However, even over short distances animals have to be able to navigate accurately. The exposure to the environment, for example while searching for food, is critical especially for small insects. A well-developed navigation system may limit the time spent outside a safe refuge. Sophisticated navigational skills evolved to complement the animal's sensory capacities and the environmental demands. In order to unravel the underlying principles, a lot of behavioral and neurobiological studies have been performed in bees and desert ants. These social insects are particularly suited to study navigation as they exhibit a quite complex, but straightforward and robust orientation behavior. The foragers of such eusocial taxa are specialized in navigation in order to find food. Their behavior is quite predictable: as central-place foragers, they are highly motivated to return to their nest after a successful foraging trip.

Desert ants, *Cataglyphis*, are outstanding navigators inhabiting a harsh and unfriendly environment. At high temperatures that can reach up to 50° Celsius, these diurnal scavengers search the desert floor for food, mostly other insects that have died of the heat. The ants' high physiological thermotolerance (Gehring and Wehner, 1995) and their extremely long legs that allow for high running speeds (0.6-0.7 m/s, Wehner (1983); Wahl et al. (2015)) which produce a cooling airflow enable the ant to be still active at extreme temperatures (Sommer and Wehner, 2012). However, the ants' survival depends on minimizing the time outside the safe nest, as they could fall prey to their predators or die of desiccation. Thus, over evolutionary time, a highly sophisticated effective navigation system evolved to optimize foraging trips. Although representatives of desert ants inhabit different environments, predominantly distinguished by the rate of vegetation, they apply basically similar strategies for navigation. They combine innate navigation mechanisms with learned cues that they have experienced in the environment during earlier foraging trips. From the first moment an ant leaves its nest to forage for food, it stays safely connected to it via its path integration system (Müller and Wehner, 1988; Wehner and Srinivasan, 2003).

Thus, during their tortuous searching paths, they are continuously informed about the actual position relative to the nest. A so-called home vector provides the necessary information of the direction and distance and allows the animal to directly return to its home.

However, depending on the habitat or the current environment a considerable amount of additional cues are usually available under natural conditions. These include visual cues, e.g. panorama and landmarks, which are used to complement path integration. Snapshots of the panorama made during the foraging trip are stored and later compared with the current view of the environment. Such visual input allows pinpointing a specific goal (Wehner and Räber, 1979; Wehner and Müller, 1985) or following a familiar route (Collett et al., 1992; Collett, 2010). However, not only visual cues can provide "landmark-like" information. Desert ants are also able to associate odors (Steck et al., 2009), tactile (ground structure: Seidl and Wehner (2006)), magnetic or vibration cues (Buehlmann et al., 2012) with the location of the nest. This multimodal approach to process all kinds of sensory input makes the desert ant navigation system especially efficient.

1.2. Path integration

Fig. 1.1.: A A salt-pan in Tunisia (Northern Africa), the natural habitat of *Cataglyphis fortis*. The characteristic scenery depicts the demands the desert ant is challenging during their foraging excursions. **B** The supreme navigator: the desert ant *Cataglyphis fortis*. **C** Path integration is the desert ants fundamental navigation mechanism. After a tortuous foraging trip (continuous line), the ant returns on a straight homewards path (dashed line); adapted from Wehner and Wehner (1990)

Path integration provides the only available navigation strategy in especially flat and featureless habitats as the salt pans of North Africa where *Cataglyphis fortis* forages (Fig. 1.1). The circuitous outbound path is integrated into a 'home vector' which reflects the actual position of the animal relative to the nest, even after several 100 m of foraging over unfamiliar terrain (Wehner and Wehner, 1990; Collett and Collett, 2000; Wehner and Srinivasan, 2003). Furthermore, an ant that has returned from a rewarding feeding site can use the reverse vector information to relocate this very same site. The home vector represents the distance and direction of the nest position and is independent of the actual environment. Thus, after a displacement to a new area, the ant would still run into the correct direction and for the correct distance as indicated by its home vector. From the moment when the ant starts its journey, it continuously monitors and records the angular and linear components of its outbound path and integrates this information into the vector (Müller and Wehner, 1988; Wehner and Srinivasan, 2003; Wehner, 2003). This integration of every path segment is not calculated as the correct arithmetical mean of all angles steered (weighted by the distance traveled in that direction) but rather via an approximate update by adding the information of the next step (its direction and distance) to the already existing home vector

of the previous location. Such an approximation leads to systematic errors under experimental situations, when the ant has to perform a one-sided turn (Müller and Wehner, 1988). However, under natural conditions the ant is able to compensate for this inaccuracy by an appropriate locomotor program, where the probable left and right turns are equal and thus systematic errors largely cancel out (Müller and Wehner, 1988). Still, the reliability of the home vector information decreases with an increasing foraging distance. That means that the calculated home vector might not lead the ant exactly to the nest entrance. If the ant has run off its home vector without reaching the nest entrance and no further information is available, it engages in a systematic search strategy. Starting from the point where the nest is expected (i.e., the end of the home vector), the ant performs search loops leading to a spiral pattern (Wehner and Srinivasan, 1981; Müller and Wehner, 1994). By adapting the size of those search loops, the ants are able to compensate for an increasing uncertainty due to larger foraging distances (Merkle et al., 2006; Merkle and Wehner, 2010).

Various cues are considered when determining the walking distance or the walking direction. The walking distance is mainly calculated by means of a step integrator but is also slightly influenced by ventral visual flow (Ronacher and Wehner, 1995; Wittlinger et al., 2006). The strategy of counting the steps was revealed by manipulating the step lengths and putting ants either on stilts or stumps. Ants with shortened legs underestimated the distance of they had traveled during their outbound journey whereas ants on stilts overshot the expected distance (Wittlinger et al., 2006; 2007a). In undulating terrain, however, ants rather measure the ground distance between nest and feeder than the actual walking distance (Wohlgemuth et al., 2001; 2002). This suggests that ants are also able to detect the slopes of their paths, the adequate sensory input, however, remains enigmatic (Wittlinger et al., 2007b; Heß et al., 2009; Wintergerst and Ronacher, 2012).

The heading direction is determined predominantly via a celestial compass. Interestingly, for the proper functionality of the path integrator, *C. fortis* has to perceive the information about the walking direction and distance simultaneously (Sommer and Wehner, 2005; Ronacher et al., 2006). In contrast, *C. cursor* was able to determine its walking distance even in complete darkness, without visual input (Thiélin-Bescond and Beugnon, 2005). Several other arthropods use idiothetic information about their directional movements for path integration (e.g., cockroaches: Durier and Rivault (1999), spiders: Seyfarth et al. (1982); Moller and Görner (1994)). Thus, an involvement of proprioceptive information to assess rotational movements should not completely be excluded also for *C. fortis* and will be further investigated here (see Chapter 3). Apparently desert ants combine a variety of strategies and rely on various cues in order to reduce the uncertainty of individual approximations. This is also the case for the determination of the ants walking direction based on celestial cues when performing path integration.

1.3. The desert ant's celestial compass system

Celestial cues are ideal for the detection of compass information, as only rotational – but not translational – movements lead to changes in the perception. The celestial compass is sun-based, thus additional cues emerge by atmospheric scattering (Rayleigh scattering) of the sun light across the celestial hemisphere, namely intensity and a spectral gradient and the pattern of polarized (POL) light. The most relevant cues that provide directional information to insects are the sun and the polarization pattern of the sky (Wehner, 1997; Wehner and Müller, 2006). The use of both compass cues has been observed in various insects, however,

the preference for one of them seem to vary between different insects, e.g. bees or ants (also between subfamilies of ants) (Duelli and Wehner, 1973; Horváth and Wehner, 1999). Despite the close physical relationship of these celestial cues, the respective signals are perceived by different areas of the eye and first processed by separate navigation systems (Wehner, 1997; Wehner and Müller, 2006).

1.3.1. The sun compass system

The use of a sun compass is from an anthropomorphic point of view the most obvious one, as the sun represents for the human eye a prominent structure in the sky. Indeed, many species across the animal kingdom (e.g., insects, birds, mammals) rely on the sun compass for navigation. Felix Santschi showed for the first time the use of the sun compass. He observed how desert ants changed their walking direction in a predictable way when a mirrored sun was presented and the view of the natural sun was occluded (Santschi, 1911). The relevant compass information is given by the azimuth position of the sun rather than its elevation (Duelli and Wehner, 1973). Point-light sources, however, are ambiguous as they can be obscured or outside the animals field of view. Thus, compass systems that rely on more extended information are more robust. In this context the sun might be interpreted rather as the center of the spectral and intensity distribution across the hemisphere than as an isolated compass cue (Wehner and Müller, 2006).

1.3.2. The polarization compass system

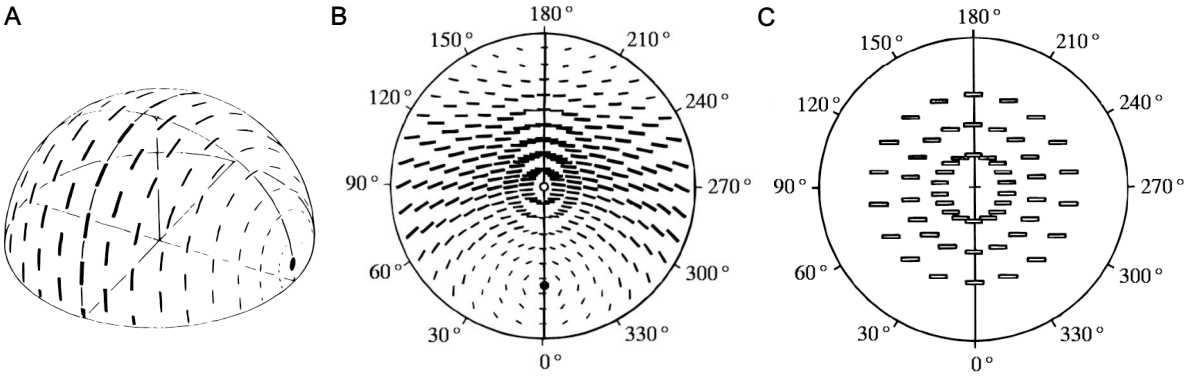

Fig. 1.2.: **A** 3-dimensional representation of the sky's polarization pattern. The electrical field vectors (e-vectors, *black bars*) are arranged along concentric circles around the sun (*black circle*). The degree of polarization in the sky increases gradually an reaches its maximum along a circle at 90° from the sun. **B** The polarization pattern viewed from an (ant's) earth-bound perspective. The symmetry plane coincides with the (anti)solar meridian. **C** The ant's simplified internal template. Adapted from Wehner (1982; 1994)

The polarization pattern in the sky is not visible for the unaided human eye. Santschi (1923) already suspected that ants exploit further features of the skylight (apart from the sun) and this could be later proven by von Frisch who discovered that insects use polarized skylight for navigation (Frisch, 1949). Due to scattering at small particles in the atmosphere, unpolarized sunlight is transformed into partially polarized light. Depending on the angle of the scatter the light is linearly polarized, thus its electric field vector (e-vector) is propagating in a single direction. The degree of polarization is maximal at a scattering angle of 90°

relative to the sun. A characteristic pattern emerges at the celestial hemisphere, consisting of e-vectors of linearly polarized light arranged as concentric circles around the sun (Fig. 1.2 A and B). From an earth's bound perspective this pattern is dynamic and the e-vectors at a specific patch in the sky change their orientation according to the sun's change in elevation (Wehner and Labhart, 2006). However, two characteristics of the pattern do not alter, the symmetry plane of the pattern defined by the (anti-)solar meridian and the particular horizontal orientation of e-vectors along the solar meridian.

Perception of the polarized light via the dorsal rim area of the insect's eye

The detection of polarized light is restricted to specialized ommatidia located in the upper part of their compound eyes, the dorsal rim area (DRA). These polarization-sensitive photoreceptors were first described in *Cataglyphis* by (Herrling, 1976). The e-vector analyzers are arranged in a fan-shaped manner, directing upwards and facing the contralateral field of view. These ommatidia consist of two blocks of photoreceptor cells with orthogonally oriented microvilli, each with rhodopsin molecules aligned in parallel. The molecules are maximally stimulated by polarized light arriving in parallel to the orientation of the rhabdoms. In ants these polarization analyzers are UV sensitive, whereas other insects possess photoreceptors sensitive to polarized blue (locust, cricket) or green (cockchafer) light (Labhart and Meyer, 1999). The strict homochromacy and the cross-arrangement of the analyzers strictly reduce or even eliminate confounding effects of spectral content or the degree of polarization (Labhart and Meyer, 1999; 2002). Although UV light intensity is lower than for other wavelengths in the clear sky, under cloudy sky it produces a pattern of polarized light with the highest degree. Furthermore, under both sky conditions a more accurate determination of the angle of the e-vector is possible for UV light (Wang et al., 2014).

The interpretation and neural processing of the polarization pattern

Most behavioral experiments are performed with bees and ants, while neurophysiological findings are predominantly provided by studies of larger insects, such as locusts and crickets. This multidisciplinary approach combining behavioral and neurophysiological data of different species is founded on their comparable neuronal structures in the central complex and thus may allow to draw a picture of how the polarization compass might work (Wehner, 2003; Wehner and Srinivasan, 2003). Based on observations in behavioral experiments, Wehner and colleagues concluded that the ant might possess a largely simplified internal template of the natural polarization pattern (Fig. 1.2 C; Rossel and Wehner (1982; 1984); Wehner and Rossel (1985); Fent (1986)). This template fits the actual polarization pattern of the sky best, when the ant is aligned along the symmetry plane of the pattern and thus allows the ant to determine the solar meridian. This matching process is hypothesized to be mediated by three interneurons, termed POL neurons, which pool the signals of the e-vector analyzers in the DRA. These neurons show tonic modulations according to the particular orientation of an e-vector. Each POL neuron is maximally stimulated at a different e-vector orientation (shifted by about 60°) and inhibited by an e-vector perpendicularly oriented (as shown in crickets Labhart (1988); Labhart et al. (2001)). Thus, the activity (e-vector tuning axis) of the POL neurons differ and depending on the orientation of the animals body lengths axis relative to the solar meridian a specific response pattern of these POL interneurons is produced. According to this pattern hypothetical compass neurons might respond, when the animal is oriented in a particular compass direction (Labhart and Meyer, 2002; Wehner and

Srinivasan, 2003). Neurophysiological findings in locusts support this model (Heinze and Homberg (2007); Sakura et al. (2008), reviewed in Homberg et al. (2011)).

1.4. Scope of the thesis

Desert ants are "champions" in spatial navigation as living under extreme conditions; they are able to accurately navigate over large distances relying on complex navigation mechanisms. By investigating the navigational toolkit of desert ants, one can understand how different cues are interpreted and weighted. Of special interest is the hierarchical organization of different navigation strategies (e.g. path integration, landmark-guided navigation) or of different cues (e.g. visual, proprioceptive) used for one strategy. The aim of this thesis is to better understand the navigational skills of desert ants, particularly the detection of directional information during path integration. I focus on the polarization compass, the most prominent cue to infer walking direction. A lot of research has already been done on the functionality of the polarization compass. However, further details of how this compass information is actually read or integrated, compared to other directional information, will be investigated here. I approached these research questions by performing different behavioral experiments. First, I applied a polarizing (POL) filter to reduce the complexity of the natural polarization pattern to a much simpler uniform pattern. Being able to selectively manipulate the polarization compass, I could provoke conflicts with respect to idiothetic information (Chapter 3) or sun compass information (Chapter 4). By means of such cue conflict experiments, the relative importance or the interplay of different cues can be investigated. I went a step further in Chapter 5 and asked, if polarization and sun compass information are fed into the same navigation center, how flexible can they be used, can they also substitute each other? These experiments provided some insights on how the ant uses these sky cues. The next chapter (Chapter 6) then focuses on the asymmetric structure of the desert ants' dorsal rim area (DRA) to test for a specific area, where POL information might mainly be detected.

2. Methodological approach and technical details

2.1. Summary

The following chapter will give an overview of the basic idea of the experiments reported in Chapters 3, 4, 5, and 6. The underlying principles of the experimental situations are presented here, while the actual experimental setups are described in detail in the materials and methods sections of the respective chapters.

2.2. Animals and location

Cataglyphis fortis (Hymenoptera, Formicidae; Forel, 1902, Wehner, 1983) was investigated in its natural habitat, the desert in North Africa. All experiments were performed in a salt pan (Sebkhet Bou Jemel, 34°55' N, 10°21' E) near the Tunisian village of Menzel Chaker. The salt pan is devoid of any landmarks and characterized by a dry hard, flat ground. This landscape provides a homogeneous panorama and ideal conditions to investigate celestial compass systems. The animals originated from various nests and each individual was tested only once.

2.3. Vector navigation and displacement experiments

Desert ants perform large foraging excursions during which they scan effectively the extensive area around the nest for food. After the ant has found a food item, it grabs this piece with its mandibles and heads for the nest on the shortest way possible, piloted by a so called home vector (Wehner, 1982). The home vector reflects the 180° reverse mean vector of the outbound run and thus enables the ant to find its inconspicuous nest entrance even after a tortuous outbound run of over several 100 meters. This vector is detached from earthbound cues and leads in case of a displacement to a heading direction parallel to the one expected without the displacement. The principle of vector navigation was used in this thesis to investigate the desert ant's celestial compass system. By manipulating the particular cues experienced during the outbound path and observing the ant's homebound run after a displacement, it is possible to draw conclusions of the significance of the respective cues for path integration in desert ants. The path integrator controls the home vector providing robust information about distance and direction of the nest already by the first visit of the feeder (Cheng et al., 2006). Additionally, previous experiments have reported that returning ants always rely on their most recent outbound run (Wehner et al., 2002). Thus to guarantee the desired home vector in the test animals, it was not necessary to determine an exact number of training runs before testing. Nevertheless, I started testing always only after a continuous flow of ants shuttled between the nest and the feeder, so most likely most of them had visited the feeder several times.

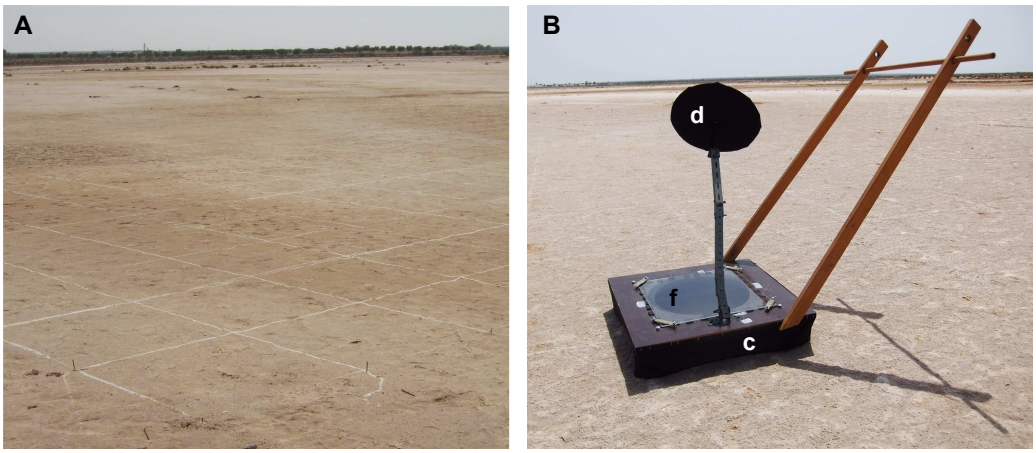

Fig. 2.1.: **A** The grid field painted with white color on the desert floor at an area devoid of any landmarks. The ants' trajectories were recorded on protocol sheets with a scaled grid. **B** Test trolley used to follow freely walking ants was equipped with four ball-bearing wheels and could be moved by the long handle. The black curtain (c) around the trolley prevented the ants from viewing the surrounding landscape or sensing the wind. The circular opening could be covered with filter sheets (f) and/or screened from the sun by a movable disc (d).

In most of my experiments, I selectively modified the celestial cues the ants experienced on their walk to an artificial feeder. Ants that had reached the feeder were individually caught and transferred inside small non-transparent containers to a distant test field, a grid (with a mesh width of 1 m^2) painted on the desert floor (Fig. 2.1 A). The grid was located at an area devoid of any landmarks. There the ant was released and its homebound run could be observed. I recorded the ant's trajectory to determine its heading directions until it performed a U-turn initiating the characteristic search loops and the completion of the home vector. Detailed information about the particular training situations and setups are given in the corresponding sections (for an overview, see Tab. 2.1).

2.4. Channel system

The training towards the feeder took place in a channel system. A plastic enclosure around the nest guided the ants directly from the nest entrance into the channel. In most of the experiments (Chapters 3, 4, and 5) U-shaped aluminum channels were used, these had a width and height of 7 cm resulting in an approx. 60° overhead strip-like window providing direct view of the sky (when the ant ran in the middle of the channel according to the "visual centering response"; Heusser and Wehner (2002)). Fine sand was glued to the bottom of the channel to provide a good walking grip and a comparable structure to the salt pan ground. The sidewalls were painted in matt grey minimizing possible light reflections. The upper parts were additionally covered with adhesive tape, preventing the ants to climb precociously out of the channel. The visual panorama inside the channel provided no landmarks and minimal optic flow. Further details about the specific setup of the individual experiments are described in the corresponding methods section.

Tab. 2.1.: Overview over the experiments

Chapter	Training	Test
3	channels + POL filters; shadowed sun	open test field
4	channels + POL filters; free sight of the sun	open test field
5	channels + POL filters or orange Perspex	trolley with orange Perspex or UV-transmitting Perspex + sun shield
6	broader channel system sidewalls consisting of wooden plates; free sight of the sky	covered eyes + ocelli; trolley with UV-transmitting Perspex + sun shield

2.5. Manipulating the celestial compass cues

In most of the experiments the ants experienced manipulated compass information during their outbound runs, i.e., while running through the channel. Filters were attached above the channel system and barriers alongside the channel could be erected in order to prevent direct view of the sun.

For manipulations during the inbound runs of freely moving ants on the open test field, the filters were carried by an experimental trolley (Fig. 2.1 B, constructed following Duelli and Wehner (1973); Fent (1986)). This gadget had a large horizontal circular aperture that could be covered with the desired filter, e.g., spectral filters (see the following paragraphs) or a movable disc to shield the sun. While recording the test run, the trolley was moved by an assistant ensuring that the ant was always in the center of the circular opening.

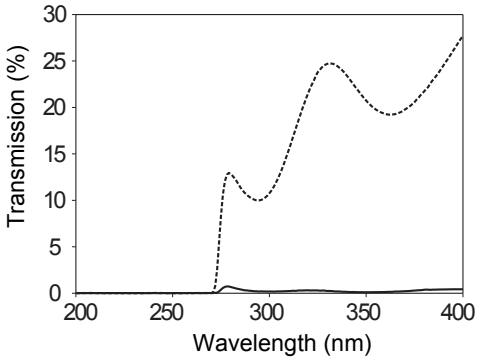

Fig. 2.2.: The transmission properties of the POL filter in the UV part of the spectrum is depicted by the *dashed curve* and is relevant for the use of the polarization compass. The quality is given by the *solid line* near zero indicating the transparency of orthogonally crossed filters. Taken from Heß et al. (2009).

Polarization filter The natural celestial pattern of polarized light could be manipulated by POL filter sheets (HN38 Polarisationsfolie linear, 0.3 mm; Fa. ITOS GmbH, Mainz, Germany). The polarized light produced by the filter extends even to the UV range of

the spectrum (300-400 nm), which is the wavelength for which desert ants can discriminate linearly polarized light (Duelli and Wehner, 1973; Labhart, 2000). Figure 2.2 depicts the transparency properties of the POL filter. Thus, while walking under the POL filter, the ants experience a 60° overhead stripe consisting of single e-vector in a specific direction while any other e-vectors are excluded.

Orange Perspex In experiments in which ants were deprived from using the POL compass, orange Perspex (Plexiglas® GS 2C04, 3 mm, Evonik Industries AG, Darmstadt, Germany) was installed above the channel. The orange sheet has a transmission less than 0.01% for wavelengths below 506 nm and do not let UV light pass through which is crucial for the proper function of the desert ant's POL compass (see transmission curve τ in Fig. 2.3 A). Under the filter only the ant's long-wavelength photoreceptors are left functional, thus not only the use of POL compass is excluded but also the perception of spectral gradients.

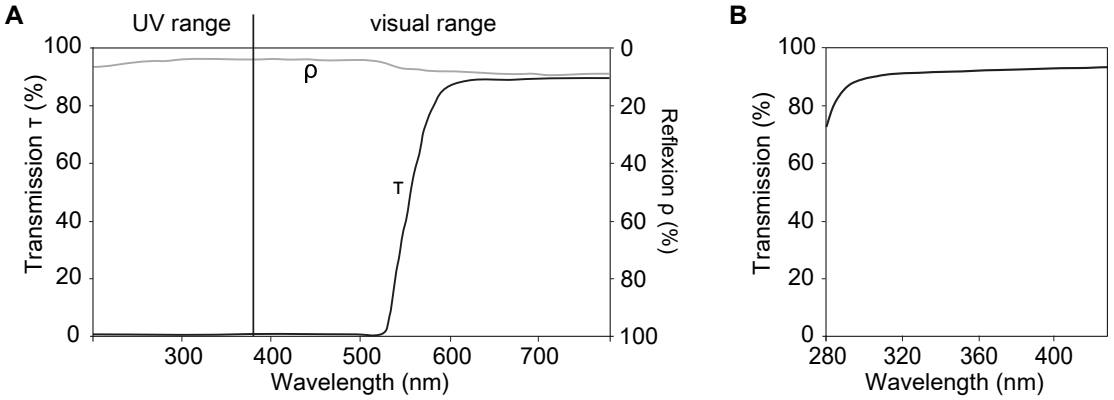

Fig. 2.3.: **A** Transmission curve of the orange Perspex which is a cut-off filter for wavelengths smaller than 530 nm, degree of transmission τ and degree of reflection ρ are presented in % (Plexiglas® GS 2C04, Evonik Industries AG, Darmstadt, Germany). **B** Transmission curve of the UV transparent perspex (Plexiglas® GS 2458, Evonik Industries AG, Darmstadt, Germany). Transmission stays high even down to wavelengths of 300 nm, the UV part of the spectrum which is relevant for the detection of polarized light.

UV-light transmitting Perspex A UV light transmitting Perspex (Plexiglas® GS 2458, 3 mm, Evonik Industries AG, Darmstadt, Germany) mounted above the trolley aperture was used in experiments where the ants had to perform their homebound trip under the trolley, but still had to be able to detect the celestial polarization pattern. In order to prevent wind blowing into the trolley causing undesired wind turbulence, I covered the trolley window with the UV-transparent Perspex (Fig. 2.3 B).

2.6. Data evaluation and statistical analysis

The quantitative determination of the desert ant's orientation abilities is mainly defined by the walking direction. To determine the mean heading directions of the ants' homing paths, I implemented a method proposed by Wehner (1968). On the protocol sheet, circles with radii corresponding to distances ranging from 1 or 2 m to 8 m on the test field were drawn at intervals of 1 m around the release point (i.e., the starting point of the trajectory). The

recorded heading direction corresponds to the intersection point of the trajectory and the circle and is determined relative to the expected direction (sun azimuth or nest depending on the training situation). These data were assembled in circular diagrams and subjected to circular statistics. All circular statistics were calculated using the software package Oriana 2.0 (Kovach Computing Services, Pentraeth, Great Britain) following the circular statistics described by Batschelet (1981). Further statistical procedures were performed according to Sachs (1999) and Zar (1999). Specific statistical tests and methods applied for individual paradigms are mentioned in the material and methods section of the corresponding chapter.

3. The dominance of the polarization compass over idiothetic cues in path integration of desert ants

In this chapter, I study the effects of a linear polarizing filter. This filter allows the selective manipulation of the polarization pattern and the control of the polarization compass information perceived by the ants, independent from other directional cues. By this means, ants can be confronted in conflict situations with artificial polarization compass information that contradicts directional information derived either from idiothetic cues (this chapter) or from the sun compass (Chapter 4), which allows to deduce their relative significance for the ant's path integration system.

3.1. Summary

[1] Desert ants, *Cataglyphis*, use the sky's pattern of polarized light as a compass reference for navigation. However, they do not fully exploit the complexity of this pattern, rather – as proposed previously – they assess their walking direction by means of an approximate solution based on a simplified internal template. Approximate rules are error-prone. Therefore it is a reasonable question whether the ants use additional cues to improve the accuracy of directional decisions. In the following I focused on "idiothetic" cues, i.e., cues based on information from proprioceptors. I trained ants in a channel system that was covered with a polarization filter, providing only a single e-vector direction as a directional "celestial" cue. Then I observed their homebound runs on a test field, allowing full view of the sky. In crucial experiments, the ants were exposed to a cue conflict, in which sky compass and idiothetic information disagreed, by training them in a straight channel that provided a change in e-vector direction. The results indicated that the polarization information completely dominates over idiothetic cues. Two path segments with different e-vector orientations were combined linearly to a summed home vector without any indication of a Bayesian approach of integration. Thus, the data presented here provide additional evidence that *Cataglyphis* uses a simplified internal template to derive directional information from the sky's polarization pattern.

3.2. Introduction

In a series of ingenious experiments, Wehner and coworkers have shown that *Cataglyphis*, primarily relies on the polarization (=POL) pattern of the sky as a compass reference to

[1] Most parts of the work presented in this chapter have been published in "The Polarization compass dominates over idiothetic cues in path integration of desert ants", Lebhardt et al. 2012 in J. Exp. Biol. (Contributions: Fleur Lebhardt: performance of experiments, data analyses, manuscript writing; Julja Koch: experimental design; Bernhard Ronacher: idea, performance of experiments, manuscript writing)

determine the walking direction for path integration (Duelli and Wehner, 1973; Wehner and Rossel, 1985; Fent, 1986; Wehner, 1989; 1994; 1997; 2003; Wehner and Labhart, 2006; Wehner and Müller, 2006). Like in other insects, this POL pattern is perceived by means of specialized ommatidia located in the dorsal rim area of their compound eyes first discovered in *Cataglyphis* (Herrling, 1976) and then described in various other insect species as well (for reviews see Labhart and Meyer (1999); Wehner and Labhart (2006)). Apart from the POL information, ants can also use the sun's position, the spectral gradient across the celestial hemisphere (Wehner, 1997; Wehner and Müller, 2006) and even the wind direction as additional or substitute compass cues – in the ants' habitats there is continuous wind usually blowing from a rather constant direction (Wehner and Duelli, 1971; Wolf and Wehner, 2000; Müller and Wehner, 2007).

The polarization pattern of the sky is complex, and the exact position of e-vector directions depends on the sun's elevation. How can insects like ants or bees use this changing pattern for their navigation? The solution proposed by Rossel and Wehner (Rossel and Wehner, 1982; Wehner and Rossel, 1985; Rossel and Wehner, 1986) is that these insects have an internal, simplified template representation of the celestial POL pattern (for ants, see Fent and others Fent (1986); Wehner (1989; 1994; 1997)) that allows them to determine the symmetry axis of the celestial POL pattern, and thus the solar meridian (see Fig. 3.1 B).

Although many features of the ant's compass system have been elucidated, some important questions have yet to be answered. For example, in his 1997 review, Wehner states that "we do not even know yet whether skylight patterns are used by these hymenopteran species simply to read a reference direction – e.g. the azimuthal position of the solar meridian – from the sky (Hypothesis I), or whether they are used to determine any particular point of the compass (Hypothesis II)". According to Hypothesis I, "a walking ant might well rely primarily on proprioceptive information derived from cuticular mechanoreceptors of its locomotor apparatus" with the danger of rapidly accumulating errors. "*Cataglyphis* might refer to skylight information simply for calibrating and, every now and then, recalibrating its internal compass scale" (pp. 177-178 in Wehner (1997)).

What kind of proprioceptors may be involved? Some mammals are able to return to a starting point by path integration even if all external cues are excluded, and the vestibular system seems to be essential for this homing performance. The semicircular canals and the statolith organs provide information on rotatory and linear accelerations, which can be integrated to monitor the animal's own movements – hence the term "idiothetic" (Mittelstaedt and Mittelstaedt, 1973) (other graviceptors are discussed elsewhere Mittelstaedt and Mittelstaedt (1996); Mittelstaedt (1996)). Successful homing based on idiothetic cues has been demonstrated both in freely moving mammals (such as golden hamsters, gerbils and humans, e.g. Etienne (1980); Mittelstaedt and Glasauer (1991); Séguinot et al. (1993)), as well as during passive displacements (Ivanenko et al. (1997); Nico et al. (2002); for a review see Wallace et al. (2008)). Remarkably, in humans, the information about self-motion during active walking was found to be dominant over visual (optic flow) cues (Kearns et al., 2002). In contrast to vertebrates, insects do not possess statoliths or semicircular canals. Instead, they use fields of mechanoreceptors (hair plates) located on various joints between body segments as gravity and probably acceleration receptors (Markl, 1962; Wittlinger et al., 2007b). There exists a plethora of other mechanoreceptors in insects, e.g. chordotonal organs (for a review see Field and Matheson (1998)), but their potential contribution to path integration is not well understood. However, there is ample evidence that arthropods may use idiothetic cues to stabilize an intended course or memorize previous movements (Mittelstaedt

and Mittelstaedt, 1973; Seyfarth et al., 1982).

In this chapter, I will present some experiments that aim at adding a piece of evidence to the above hypotheses proposed by Wehner. Experimental paradigms were designed in which ants were exposed to a conflict between different navigational cues. In particular, ants had to cope with conflicting information from the POL compass and the proprioceptors (idiothetic cues).

3.3. Materials and methods

For all experiments, ants were trained to walk to a feeding station through a linear aluminum channel that was covered with a polarizing transparency (POL filter, see Chapter 2). In the first short part of the foraging excursions from the nest to the entrance of the channel covered with the POL filter, the ants had free view of the sky, along a distance of approx. 45 cm. An ant walking in the training channel had no direct sight of the sun because of a 50 cm high barrier erected next to the channel. Two different training directions, at different nests, were used in the morning (AM) and in the afternoon (PM) to exclude the direct view of the sun: in the morning, the ants had to walk from the nest in the southwest direction (225°; Fig. 3.1 A); in the afternoon, the feeder was located in the southeast direction (135°) – the respective homing directions to the nest thus were 45° and 315°. At approximately noon, the shadowing of the training channel was not possible and therefore training and testing were suspended (see Fig. 3.2).

Due to the POL filter, the polarization information was manipulated and on their way from the nest to the feeder the ants experienced a single specific direction of the e-vector of light, as the filter transparency excluded all e-vectors except one. In this respect, the present experimental setup differed from most earlier experiments in which ants were trained under full view of the sky, and were then exposed to a restricted view of the sky or reduced POL patterns on their homebound path, by means of a trolley, which was moved along with the homing ant (e.g. Fent and Wehner (1985); Fent (1986); Müller (1989); see also Wehner and Müller (2006)). Three orientations of the e-vector relative to the channel orientation were used (orthogonal (90°), parallel (0°), and oblique (135°)), and various combinations of these.

The first group of experiments consisted of three types of experiments (Fig. 3.1 C-E). As a control, ants were trained in a 6.6 m linear channel with uniform e-vectors: orthogonal, parallel, and oblique (Fig. 3.1 C; note that the orientation of the schemes in Fig. 3.1 C-G does not correspond to the experimental situation; all channels were oriented on the field as shown in Fig. 3.1 A, depending on the time of day). In the first cue conflict experiment, ants were trained in a channel with a 90° turn (after 4 m; the second leg was 3.3 m); this channel was covered with a constant (orthogonal) e-vector pattern (Fig. 3.1 D). In a second cue conflict experiment, ants were trained in a linear channel covered with different combinations of two e-vectors; e.g. 3.3 m orthogonal followed by 3.3 m parallel (Fig. 3.1 E). In the latter series of experiments, I used the following combinations of e-vector orientations: 90° and 0°, 0° and 90°, 90° and 135° (all equal length of the two segments), and 90°, 0° and 90° (the two 90° segments combined had the same length as the 0° segment). In preliminary experiments it has been observed that the ants tended to turn back at the sharp transition from a 0° to a 90° e-vector. To reduce confusion of the ants, I covered the border between the two e-vector orientations with a 15 cm piece of orange Perspex, so that at the transition the ants had to walk a 15 cm distance without POL compass information (Ronacher et al., 2006); this 15 cm distance is not included in the length details given above. In the first cue

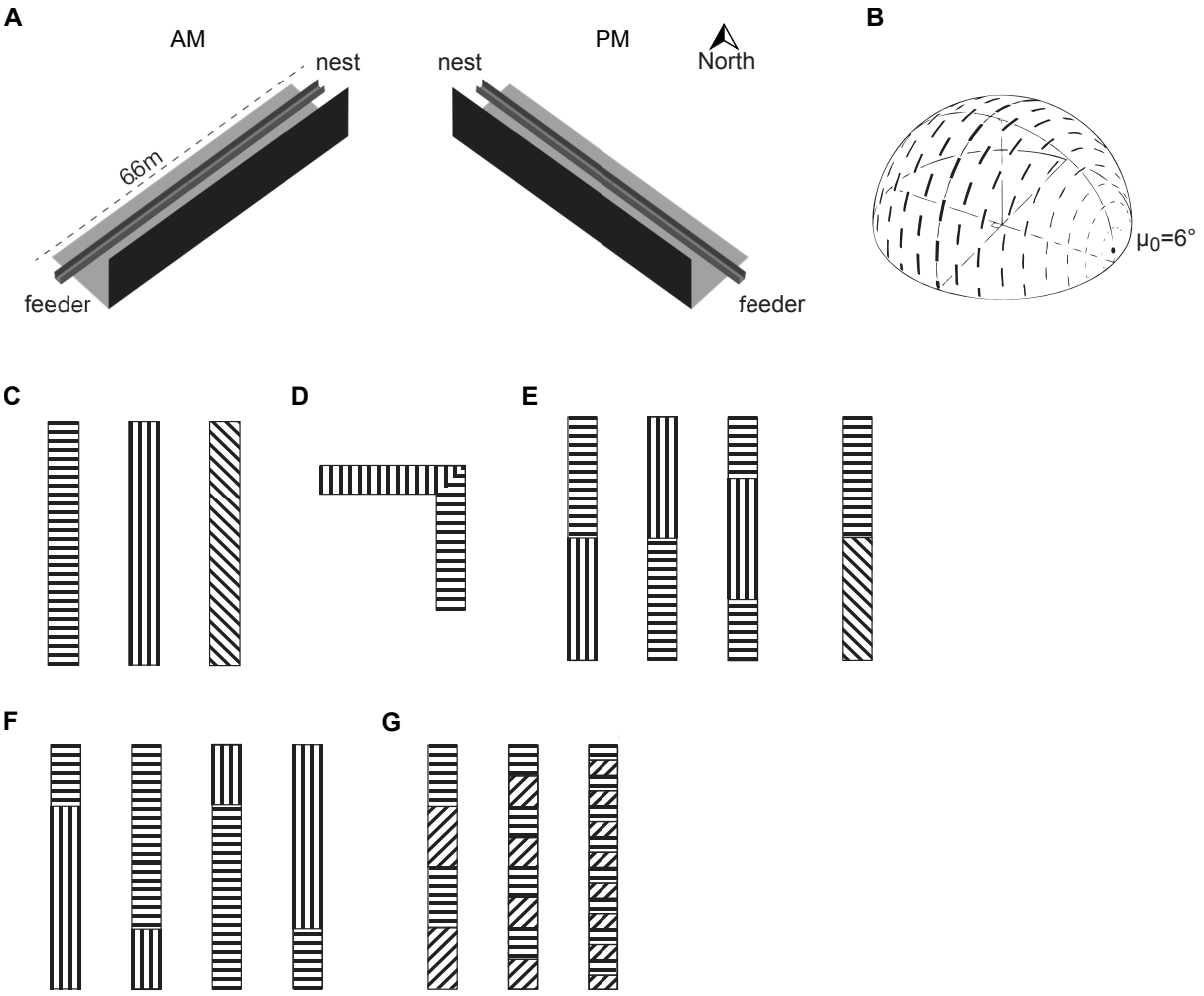

Fig. 3.1.: **A** Experimental setup showing the orientation of the channel used in the morning (left) and the afternoon (right). In the morning, the ants had to walk from the nest in the southwest direction (225°); in the afternoon, the feeder was located in the southeast direction (135°); the respective homing directions to the nest thus were 45° and 315°. **B** Sky polarization pattern at sunrise; the sun elevation (μ) was 6° (from Wehner 1982). **C** Straight channels with three different orientations of the e-vector (channel length with polarization (POL) cover of 6.6 m; channels not drawn to scale). Note that the orientation of the channels in (C-G) does not correspond to the experimental situation; on the field all channels were oriented as shown in (A), depending on the time of day. **D** First cue conflict paradigm: channel with 90° bend, covered with uniform POL filter orientation (e-vector orthogonal to the channel direction). Second cue conflict paradigm: change of e-vector orientation in a straight channel (**E**) after half (each POL pattern covered a distance of 3.3 m) and (**F**) after one-fourth or three-fourths (POL filter of 2 or 6 m length, respectively) of the training distance. **G** Channels of approx. 8 m length covered with alternating segments of two different e-vectors (0° and 45°). Schemes are not drawn to scale. Modified after Lebhardt et al. (2012).

conflict experiment (Fig. 3.1 D), however, the bend was not covered by orange Perspex, and thus the ants performed their turning movement under sight of the (orthogonal) e-vector.

In a subsequent series of experiments, I varied the relative lengths of the POL filters in combinations of short and long segments (i.e., one-fourth (2 m) and three-fourths (6 m) of the total length of the training channel (8 m), respectively). Segments of orthogonal and parallel POL filters were combined in all possible variations, that means starting either with a long or a short segment of a specific e-vector orientation (see Fig. 3.1 F).

In a second group of experiments (Fig. 3.1 G), the ants were presented with an e-vector pattern which repeatedly changed along the entire training distance, consisting of an orthogonal and an oblique e-vector orientation. For both e-vectors the same number of POL filter segments were used, thus all segments of the respective e-vector added together resulted in the same length. However, the constantly changing e-vector direction caused a permanent alternating virtual walking direction along the rather straight channel. Here the transitions between the changing e-vector patterns were separated by small cardboard pieces of 5-10 cm length instead of the 15 cm orange Perspex.

3.3.1. Data analysis and statistics

The homing directions at 2, 3, and 4 m were plotted in circular diagrams and subjected to circular statistics. The length of the mean vector and the circular standard deviation describe the concentration of data around a specific angle. To test whether a population's mean angle corresponded to a theoretical value, the One-sample test was applied (Zar, 1999). Viewing a single e-vector direction in the zenith yields ambiguous directional information. For example, having been trained previously with an e-vector parallel to the channel, the ant can choose to walk either 90° to the left or to the right of the sun azimuth on the test field, as these are the positions of a "vertical" e-vector, at least when the sun is at the horizon (see Fig. 3.1 B; the terminology relates to the e-vector orientation relative to the meridian when seen from the inside of the celestial hemisphere, cf. Wehner (1982; 1997)). Ideally, this leads to a bimodal distribution of homing directions in a circular plot. Hence, the mean vector becomes very small in spite of a strong clustering of the walking directions. In the case of a clear bimodal separation of data, I applied the One-sample t-test separately to each half of the bimodal distribution (see Results). As an alternative, the bimodal distribution was transformed to a unimodal distribution before applying significance tests (e.g. Batschelet (1981); Zar (1999)).

To compare two distributions, I used the Mardia-Watson-Wheeler test, after transformation to a unimodal distribution. In some cue conflict experiments, a more complex, quadrimodal distribution of homing directions was expected, for which no simple formulas exist in circular statistics. Two different types of tests were applied. First, I compared the counts in a 30° sector around the expected directions with the counts outside this range, and tested whether more ants than the expected 0.33 proportion headed in the predicted directions. The procedure was repeated for a 45° sector around the expected directions when applicable. As a second test of whether the actual homing directions of ants would correspond to these expectations, a Monte-Carlo simulation in combination with the Kolmogorov-Smirnov test was applied; the details of this procedure will be described in the Results section. In addition, for the first experiments (Fig. 3.1 C-E), the length of an ant's home vector was determined as the distance between the release point and the point where the ant switched from a straight path to search loops (Wehner and Srinivasan, 1981). To compare these data with the actual distances between nest and feeder, I estimated the confidence intervals of the

medians, according to the procedure given by Sachs (p. 336 in Sachs (1999)). All statistical tests were two-sided.

3.4. Results

3.4.1. Training with a single e-vector orientation

In a first set of experiments, an ant was exposed to a single e-vector direction during its foraging excursion in a straight channel (see Fig. 3.1 C). Performing its homebound run on the test field, now with full view of the sky's polarization pattern and the sun, the ant should orient in a particular direction relative to the sun azimuth, depending on where on the sky it expects to see that specific POL direction (see Wehner (1997)). For example, when trained with the e-vector orthogonal to the walking direction, the expected homing directions are along the solar meridian, either towards the sun azimuth or in the opposite, antisolar direction, as horizontal e-vectors are restricted to the solar-antisolar meridian (see Fig. 3.1 B). Obviously, during the day the sky-bound homing directions will change relative to the earth coordinates of the test field. In Figure 3.2 A, the actual homing directions of the ants recorded at different times of the day, are shown in earth coordinates (0° corresponding to North). In this graph, the shifts of the solar and antisolar direction are represented by solid and dashed curves, respectively. The "correct" homing directions, towards the nest, are indicated as horizontal lines at 45° and 315° (different training directions were used in the morning and in the afternoon, to exclude the direct view of the sun; Fig. 3.1 A).

Evidently, after this training the ants were not able to walk in the respective nest directions. Most ants headed in the solar direction, whereas only three animals chose the antisolar sector (Fig. 3.2 B). To quantify the accuracy of orientation, the homing directions were plotted relative to the sun's direction in a circular diagram (Fig. 3.2 B; sun azimuth at 0°). Focusing on the data in the upper half of the diagram, the length of the mean vector ($r = 0.96$) and the moderate circular standard deviation (± 15.8°) indicate a strong concentration of homing directions. The mean vector of this distribution ($\mu = 357.4°$) was not significantly different from the expected value 0° (One-sample t-test, 95% confidence interval for $353.2 < \mu < 1.7°$, N = 54).

The training with an e-vector direction parallel to the channel's axis mimics – from the ant's perspective – a foraging excursion in a direction at right angles to the sun azimuth; this is the expectation according to the ant's simplified internal template (Wehner (1997), see also Fig. 3.1 B). For different times of the day, the two expected directions are shown in Figure 3.2 C as dashed curves, whereas the solar direction is plotted as a solid curve. The right diagram shows again the orientation in coordinates relative to the sun's position (Fig. 3.2 D). Evaluating the right and left half of the diagram separately, mean (± circ. SD) vectors were 81.6 ± 12.2° and 267.7 ± 12.8° ($r = 0.978$ and 0.975, N = 14 and 42, respectively). The mean angle of 267.7° did not deviate significantly from the expected 270° ($p > 0.05$), whereas the mean angle of 81.6° deviated significantly, although weakly, from the 90° expectation ($0.05 > p > 0.01$). After training with the 135° orientation of the POL filter (Fig. 3.2 E, F), the homing directions again clustered near the expected values of 135° and 315°. Evaluating the two halves of the diagram separately, the mean vector of 309.8 ± 12.4° (N = 21) did not deviate from the expectation ($p > 0.05$), whereas the opposite vector (118.9 ± 9.0°, N = 28) deviated significantly from 135° ($p < 0.01$). Possible causes for the deviations from the expected values shown in Figure 3.2 D and F will be discussed later.

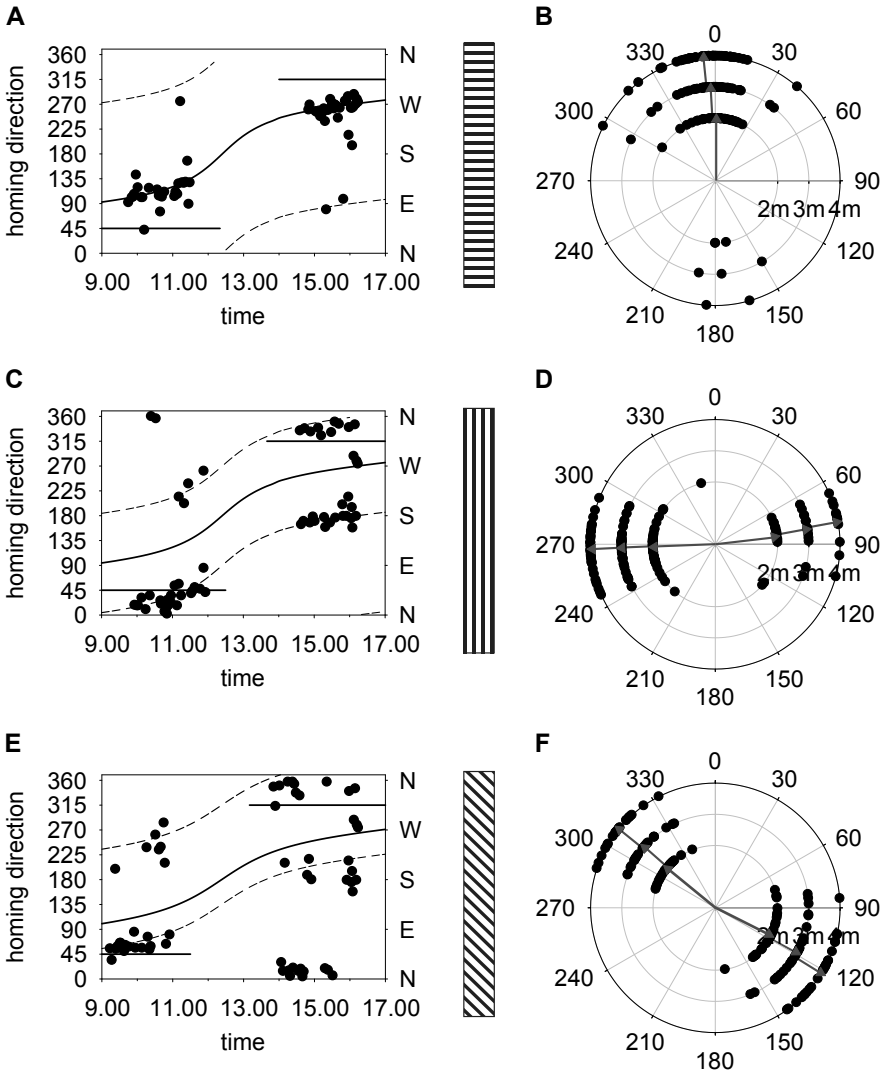

Fig. 3.2.: Homing directions of ants recorded on the test field, after training with a single e-vector direction (as in Fig. 3.1 C). Left diagrams (**A, C, and E**): direction of the homebound path at different times of the day, taken at 3 m distance from the release point. Curves represent the sun azimuth (*solid lines*) and the change in expected homing directions during the day (*dashed lines*); 0° corresponds to north (the four points of the compass are indicated on the right ordinate); *horizontal lines* at 45° and 315° indicate the nest position. The sun azimuth curves differ slightly between the diagrams because of the different test days. Each *point* represents the course of one ant. Right diagrams (**B, D, and F**): homing directions relative to the sun azimuth (at 0°), measured 2, 3, and 4 m from the release point. *Grey arrows*: mean vectors. **A, B** Orthogonal e-vector orientation (90°). Lengths of mean vectors were > 0.96 (evaluated for the solar half). At 2 and 3 m, the direction was not significantly different from 0°; at 4 m, the difference was significant ($0.01 < p < 0.05$) (N = 56, 54, and 52 at 2, 3, and 4 m, respectively). **C, D** Parallel e-vector orientation (0°). Mean vectors were evaluated separately for the left and right halves (all $r > 0.94$). Mean vectors were not significantly different from the 270° expectation at all distances (N = 43, 42, and 37); although the mean vector was not significantly different from 90° at 2 m, at 3 and 4 m the difference was significant ($0.01 < p < 0.05$ and $p < 0.01$, respectively; N = 14, 14, and 12). **E, F** Oblique e-vector orientation (135°). Mean vectors were evaluated separately for the left and right halves. The mean vector was not significantly different from 315° at 3 m, but this difference was significant at 2 m ($0.01 < p < 0.05$) and at 4 m ($p < 0.01$; all N = 21). Mean vectors were significantly different from the expected 135° (all $p < 0.01$; N = 30, 28, and 25). Taken from Lebhardt et al. (2012).

When insects experience a single e-vector direction in the zenith as a compass cue, one expects a bimodal distribution of heading directions (Wehner and Strasser (1985); Wehner (1994), see also Fig. 3.2 D and F). This bimodality was absent in the experiment with orthogonal e-vector orientation – ants showed a strong bias to the solar azimuth (Fig. 3.2 B) – whereas the other two training conditions exhibited a bimodal distribution of homing directions (Fig. 3.2 D, F). A closer look at Figure 3.2 C and E, however, reveals a similar bias in these data. In the parallel e-vector training, the ants strongly preferred one of the optional homing directions during the morning (stippled curves in Fig. 3.2 C): 27 animals headed to the 270° sector, and only four to the 90° sector; this bias was almost gone in the afternoon (15 versus 10). In the oblique e-vector training (Fig. 3.2 E), the bias (17 versus 7) was directed to the 315° sector in the morning, and reverted during the afternoon (4 versus 21). Possible causes for these deviations from bimodality will be discussed later.

3.4.2. Cue conflict experiments

In the next set of experiments, I put the sky compass cue in competition with the idiothetic cues derived from the animals' own movements. The inset in Figure 3.3 A depicts the situation of the channel with a rectangular bend in which, however, the continuous 90° POL filter mimicked a linear course. This experiment could be performed only in the late afternoon (16:00-17:15 h) because both legs of the channel had to be shaded against direct view of the sun. Figure 3.3 B shows some sample tracks of individual ants, demonstrating the straight path segments until they switched to search loops (see Wehner and Srinivasan (1981)). The outcome of this experiment is very clear: the ants ignored the actual bend of the channel, and they behaved exactly like animals trained in the straight channel with 90° POL filter direction (compare Fig. 3.3 A and Fig. 3.2 B). The two distributions in Figure 3.2 B and Figure 3.3 A did not differ significantly (Mardia-Watson-Wheeler test after transformation to unimodality, $W = 3.297, p = 0.192$).

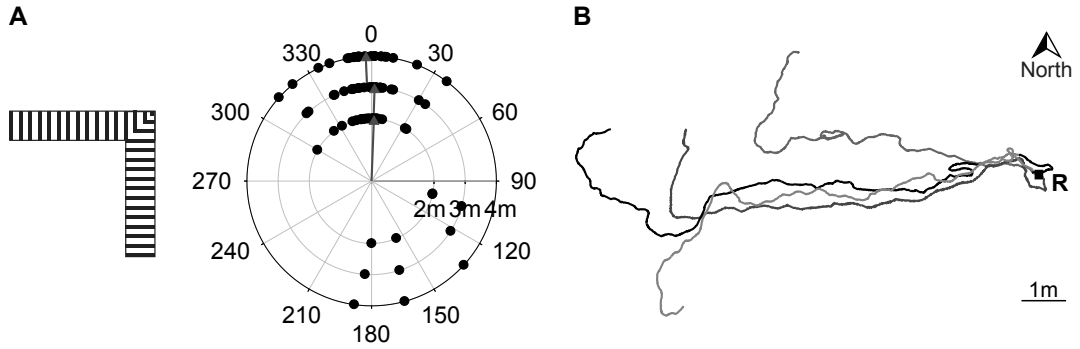

Fig. 3.3.: **A** Homing directions of ants on the test field, after training in a channel with 90° bend, covered by a POL filter with orthogonal e-vector directions was not different from that shown in Fig. 3.2 B (Mardia-Watson-Wheeler test: $W = 3.297$, $p = 0.192$). **B** Sample tracks of four individuals. R = release point. Reprinted from Lebhardt et al. (2012).

A "reciprocal" experiment was performed in a straight channel, but now simulating a virtual bend by a change in the POL filter direction. In this series of experiments I used four combinations of e-vector orientations (see Fig. 3.1 E): 90° and 0°, 0° and 90°, 90° and 135° (all equal length of the two segments), and 90°, 0° and 90° (the two 90° segments combined had the same length as the 0° segment).

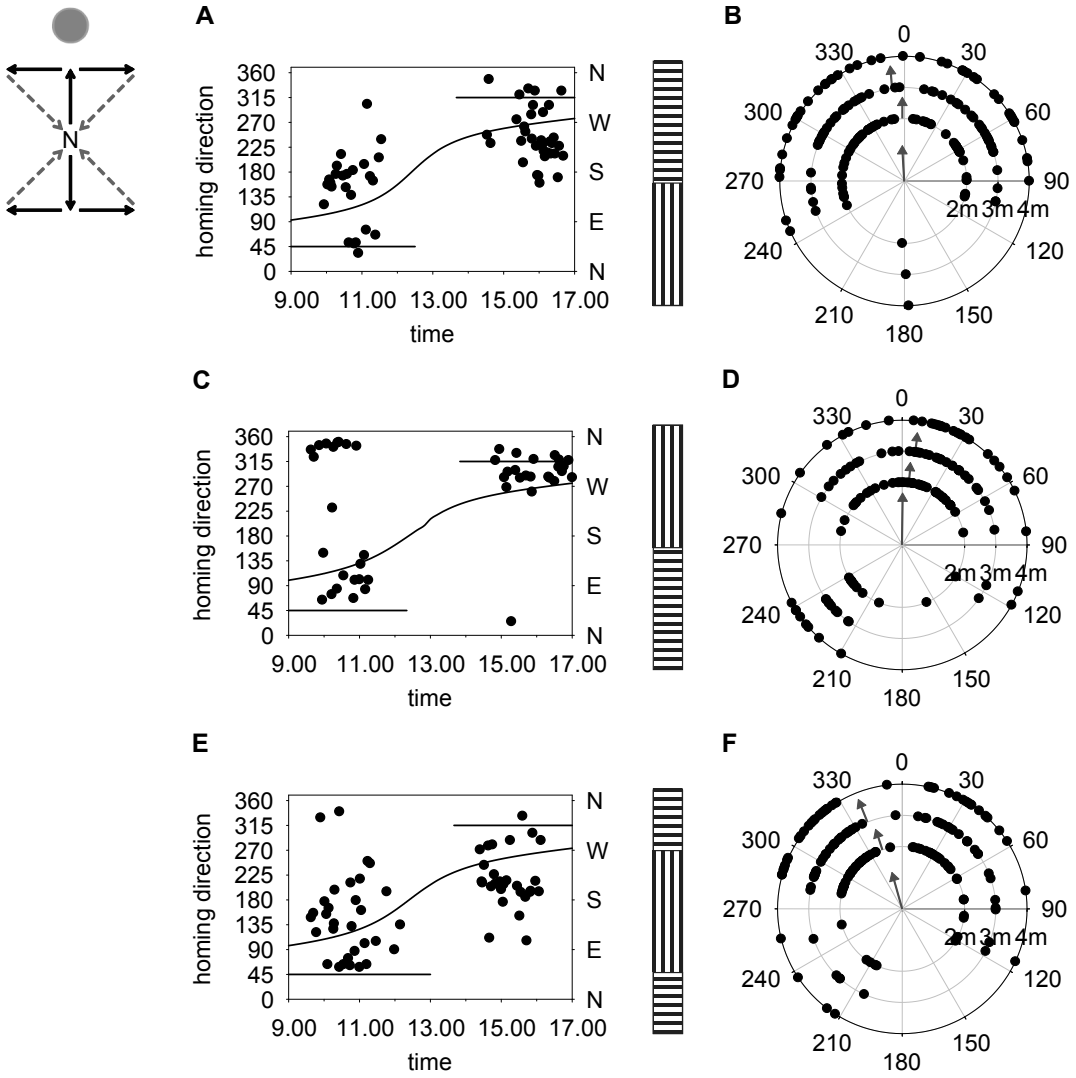

Fig. 3.4.: Cue conflict experiments in a straight channel simulating an "optical bend" by combining 0° and 90° e-vector directions. Left: scheme of expected homing directions. N = nest (the *grey disc* marks the sun azimuth). **A, C, E** Distribution of homing directions during the day; as in Fig. 3.2, the *solid curve* represents the sun azimuth; expected homing directions are not indicated in these diagrams. *Horizontal lines* at 45° and 315° indicate the respective nest positions. **B, D, F** Homing directions plotted relative to the sun azimuth. The respective vector lengths are small compared with those shown in Fig. 3.2 because of the broad distribution of homing directions. For the correspondence with the expected homing directions, see Fig. 3.5. In the sketches of the channels, the upper part represents the e-vector directions seen first by the ants on their outbound foraging trips (cf. Fig. 3.1 A). For further details, see Results. Adapted from Lebhardt et al. (2012).

3. The dominance of the POL compass over idiothetic cues

Because a single e-vector orientation leads, in principle, to a bimodal distribution of homing directions (as in Fig. 3.2 D and F), the expected homing directions in this type of experiment become more complex. For the combination of 90° and 0°, in principle a quadrimodal distribution of homing directions is expected (see scheme on the right of Fig. 3.4) because an ant trained with the orthogonal (90°) e-vector first has two options, the solar or antisolar direction. When the POL pattern then is changed to a parallel (0°) e-vector, it may choose to either run to the left or to the right of the sun position. As the two channel segments with 90° and 0° orientation of the e-vector had the same length (3.3 m), the combination leads to expected homing directions at 45°, 135°, 225°, and 315°, respectively, provided that the ants combine the two segments in a linear way (see inset in Fig. 3.4). A potential drawback of this experimental paradigm is that it may be difficult to distinguish such a quadrimodal distribution from a uniform distribution of homing directions. I expected that the strong preference of the solar direction observed in the experiment shown in Figure 3.2 A and B could reduce the ambiguity described in the scheme of Figure 3.4, and would lead to an actual preference of fewer than four directions. This was indeed the case (Fig. 3.4). In particular, there were virtually no individuals heading in the 135° direction, and the 225° quadrant was also underrepresented (Fig. 3.4 B, D, and F). As circular statistics books (Batschelet, 1981; Zar, 1999) offered no ideal solution for a statistical treatment of this type of data, I applied a Monte-Carlo simulation approach, combined with a Kolmogorov-Smirnov test (Sachs, 1999). First, the expected distribution of homing directions using two Gaussian distributions was calculated with the "ideal" mean values at 0° and 90° (or 0° and 270°) and a standard deviation of 19°, which is well in the range of standard deviations observed in Figure 3.2 (range of circular SD between 10.5° and 22.8°).

Figure 3.5 compares the observed homing directions at 3 m distance from the release point (grey columns) with the expected distributions. Then the Kolmogorov-Smirnov test was used to check for significant differences between the expectation and the actual data; an expectation with four peaks weighted by the number of data in the respective quadrants was applied. Figure 3.5 A demonstrates a reasonable agreement between the observed and expected distributions in the combination of orthogonal-parallel e-vectors (the data at 4 m distance yielded very similar statistics; in the following, the 4 m probabilities are given in parentheses). The Kolmogorov-Smirnov test indicates that the differences were not significant ($D = 0.1264$, $p = 0.31$, $N = 58$ ($p = 0.72$, $N = 49$)). For the combination of parallel-orthogonal e-vectors (Fig. 3.5 B), the difference between the expectation and the data was significant ($D = 0.213$, $p = 0.025$, $N = 48$ ($p = 0.004$, $N = 39$)). However, there was good agreement if the expected peak at + 45° was shifted to 35° (now $D = 0.1310$, $p = 0.386$ ($p = 0.32$, $N = 39$)). Figure 3.5 C shows the results of the e-vector combination orthogonal-parallel-orthogonal. These data corresponded well to the expectation ($D = 0.1165$, $p = 0.40$, $N = 59$ ($p = 0.22$, $N = 46$)). In summary, the linear combination of the two directions (0° and 90°, or 0° and 270°) described the observed homing directions remarkably well (Fig. 3.5).

As an additional, less sophisticated statistical test, it was checked whether a higher proportion of walking directions fell into 30° sectors centered on the four expected homing directions (45°, 135°, 225° and 315°), i.e., "hits", or in the surrounding sectors, i.e., "misses". The results indicate a high proportion of hits in three experiments. For the parallel-orthogonal e-vector combination (Fig. 3.4 D) the proportions were 25 hits and 23 misses - compared with the uniform expectation of 16 hits *versus* 32 misses ($\chi^2 = 7.59$, $p < 0.01$). For the orthogonal-parallel-orthogonal combination (Fig. 3.4 F), there were 31 hits and 28 misses ($\chi^2 = 9.79$, $p < 0.01$). For the orthogonal-oblique e-vector combination (Fig. 3.6 B), there

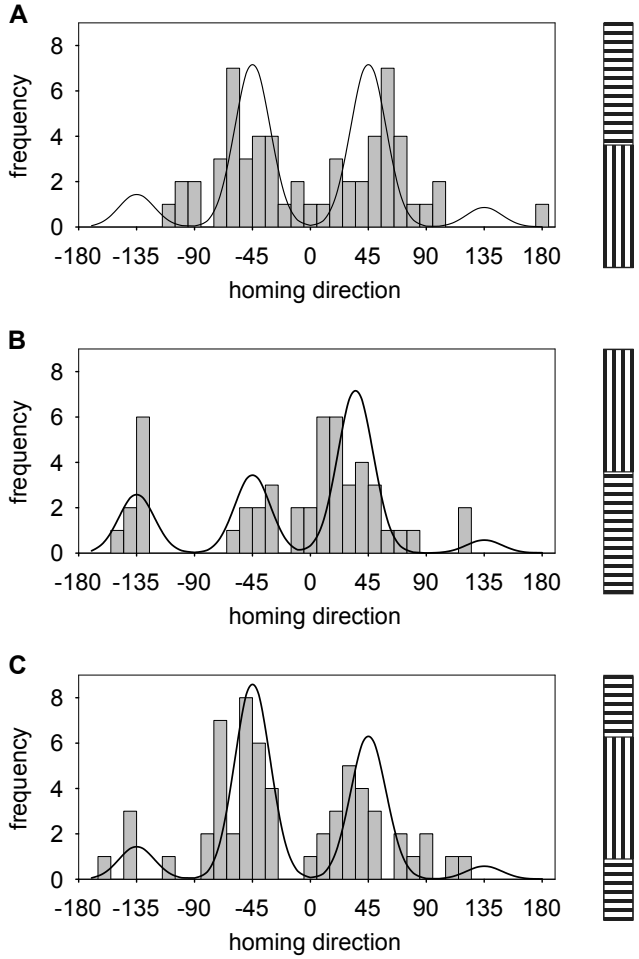

Fig. 3.5.: Statistical evaluation of the data shown in Fig. 3.4. Homing directions are shown as frequency histograms (*grey bars*). *Curves* represent the expected homing directions; the height of the expectation curves was adjusted by the number of actual occurrences in the respective quadrants. For further details, see Results. Adapted from Lebhardt et al. (2012).

were 24 hits and 18 misses ($\chi^2 = 10.71$, $p \approx 0.001$). For the orthogonal-parallel e-vector combination (Fig. 3.4 B), there was no significant accumulation in the 30° sector (22 hits *versus* 36 misses); however, in a 45° sector around the expected directions the counts were 36 hits *versus* 22 misses, approaching significance ($\chi^2 = 3.38$, $p = 0.066$). Taken together, this alternative test supports the notion that the ants headed more often than expected by chance in the directions predicted for these cue conflict experiments.

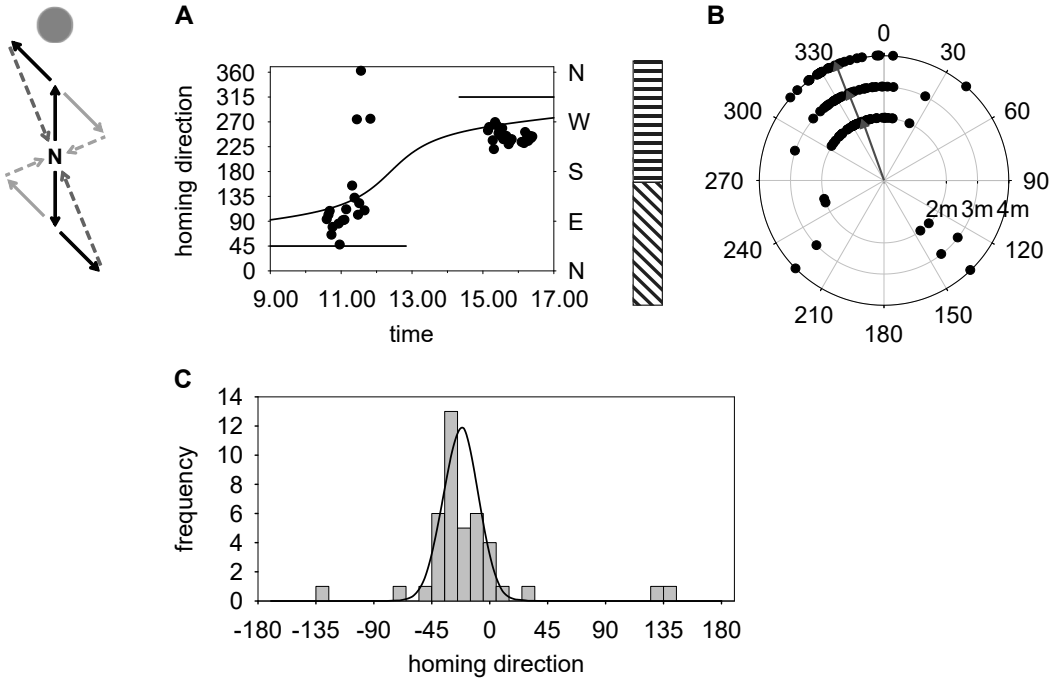

Fig. 3.6.: Cue conflict experiment in a straight channel simulating an "optical bend" by combining 90° and 315° e-vector directions. Inset on the left: scheme of expected homing directions (cf. Fig. 3.4). **A, B** Observed homing directions (conventions as in Figs. 3.2, 3.4). The *solid curve* represents the sun azimuth. **C** Statistical data evaluation. The observed mean vector direction at 3 m ($\mu = 336.7°$) is indistinguishable from the expected value of 337.5° (combination of 360° and 315°; Kolmogorov-Smirnov test: $D = 0.114$, $p = 0.69$). Reprinted from Lebhardt et al. (2012).

The combination of an orthogonal and an oblique e-vector orientation (90° and 135°) was chosen because it represents a (virtual) 45° bend in one direction versus a 135° bend in the other direction (see scheme in Fig. 3.6). Müller reported that it was much more difficult to induce ants to make a sharp turn leading backwards when trained in channels with view of the sky (Müller, 1989). Hence, we expected that this combination of two e-vector orientations would further reduce the ambiguities introduced by a single e-vector orientation. Indeed, this experiment yielded a strong concentration of homing directions around 337.5°, that is, the expected value for a linear combination of 360° and 315° (mean vector at 3 m: $\mu = 336.7 \pm 35°$, $r = 0.832$, $N = 41$; Fig. 3.6 B). Figure 3.6 C shows an almost perfect correspondence between expected and observed homing directions in this experiment (Kolmogorov-Smirnov test: $D = 0.114$, $p = 0.69$, $N = 41$ ($p = 0.07$, $N = 36$)).

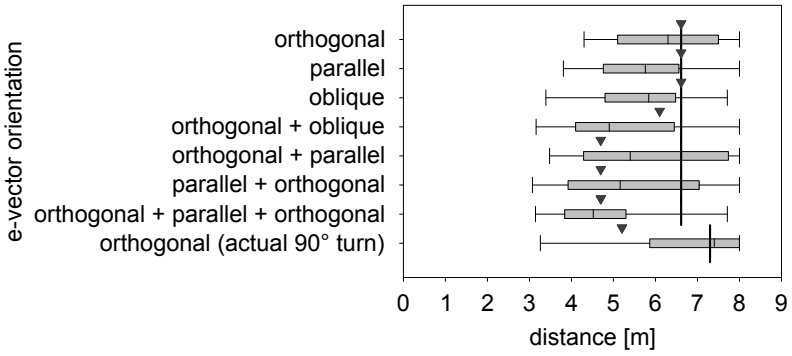

Fig. 3.7.: Length of home vectors for the eight training paradigms, i.e., distance between release point and begin of search loops. Shown are medians, quartile ranges (*grey bars*), and 10th and 90th percentiles (*whiskers*). *Bold vertical bars* indicate the expectation according to the actual walking distances under the POL filter, i.e., distance between channel entrance and feeder. *Arrowheads* indicate expected vector lengths if the ants had perceived an actual (experiment of Fig. 3.3) or virtual bend of the channel (Figs. 3.4, 3.6). From top to bottom, the number of individuals tested is $N = 59, 57, 51, 45, 60, 50, 61$, and 30. Adapted from Lebhardt et al. (2012).

3.4.3. Length of home vectors

From the paths recorded on the test field I extracted the distance between the release point and the first distinct turning of the ant. This turn indicates the switch from the rather straight path to the characteristic search behavior, and thus the length of the home vector (see Wehner and Srinivasan (1981)). Figure 3.7 presents a compilation of the homing distances observed in the different experimental paradigms. Shown are medians, quartile ranges (grey bars) and 10th and 90th percentiles (whiskers). The actual distances an ant had covered in the training channel under the POL filter are indicated by bold black bars, whereas triangles represent the distances for a virtual (or actual) bend between nest and feeder in the cue conflict experiments. For path lengths longer than 8 m, the switch to search loops could not be recorded exactly; therefore, these data were fixed at 8 m. Although the spread of observed distances is large, some trends are visible (Fig. 3.7). After training with a single e-vector direction, the ants tended to underestimate the true distance (the difference to the expected 6.6 m was significant at $p < 0.01$ for parallel and oblique e-vector orientations, but not significant for orthogonal e-vector orientations). A shortening of home vectors, however, is not uncommon if the training and test situations differ (Müller, 1989; Grah et al., 2005). In the cue conflict experiments with combinations of orthogonal and parallel e-vectors (cf. Fig. 3.4), the observed distances were always significantly smaller than the actual walking distances ($p < 0.01$), whereas they did not differ significantly from the virtual nest-feeder distance indicated by the triangles (4.67 m). In the combination of orthogonal and oblique e-vectors (cf. Fig. 3.6), the actual and expected virtual homing distances are rather similar, and the ants showed an underestimation for both (observed lengths of home vectors compared with the walking distance, $p < 0.01$; compared with the expected distance marked by the triangle, $p < 0.05$). Remarkably, in the first cue conflict experiment with the 90° bend of the channel (see Fig. 3.3), the median distance is close to the walking distance in the channel ($p > 0.05$); however, it differs significantly from the real distance between nest and feeder ($p < 0.01$; note that in this experiment, for technical reasons, the two legs of the channel were 4 and 3.3 m, and thus the diagonal was 5.19 m). This last result corroborates the

conclusion of Figure 3.3 that the ants interpreted this experimental paradigm as a straight path.

3.4.4. Bayesian interpretation of the cue conflict?

In order to better understand how individual subsequent path segments are combined into the home vector, I varied the respective POL filter lengths of different e-vectors in ratios of one-fourth and three-fourth of the entire training distance. A putative stronger significance of the first or the last section of the training route would then be more apparent than it would be for the earlier described cue conflict situations (cf. Fig. 3.4). Again, combinations of orthogonal and parallel e-vectors were used. The prediction of a quadrimodal distribution as observed for the experiments in Figure 3.4 also applies here. However, because of the new combination of lengths the peaks of the expected distribution are shifted towards 22.5°, 157.5°, 192.5°, and 337.5° for a combination of a long orthogonal and a short parallel POL filter and towards 67.5°, 112.5°, 247.5°, and 292.5° for a long parallel and a short orthogonal POL filter segment. The data were analyzed the same way as before and the recorded homing directions at 2, 3, and 4 m are plotted relative to the sun azimuth in circular diagrams in Figure 3.8 A, C, E, and G.

Analogous to the cue conflict experiments presented in Figure 3.4, I used a Chi-squared test to test if the recorded homing directions accumulated significantly within a 30° sector around the expectations. This analysis revealed for all four experimental conditions that a significant amount of ants headed towards the expected directions (χ^2-tests for the 3 m data Fig. 3.8 A: $\chi^2 = 10.78$, $p \sim 0.001$; Fig. 3.8 C: $\chi^2 = 20.44$, $p < 0.001$; Fig. 3.8 E: $\chi^2 = 24.50$, $p < 0.001$; and Fig. 3.8 G: $\chi^2 = 4.06$, $p < 0.05$). A theoretical distribution representing the expected homing directions was calculated as described previously, but this time the respective vectors were weighted according to the lengths of the corresponding POL filter segments. However, the putative quadrimodal distribution is here less obvious because of the close vicinity of the expected heading directions (e.g. peaks at 337.5° and 22.5° or 157.5° and 192.5° for the long orthogonal and short parallel POL filter combination). Comparing the frequency distributions of the ants' homing directions with the theoretical distributions yielded good agreements for 2 out of 4 cases for the 3 m (Fig. 3.8) and 3 out of 4 cases for the 4 m data (given in parentheses). The distributions of the heading directions of ants that have been trained with a combination of first a parallel and then an orthogonal POL filter orientation coincided with the expectation, irrespective of the individual segment length (Fig. 3.8 B: $D = 0.1493$, $p = 0.101$, $N = 67$ ($p = 0.285$, $N = 57$), and H: $D = 0.1475$, $p = 0.080$, $N = 74$ ($p = 0.265$, $N = 64$)), whereas the results from the combination of a long orthogonal and a subsequent short parallel POL filter were significantly different for the 3 m but not for the 4 m data (Fig. 3.8 D: $D = 0.2008$, $p = 0.008$, $N = 68$ ($p = 0.062$, $N = 58$)). However, the theoretical distribution and the frequencies of the ants' homing directions after the training under a short orthogonal and a long parallel POL filter combination did significantly differ for the 3 m and the 4 m data (Fig. 3.8 F: $D = 0.1796$, $p = 0.032$, $N = 64$ ($p = 0.028$, $N = 51$)). In both cases of disagreement with the theoretical values, I shifted one of the expected peaks for 10° either towards 0°, i.e., the sun azimuth (Fig. 3.8 F: from 67.5° to 57.5°), or away from the sun azimuth (Fig. 3.8 D: from 337.5° to 327.5°). By this means very good accordance of the experimental data with the theoretical distribution could be achieved for the long orthogonal and short parallel POL filter training (Fig. 3.8 D: now $D = 0.1336$; $p = 0.177$) and the short orthogonal and long parallel POL filter combination (Fig. 3.8 F: now $D = 0.1193$; $p = 0.323$ ($D = 0.1405$; $p = 0.267$)).

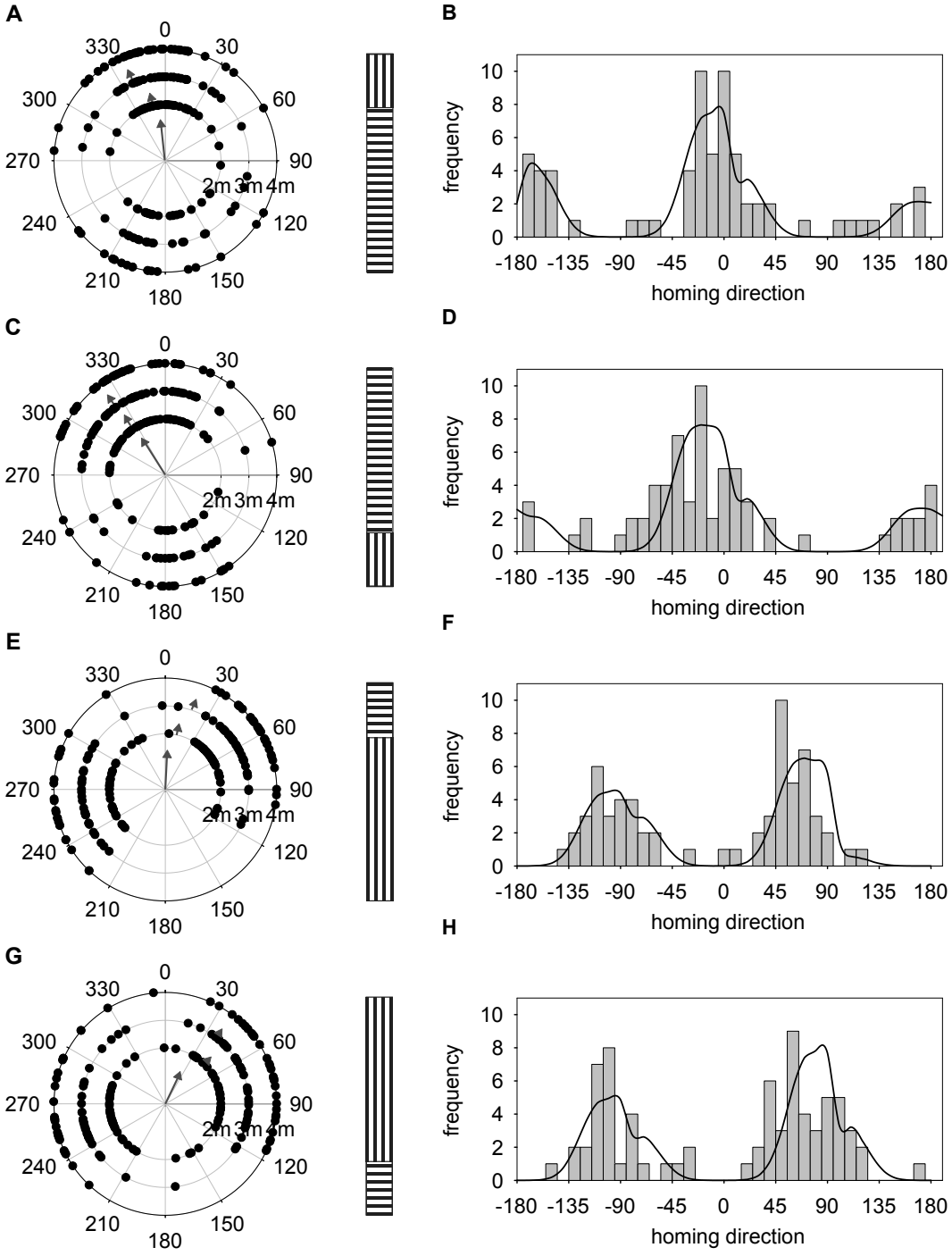

Fig. 3.8.: Homing directions of desert ants after training under a POL filter with a particular e-vector orientation and followed by a second POL filter orientation rotated by 90° of different lengths. **A, C, E**, and **G** Circular diagrams depict the ants' homing directions relative to the sun azimuth. The frequencies of the respective homing direction (*grey bars*) and the expectations (*curves*) are plotted in **B, D, F**, and **H**. For further description see Figs. 3.2 and 3.5.

3.4.5. Multiple visual bends influence the ant's homing performance

A putative impact of repetitive visual bends was investigated in the experiments illustrated in Figure 3.9. In three different training situations, I presented ants with combinations of 2 m, 0.5 m, and 0.15 m long POL filter segments for the e-vector orientations of 90° and 45° repeatedly alternated along a training distance of approx. 8 m (see the three different schemes of Fig. 3.1 G).

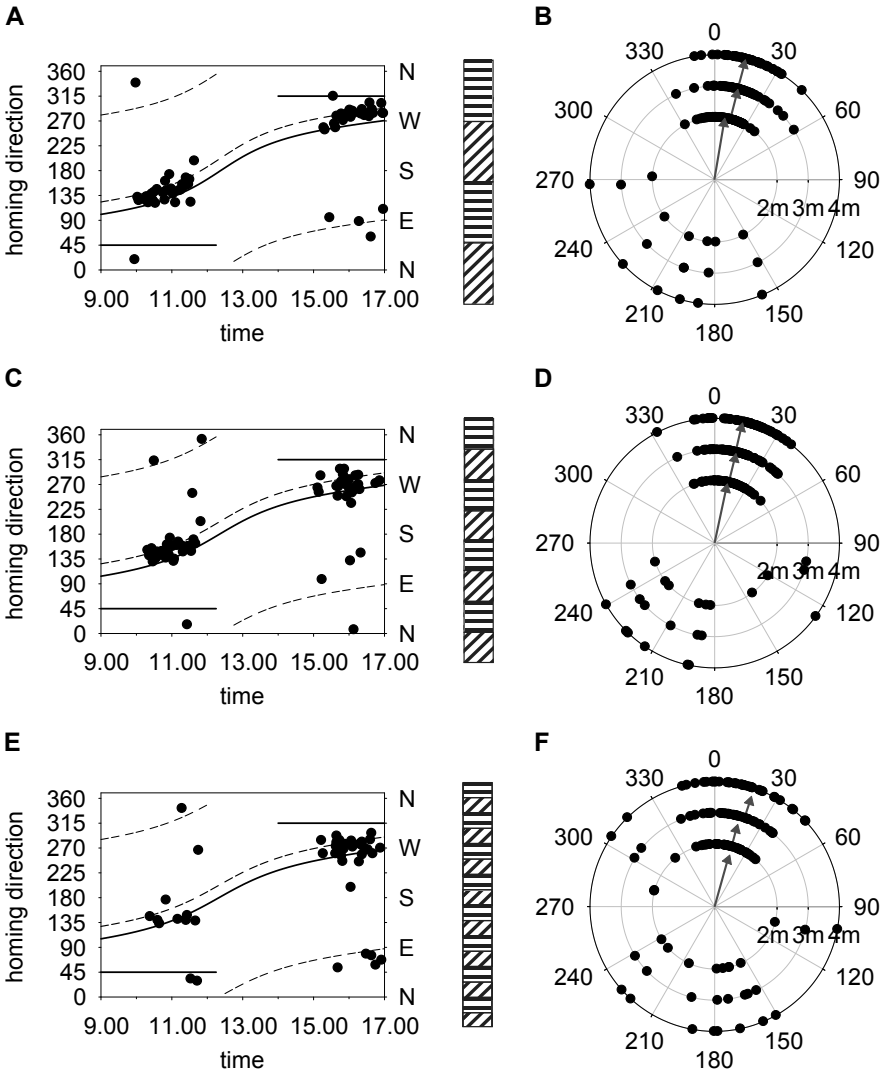

Fig. 3.9.: Homing directions after training with constantly changing e-vector orientations consisting of 90° and 45° e-vectors plotted relative to the earth coordinates (**A, C, E**) and relative to the sun azimuth (**B, D, F**). The ant's orientation abilities are hardly affected and result for the 3 m data in mean vectors angles ($\mu = 13.7°$ - $14.7°$, $N = 41 - 65$) close to the expected 22.5° (not significantly different, One-sample t-test) and relatively large mean vectors lengths ($r > 0.647$). For further details see Fig. 3.2.

Figure 3.9 depicts the distribution of homing directions at different times of the day (A, C, and E) and plotted relative to the sun azimuth (B, D, and F). The latter were subjected to circular statistics. The mean vectors for the 2 m and 0.5 m segmentation resulted in mean angles of $\mu = 14.7 \pm 37°$ and $r = 0.809$ ($N = 65$) and $\mu = 13.7 \pm 41°$ and $r = 0.773$ ($N = 65$;

Fig.3.9 B and D, respectively) and the mean homing directions after the 0.15 m POL filter segmentation resulted in $\mu = 13.8 \pm 54°$ and $r = 0.647$ ($N = 61$, Fig. 3.9 F). None of the mean vectors deviate significantly from the expected value of 22.5°, although this might be due to the relatively large circular standard deviations, especially in the latter case. The ambiguity of the directional information and the bimodality of the distributions appears to be slightly stronger pronounced in the experiments with shorter POL filter segments and consequently more POL filter changes; only 9% of the animals in Figure 3.9 B and 15% in F walked towards the "antisolar" direction, interestingly then with much larger scatter. Thus, for the further statistical analysis and a better comparison between the different training situations, I focused only on the data lying in the upper part of the diagram in a 180° sector around the expected 22.5° (thus between 292.5° and 112.5°). Now, the distributions have reduced circular standard deviations (ranging from ± 10° to ± 27°) and evidently larger mean vector lengths ($r > 0.893$); but also all distributions now deviate significantly from 22.5° ($\mu < 15.7$, One-sample t test).

According to the Mardia-Watson-Wheeler test the distributions of the 2 m and 0.5 m segmentation was considered indistinguishable (Fig. 3.9 B and D: $p > 0.414$ and $W < 1.764$, for all 2-4 m). The same is true for the comparison of the 0.5 m and 0.15 m segmentation (C and D: $p > 0.074$ and $W < 0.5196$), although the 2 m data of these distributions nearly reach significance ($p = 0.051$) and significantly differ with respect to their circular standard deviations ($p = 0.033$; Wilcoxon-Mann-Whitney test for dispersion). However, the distributions of the 0.15 m segmentation differ significantly from the 2 m segmentation in two out of three cases (3 and 4 m data: $p < 0.024$, $W > 7.567$; but 2 m data: $p = 0.092$ and $W = 4.771$) and have significantly different circular standard deviations for the 3 and 4 m data ($p < 0.01$, and $p = 0.06$ for the 2 m data). Thus, comparing the distributions with each other revealed at least a difference between the "longest" (2 m) and the "shortest" (0.15 m) segments.

In the following, I check for differences between the observed distributions of homing directions and the expected heading directions according to the applied POL filter combination. First, using the χ^2 test to compare the hits and misses of homing directions lying within or outside the 30° sectors around the two expected homing directions, i.e., 22.5° and 202.5°, resulted in a significantly higher representation within the expected sectors for all cases (Fig. 3.9, $\chi^2 = 8.39 - 37.69$, $p < 0.01$ for B, D, and F). This represents a good agreement between the data and a theoretical assumption of a linear combination of the two e-vector orientations. Thus is additionally investigated by the second approach of a Monte-Carlo simulation (see Section 3.4.2). The frequency distributions of the recorded homing directions and theoretical distribution obtained by the Monte-Carlo calculation are depicted in Figure 3.10 as frequency histograms (grey columns) and curves, respectively. The comparison between the observed distributions and the expectation for the respective segmentation resulted for all three cases in significant differences ($p < 0.04$, N = 65, 65, 61; Fig. 3.10 A-C). This significance were dissolved, when the peak expected at 22.5° was shifted by 10° to 12.5°, leading then to good congruence in all cases (Fig. 3.10 A, 3 m data: $D = 0.144$, $p = 0.135$ (4 m data: $D = 0.172$, $p = 0.077$); B, 3 m data: $D = 0.056$, $p > 0.5$ (4 m data: $D = 0.142$, $p = 0.076$); C, 3 m data: $D = 0.148$, $p = 0.138$ (4 m data: $D = 0.146$, $p = 0.155$)). The Monte-Carlo simulation was calculated as mentioned before, however, this kind of a simple combination of only two theoretical Gaussian distributions with the "ideal" mean values at 0° and 45° does not fully reflect the complex situation of multiple, though, repeated e-vector changes. A mathematical vector addition of repeated results instead in smaller standard

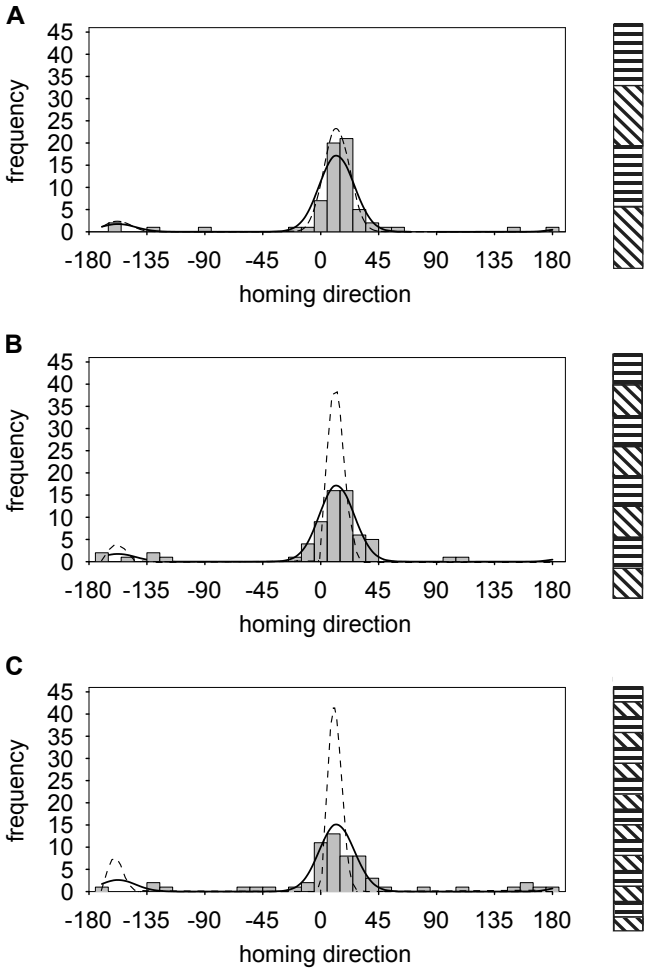

Fig. 3.10.: Homing directions from Fig. 3.9 plotted as frequency histograms for statistical analysis. *Grey bars* = data, *curves of continuous lines* = expected distributions based on a Monte-Carlo simulation approach as calculated before (see Fig. 3.5), *curves of stippled lines* = expected distributions based on a second Monte-Carlo simulation approach (taking the repetitive changes of e-vector orientations into account).

deviations and steeper peaks, as the probability to read the respective e-vector correctly is higher the more frequently the POL information is presented (stippled curves in Fig. 3.10). Thus, for the smallest segmentation of 0.15 m the theoretical distribution would result in a curve with a quite high and steep peak, although obviously the experimental data are wider spread (compare grey columns and stippled curve in Fig. 3.10 C).

3.5. Discussion

The experiments reported here aimed at revealing the respective influences of sky compass information and idiothetic cues on the navigation of *C. fortis*. In different experiments, the ants were exposed to a situation in which the idiothetic information about the actual movement direction disagreed with the information from the POL compass. All these experiments supported the same conclusion: the ants relied primarily on the sky compass and ignored conflicting idiothetic information. Remarkably, the exposure to a rather artificial situation – with only a single e-vector direction available in the training channel – did not impair the accuracy of homing paths on the test field (see the low circular standard deviations in Fig. 3.2). Even in some of the cue conflict experiments, the clustering of homing directions was very tight (Figs. 3.3 and 3.6). The results will now be discussed in detail.

3.5.1. Training with a single e-vector direction

Ants that saw only a single e-vector orientation during an extended path segment behaved quite normally on the test field now with full view of the sky. The ants followed rather straight homebound paths (Fig. 3.3 B) and mostly adhered to the expected directions that correspond to the position of these e-vectors in the sky and in their internal template (see Fig. 3.1 E; see Wehner (1997)). Hence, a single e-vector direction seen during training allows for a quite accurate navigation on the test field – this is evident from the large mean vectors ($r = 0.92 - 0.98$) and the small circular standard deviations shown in Figure 3.2 (circ. SD range = 10.7 - 22.8°). The variances are in the same range as reported in earlier investigations (e.g. Müller (1989); Wehner (1997); Wehner and Müller (2006)). However, a few significant deviations from the expected homing directions occurred.

The first was the strong bias towards the solar direction (visible in Fig. 3.2 B and Fig. 3.3 A), which is in contrast to the bimodal distribution expected for a single e-vector stimulus in the zenith (Wehner and Strasser, 1985; Wehner, 1994). However, on closer examination of different test times, less obvious biases were also visible in the other experiments (see Results, Fig. 3.2 C, E and Fig. 3.4).

When trying to explain an obviously general lack of bimodality in several of these experiments, one should be aware that a tiny additional influence may be sufficient to turn the balance between two equivalent homing directions. As mentioned in the Introduction of this chapter (Section 3.2), ants can use several additional or substitute compass cues: the sun's position, the spectral gradient across the celestial hemisphere (Wehner, 1997; Wehner and Müller, 2006), and even the wind direction, which is rather constant for longer time periods in the study sites (Wehner and Duelli, 1971; Müller and Wehner, 2007). The direct view of the sun was shielded in our training paradigm (Fig. 3.1 A). Hence spectral gradients on the sky and wind remain as major additional compass cues that could have caused these biases.

On its outbound run in the morning, an ant experienced a spectral gradient with more UV on its right side (see Fig. 3.1 A). Thus, for its homebound run on the field it should

prefer that of the two possible homing directions which yields more UV on its left side. This consideration perfectly explains the strong morning bias for 310° and the reversed afternoon bias for 120° found for the oblique e-vector training (Fig. 3.2 E and F). The same argument is able to explain the strong morning bias to 270° in the parallel e-vector training (Fig. 3.2 C). In the afternoon, however, a preference for 90° would have been predicted according to the spectral gradient hypothesis, which was not observed (10 ants heading to 90° versus 15 heading to 270°). For the cue conflict experiments shown in Figure 3.4, I also observed a bias for certain directions, depending on the training type and test times. The spectral gradient hypothesis is in perfect agreement with the opposing biases found both in the morning and afternoon in the parallel-orthogonal e-vector training (Fig. 3.4 C). The data shown in Figure 3.4 E are equivocal with respect to the hypothesis, as they do not exhibit such a strong bias. However, the preferred directions in the morning and afternoon sessions, shown in Figure 3.4 A, reveal a bias that is opposite to the predictions from the spectral gradient.

The strong preference of the solar azimuth in the experiments with orthogonal e-vector orientation (Fig. 3.2 B, Fig. 3.3) cannot be explained by the spectral gradient hypothesis. Conceivably, an additional influence of wind - which blew mostly from a northern to a northeastern direction in the morning, while turning in the afternoon to the southeast or south - may have caused these preferences. However, as wind direction and wind speed was not continuously recorded during these experiments, this possibility must remain tentative. Hence, the most likely explanation is that ants interpret a single orthogonal e-vector usually as belonging to the antisolar meridian, already suggested by Fent (1986).

In Figure 3.2 D, a small but significant ($p < 0.05$) deviation from the 90° expectation was observed, whereas in Figure 3.2 F, the deviation from the 135° expectation amounted to approx. 16° ($p < 0.01$). It is unlikely that these deviations could have been caused by an additional influence of spectral gradients or wind. Wind probably can be ruled out, as the wind compass is neglected if put in competition with the POL compass (Müller and Wehner, 2007). Another explanation for these deviations may be that during training the ants first walked a short distance of approx. 45 cm between nest entrance and channel opening with full sight of the sky, and here experienced a different compass direction, compared with the POL pattern in the channel (see Section 3.3). This could have introduced a deviation from the solar meridian of up to 5°; remarkably, this effect was smaller in the morning and larger in the afternoon, which fits the data shown in Figure 3.2 C-F. Taking this potential effect into account, the deviations from the 90° value in Figure 3.2 D are not longer significant; however, this effect can not completely explain the larger deviation from 135° in Figure 3.2 F.

3.5.2. Additional evidence for a simplified internal template

It has to be emphasized that the expected directions shown in Figure 3.2 C-F correspond to the predictions of a simplified, internal template that has been elaborated previously (Rossel and Wehner, 1982; Fent and Wehner, 1985; Fent, 1986; Rossel and Wehner, 1986). However, it is only at sunrise and at sunset that this template fits the actual distribution of e-vectors on the sky. At other times of the day, in particular around noon, there are deviations (for a detailed discussion, see Wehner (1982; 1989; 1994; 1997)). The "vertical" e-vector (in my paradigm corresponding to the e-vector parallel to the channel; Fig. 3.2 D), for example, is shifted towards 45-60° azimuthal distance to the sun at 11:00 h (Coulson et al., 1960). Thus, if the ants had relied on the actual sky position of the vertical e-vector, at around noon their homing direction should have deviated by 30°-45° from the 90°/270° expectation. I checked

the homing directions shown in Figure 3.2 C, D separately for times early in the morning (or late in the afternoon) and times between 11:00 and 15:00 h, and found no difference: the mean vectors at 2, 3, and 4 m differed by only $-2.0°$, $+4.3°$, and $-0.8°$, respectively (Mardia-Watson-Wheeler test: $p > 0.65$ in all cases, $N = 36$ and 21, 35 and 21, and 31 and 18 animals, respectively). Thus, the results provide an independent piece of evidence supporting the model proposed by Wehner, i.e., that the ants navigate by comparing the sky's polarization pattern with a simplified internal template for POL directions (for a review, see Wehner (1994; 1997)). In this template, the vertical e-vectors are fixed at 90° distance to the solar meridian, in contrast to the sky's polarization pattern, in which the azimuth positions of vertical (and other) e-vectors depend on the sun's elevation (Wehner, 1982; 1994; 1997).

3.5.3. Cue conflict experiments

Both types of cue conflict experiments of an actual bend or a visual bend showed that orientation in *C. fortis* is based on POL information as the completely dominant cue, rather than on idiothetic information. In the experiment shown in Figure 3.3 A – with a 90° bend in the channel – the ants behaved exactly like those trained in a straight channel. In the experiments shown in Figures 3.4 and 3.5, a marked influence of idiothetic cues would have led to a distinct deviation from the 45° and 315° expectations. In general, the data of Figures 3.5 and 3.6 correspond quite well to the theoretical expectations. The only exception (Fig. 3.5 B) where a significant deviation existed between data and theoretical curves became non-significant if we shifted the 45° peak of the expectation by only 10°. This deviation is not larger than the deviations found in the experiments with a single e-vector orientation (see Fig. 3.2 D, E). Hence, the ants seem to combine the path segments corresponding to two e-vector orientations (0° and 90°) in a linear fashion. This interpretation is corroborated by the results shown in Figure 3.6, in which a strong concentration of homing directions and an almost perfect correspondence between expected and observed homing directions was found.

Deviations from the expected directions (see scheme in Fig. 3.4) could have several causes. One could be an influence of additional idiothetic cues – if an ant perceives the straightness of the channel via its proprioceptors, this could lead to a compromise direction between the visual 90° bend and the straight path, resulting in a smaller virtual turning angle, e.g. 60°. In addition, ants that are trained in a channel system (with sight of the sky) that forces them to a sharp turn later exhibit systematic navigational errors in their homing directions recorded on a test field (Müller and Wehner, 1988). As the combination of 0° and 90° e-vectors simulates a 90° turn of the channel, ants should exhibit this type of "integration error" (Müller and Wehner, 1988). The expected error for a 90° turn and equal length of the two legs is approx. 12° (Fig. 3.5); for a 45° turn the error is approx. 5.6° (Fig. 3.6). The shift of the distributions shown in Figure 3.5 B and C towards 0°, compared with the expectations, may be due to this type of error. However, the data shown in Figure 3.5 A rather indicate a trend in the opposite direction. In Figure 3.6 C, no deviation from the expected homing directions is visible; however, in this paradigm the integration error would be rather small ($< 6°$).

A deviation could also result from a different weighting of the first and second channel segment. A stronger weighting of the second path segment would then yield different distributions of homing directions for a combination of a short orthogonal followed by a long parallel e-vector segment than for the reverse combination (cf. Fig. 3.11 A and B). Such a difference could not be observed. Instead, the homing directions coincided nicely with the expectation of a linear combination of the two unequal path segments independent of their

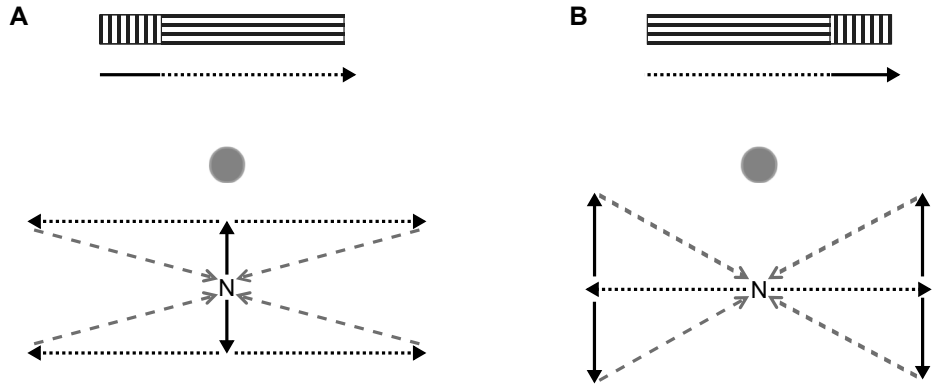

Fig. 3.11.: **A** Upper scheme: training situation with a combination of a short orthogonal and a long parallel POL filter segment. Lower scheme: the expected heading directions (*grey arrows*) relative to the sun (*grey circles*) considering a stronger weighting of the latter path section, i.e. the parallel POL filter (*dotted lines*). **B** In the reverse case (long parallel and subsequent short orthogonal POL filter) the orthogonal POL filter segment is stronger weighted, resulting in different heading directions with a stronger bias towards the (anti-)solar direction. N = nest

order and scattered predominantly within a 30° sector around the expected values (67.5°, 112.5°, 247.5°, and 297.5°). In contrast, the Monte-Carlo simulation revealed significant deviations for two POL filter combinations (Fig. 3.8 D, F), which could be resolved by shifting only one of the peaks about 10° (cf. Fig. 3.5 B). Interestingly, the shift had to be done in two different directions with respect to the expectations. Thus, at least these alterations done for Figure 3.8 D and F are somehow contradicting and provide no conclusive explanation for a stronger influence of the more recently experienced compass information on the homing direction.

In order to better understand the mechanism of how integration of POL information might be accomplished, the ants were presented with multiple visual bends during their outbound runs. In general, they still performed well oriented homebound paths, however, with an increasing number of changes of the e-vector direction, more ants headed towards the "antisolar" direction (Fig. 3.9 F). As their homing directions are quite randomly distributed, it seems rather unlikely that they were really heading for the antisolar azimuth. The larger scatter could in theory result of an non-expected e-vector combination, for example of a 180° and a 45° e-vector (instead of the corresponding 225°). Although, as earlier described, ants prefer to walk obtuse instead of acute angles (see Fig. 3.6), this might have happened in these experiments (Fig. 3.9, caused by the shorter POL filter segments and their repeatedly changing direction). Anyhow the larger standard deviation along with more POL filter changes persisted even when the "antisolar" data were excluded. Interestingly, for all distributions the simulated expected values had to be shifted towards the sun azimuth, suggesting a stronger weighting of orthogonal e-vectors compared to oblique e-vectors. An alternative explanation is that an oblique e-vector pattern actually reflects a direction nearer to the sun azimuth than at 45°, as reported by Fent (Fent, 1986). Furthermore, the comparison of a mathematical calculated theoretical distribution (stippled curve in Fig. 3.10 C) and the actual data hint at the assumption that shorter POL filter segments or their constantly changing orientation interferes with some noise, leading to less accurately read POL information and consequently to a less precise determination of the correct homing direction (i.e.,

larger circular standard deviations).

In summary, the results show that in path integration the polarization compass completely dominates over idiothetic cues. In addition, the good correspondence between expected and measured homing directions in the cue conflict experiments (Figs. 3.4-3.6), does not only support the template hypothesis (Wehner, 1994; 1997), but also suggests as the most parsimonious explanation that two path segments with different e-vector directions are combined in a linear way.

4. Interactions of the polarization and the sun compass in path integration of desert ants

This chapter will describe how desert ants evaluate information from different celestial cues, namely the polarized light and direct sun light. The results reveal a strong connection linking sun and POL compasses. The interaction of these two compass systems leads to interesting insights and further questions on the flexibility of such connected compass systems (addressed in Chapter 5).

4.1. Summary

[1] Desert ants, *Cataglyphis fortis*, perform large-scale foraging trips in their featureless habitat using path integration as their main navigation tool. To determine their walking direction they use primarily celestial cues: the sky's polarization pattern and the sun position. In this chapter I aim to examine the relative importance of these two celestial cues by performing cue conflict experiments. I manipulated the polarization pattern experienced by the ants during their outbound foraging excursions, reducing it to a single electric field (e-)vector direction with a linear polarization filter. The simultaneous view of the sun created situations in which the directional information of the sun and the polarization compasses disagreed. The heading directions of the homebound runs recorded on a test field with full view of the natural sky demonstrate that none of both compasses completely dominated over the other. Rather the ants seemed to compute an intermediate homing direction to which both compass systems contributed roughly equally. Direct sunlight and polarized light are detected in different regions of the ant's compound eye, suggesting two separate pathways for obtaining directional information. In the experimental paradigm applied here, these two pathways seem to feed into the path integrator with similar weights.

4.2. Introduction

While foraging in their featureless natural habitat, desert ants, *Cataglyphis fortis*, compute the home vector inferring the necessary information about the walking direction from the sky's polarization (POL) pattern or the azimuthal position of the sun. Besides these main compass cues, the POL and the sun compasses, it has been report that ants in specific situations also can use information from the spectral gradient of the sky or even from wind

[1] The work presented in this chapter has been published in "Interaction of the polarization and the sun compass in path integration of desert ants", Lebhardt & Ronacher 2014a in J. Comp. Physiol. A (Contributions: Fleur Lebhardt: idea, experimental design, performance of experiments, data analyses, manuscript writing; Bernhard Ronacher: discussion, manuscript writing)

blowing from a constant direction to determine their walking direction (Wehner, 1994; 1997; 2003; Wehner and Müller, 2006; Müller and Wehner, 2007).

This multitude of directional information (sun position, POL pattern, spectral gradient, wind) has to be evaluated and weighted to avoid ambiguities for the computation of a specific unequivocal homing course. One possibility to deal with this problem would be that the integration of information will be adjusted depending on its relative reliability for the actual navigation task, possibly suggesting a Bayesian type of cue integration (for reviews see Deneve and Pouget (2004); Cheng et al. (2007); Collett (2012)). However, another way would be a strict hierarchy, i.e., the exclusive dominance of one compass cue, whereas the information given by other cues is discarded; only in case that the dominant cue is not available the information of the "back-up cues" would be considered. Cue conflict experiments offer a straightforward approach to investigate the interaction of different compass cues. First insights into the integration of POL and sun compass information were obtained in an experimental paradigm that restricted the ants' view of the celestial POL pattern. This manipulation led to systematic navigational errors that persisted even if the sun was visible, which allows accurate navigation if presented alone (Wehner and Müller, 2006). The authors concluded that in desert ant navigation the POL compass dominates the sun compass (for a similar conclusion see also Duelli and Wehner (1973)).

With the experiments described in the previous chapter I could show that ants navigate accurately even under a very restricted, uniform POL pattern generated by a linear polarizing filter (POL filter) while the view of the sun was occluded. If, for example, ants are trained under a POL filter that was oriented orthogonally to the ants' walking direction this e-vector orientation mimics a walking direction along the solar meridian. On the test field, with full view of the sky, ants indeed chose homing directions along the solar meridian (see Chapter 3). Such a uniform POL pattern was now used to provide POL compass information that could be decoupled from the actual position of the sun. Applying this paradigm allowed me to create an artificial situation setting sun and POL compass information in direct conflict, in order to reveal the computation and the interaction of these two major compass cues.

4.3. Materials and methods

4.3.1. Manipulation of compass cues

The POL information experienced by the ants during training was manipulated using a POL transparency (HN38 Polarisationsfolie linear, 0.3 mm; Fa. ITOS GmBH, Mainz, Germany; see also Chapter 2). The POL transparency provided linear polarized light, also in the UV range, the wavelength range in which ants perceive polarized light (for transmission curve of the POL filter and further details see Chapter 2). In the first experimental paradigm, the ants experienced particularly restricted POL information along the entire training, i.e., a 7.5 m long, approximately 60° broad overhead stripe with a single e-vector orientation. Earlier experiments have shown that this type of directional information is sufficient to allow the ants to navigate accurately (see Chapter 3). However, in contrast to the earlier experiments in the present paradigm the ants had also visual access to the sun while walking under the POL filter. As a consequence, the training direction (Fig. 4.1 A, grey arrow) could be determined relative to two different reference directions: the sun azimuth and the POL filter orientation (here parallel to the walking direction). Hence, on the open test field, two extreme homing directions are possible (Fig. 4.1 B): the orange arrow indicates

the expected home path according to the sun compass. The blue arrow represents the POL compass direction (here perpendicular to the solar meridian, in case of an e-vector orientation parallel to the walking direction, as shown in A). If the ants relied exclusively on the POL cue, their walking directions on the test field should follow the sun's azimuthal course.

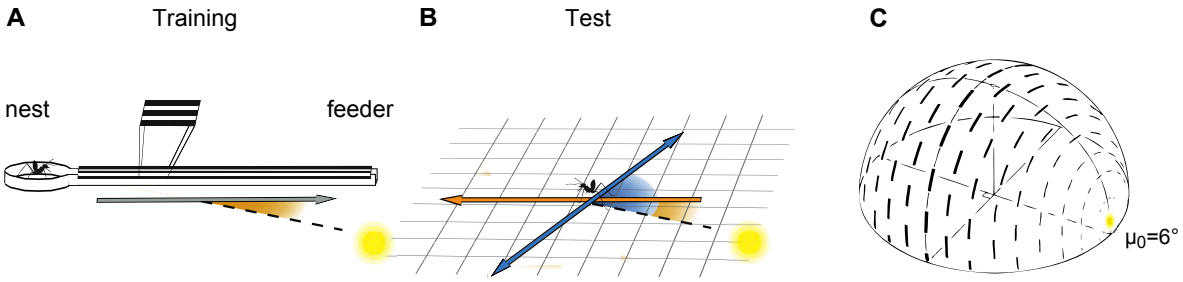

Fig. 4.1.: **A** Scheme of the training situation with a parallel orientation of the POL filter. The *grey arrow* gives the training direction imposed by the channel; the angle between the *grey arrow* and the *stippled line* indicates the nest direction relative to the sun azimuth, while the POL filter indicates a nest direction at a right angle to the sun azimuth. **B** On the test field with full view of the sky, the ant has two extreme options for its homing direction: based on the POL compass it would take a direction perpendicular to the solar meridian (*blue arrow*); based on the sun compass it can determine the unequivocal nest direction (*orange arrow*), or it can adhere to a combination of the two cues. If the ant relies on the POL information, its homing direction will change, depending on the time of the day (and the corresponding position of the e-vector direction on the sky according to the internal template). The *yellow circles* in A and B depict the sun. **C** The natural hemisphere with the polarized scattered sunlight arranged in concentric circles around the sun (*black bars* indicate e-vector orientation, *yellow circle*: sun at an elevation of $\mu = 6°$ above horizon; modified from Fent (1986)). Adapted from Lebhardt and Ronacher (2014a).

To meet the requirements of an effective cue conflict situation, it had to be ensured that the channel was directly illuminated by the sun for the entire training period and, therefore, guaranteed that the ants had direct view of the sun during their outbound run (Fig. 4.2). Thus, the time during which tests could be performed depended on the particular orientation of the training channel and was limited by the sun's elevation as the aluminum channels provided a maximum viewing angle of 60°. I applied three different e-vector orientations of the POL filters relative to the walking direction (orthogonal, parallel, and oblique). For each e-vector orientation, I chose two particular training directions, so that the discrepancy of the directional information between the POL compass and the sun compass was maximal at different times of the day and changed during the test period: 270° or 360° (= 0° corresponds to North) for the e-vector patterns orthogonal or parallel to the walking direction, and 135° or 225° for an e-vector orientation oblique (i.e., 45°) to the walking direction. The actual nest direction was thus 90°, 180°, or 315°, and 45°, respectively. In a second series of experiments, I either changed the walking direction with an unchanged POL pattern or changed the POL pattern while the actual walking direction remained constant (cf. Chapter 3, Figs. 3.3 and 3.4). In the former case, the ants were forced to follow a 90° bend of the channel system while the POL information mimicked a straight walking direction. In the reciprocal experiment, the ants experienced a 90° turn of the e-vector orientation while walking in a straight channel. In both cases, they experienced a sudden change of one cue relative to the other.

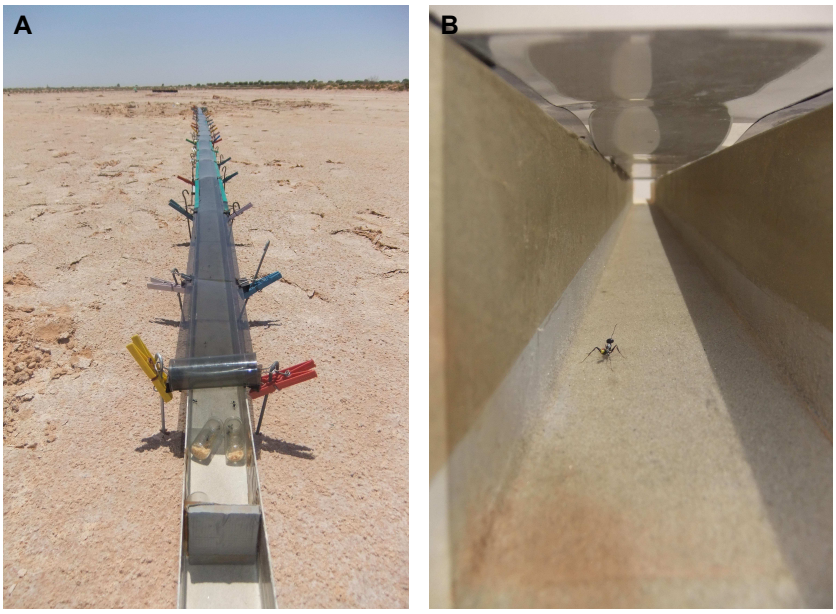

Fig. 4.2.: **A** Foto of the experimental setup **B** Close-up of the channel, the ant walks under an overhead stripe of polarized light produced by the POL filter and simultaneously sees the sun.

4.3.2. Data evaluation and statistical analysis

For each homing ant, I determined its heading direction at 2, 3, and 4 m from the release point on the test field. This measure provided a good representation of the initially fairly straight walking directions of the ants (see Fig. 4.3 J). I measured the deviation of the recorded homing directions from the expected POL compass direction based on the experienced e-vector pattern during training and checked for a dependence on the angular distance between POL compass and sun compass direction. In the Figures of this chapter, I plotted the 3 m data relative to the expected POL direction and against the angular distance between the POL compass and the sun compass direction. Evaluation of the 2 and 4 m data yielded the same results and conclusions. Since two homing directions are expected for a single e-vector orientation due to the symmetry of the POL pattern, I referred each of our data sets always to the more likely expected POL direction; i.e., the one with the smaller angular distance to the recorded homing direction. I subsequently subjected the data to a linear regression analysis and performed a one-way ANCOVA as well as adequate post hoc tests using the PAST software package (version 2.17, http://folk.uio.no/ohammer/past; Hammer et al. (2001)).

4.4. Results

4.4.1. Interactions of sun and polarization compasses in the first cue conflict paradigm

During training, the ants had direct view of the sun while at the same time experiencing an overhead stripe with a single e-vector orientation. If an ant relies exclusively on the POL cue it would navigate in a direction relative to the sun azimuth in which it expects

the experienced POL information in the sky (Wehner, 1997). For example, trained with an e-vector orientation orthogonal to the walking direction, the ant determines its homing direction relative to the solar meridian, i.e., either towards the sun or in the opposite direction (see Chapter 3). Alternatively, as the ant could also see the sun during the training, it could determine its walking direction on the basis of the sun's position during the outbound run. Relying on the sun compass information only, the ant would be able to head for the correct nest direction irrespective of the time of the day. Since in my experiments the animals were tested immediately after training, they did not have to compensate for the movement of the sun – although they are able to do so (Wehner and Müller, 1993).

The experimental paradigm now challenged the ant's navigational system with a conflict situation where the two homing directions, according to POL and sun compasses, pointed in different directions and deviated from each other to varying degrees, depending on the time of the day (see Fig. 4.1). In Figure 4.3 A and B, the heading directions of the ants tested at different times of the day are plotted according to the earth coordinates (0° corresponds to North). The shift of the solar azimuth during the day is shown as a solid curve, whereas the dashed line represents the "antisun" azimuth. The expected heading directions according to the POL compass based on the orthogonal e-vector orientation experienced during training correspond to the solar or antisolar direction and, therefore, should align on the red solid or the stippled curve. The horizontal straight lines (at 90° in Fig. 4.3 A, and at 180° in Fig. 4.3 B) depict the "correct" nest direction, i.e., the expected direction derived from the sun compass. As evident in both graphs (Fig. 4.3 A, B), after training with contradictory sun and POL compass information the ants did not adhere to the expected homing directions according to either cue. Rather, most ants headed in a compromise direction between the two "pure" compass directions. Remarkably, in Figure 4.3 A, the preferred direction according to the POL information changed around noon, from solar to antisolar (solar noon was around 12:22 h during the entire test period). This change was not evident with the other training direction (Fig. 4.3 B). The results of Chapter 3 have shown that the artificial POL pattern, a single e-vector orientation imposed by a POL filter, allows a solid prediction of and does not affect the accuracy of the homing direction. Thus, the impact of the sun compass on the experiments described here can be quantified by how far the ants' heading direction deviate from the POL direction that the ants select when relying exclusively on the experienced e-vector orientation. Hence, to quantify this "intermediate" homing direction, I plotted an ant's heading direction against the angular distance between the POL compass and the sun compass direction (Fig. 4.3 C). The slope of the linear regression function in Figure 4.3 C yields an estimate of the relative weights of both compass cues. The deviations of the ants' heading directions relative to the predicted POL compass direction increased linearly with increased angular distance between the POL compass and the sun compass directions (the latter represented by the diagonal). The distribution of the ants' heading directions can be described by the linear regression function $y = 0.4x - 2.24$ ($R^2 = 0.60$, $N = 121$). The slope represents the mean deviation from the POL compass direction (for the two channel orientations separately, nest in 90°: $y = 0.37x + 0.85$; $R^2 = 0.62$, $N = 89$; Fig. 4.3 A, and nest in 180°: $y = 0.44x - 10.95$; $R^2 = 0.60$, $N = 32$; Fig. 4.3 B, respectively; the slopes do not deviate significantly from each other; one-way ANCOVA: $p = 0.31$).

The experiments were repeated using two additional e-vector orientations relative to the walking direction. In all situations, the ants behaved similarly and chose homing directions lying approximately half way between the expected sun and POL compass direction (Fig. 4.3 D, E, G, H). For the parallel e-vector orientation (Fig. 4.3 D-F), a linear regression was

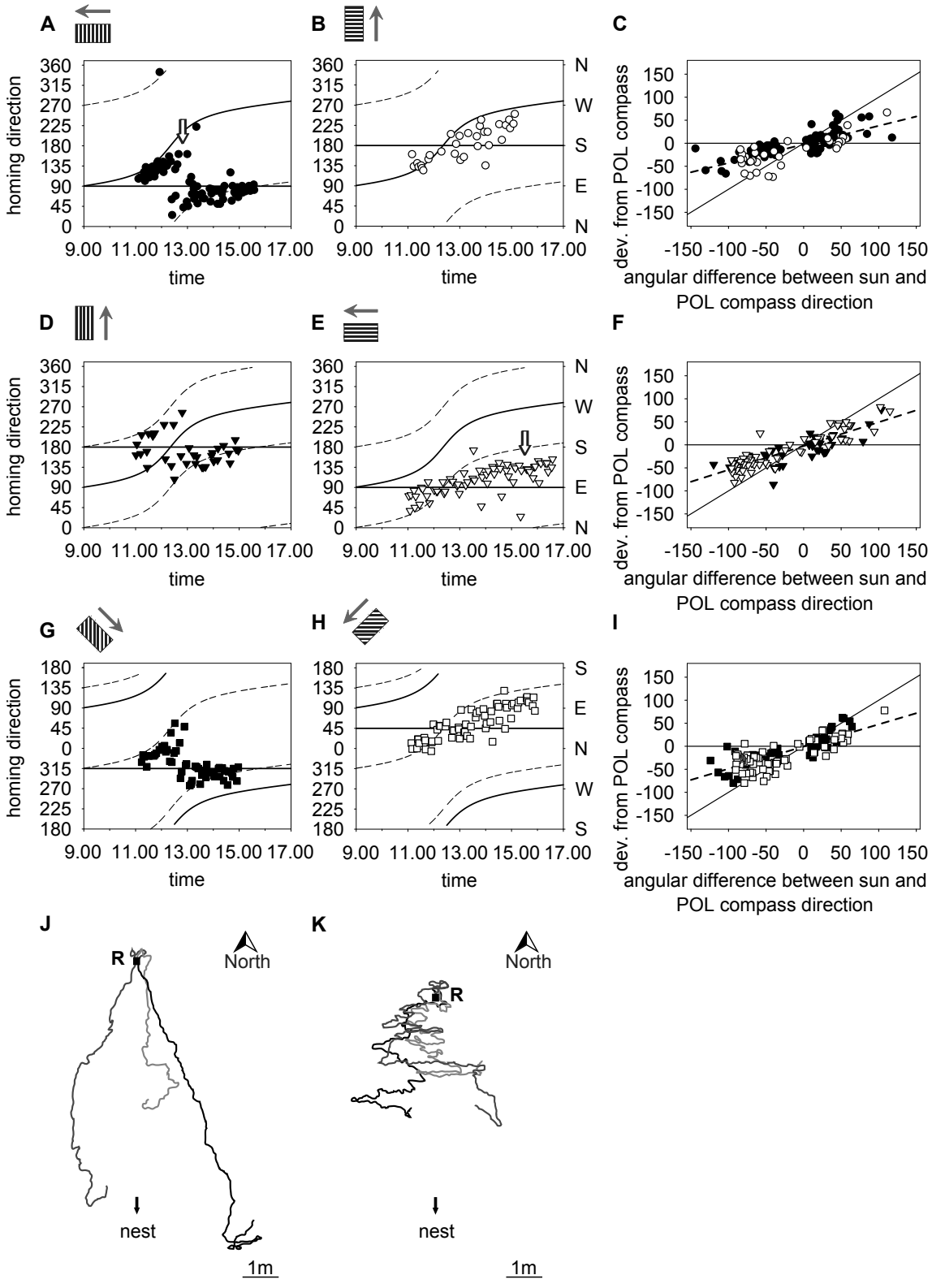
A
B
C
D
E
F
G
H
I
J
K
homing direction
360
315
270
225
180
135
90
45
0
9.00 11.00 13.00 15.00 17.00
time
N
W
S
E
N
dev. from POL compass
150
100
50
0
-50
-100
-150
-150 -100 -50 0 50 100 150
angular difference between sun and
POL compass direction
S
E
N
W
S
R
North
nest
1m

Fig. 4.3.: Homing directions of individually tested ants after training with a single e-vector orientation and direct view of the sun. The *symbols* in the diagrams of the left and middle columns depict the recorded homing path of single ants at 3 m distance from the release point at different times of the day; each symbol represents the heading direction of an individual. The *straight lines* represent the actual nest direction; the *solid curves* represent the solar azimuth and the *dashed curves* the POL compass-based homing direction. The diagrams are scaled according to the earth coordinates (0° = North). Small insets depict the training directions (cf. *grey arrow* in Fig. 4.1 A) and the respective POL filter orientation. In the right column, the data are plotted relative to the POL compass direction (*ordinate*) and the angular distance between the POL and sun compass direction (*horizontal line*). The *horizontal line* represents the POL compass direction and the *diagonal line* the sun compass direction. In each diagram, a linear regression (*stippled line*) describes the distributions of the data (**C**, **F**, **I**). **A**, **B** Linear regression analysis for each channel orientation of the orthogonal e-vector situation separately: A) nest in 90°: $y = 0.37x + 0.85; R^2 = 0.62, N = 89$ and B) nest in 180°: $y = 0.44x - 10.95; R^2 = 0.60$, $N = 32$, respectively; the slopes do not deviate significantly from each other; one-way ANCOVA: $p = 0.31$. **D**, **E** The two training situations with parallel e-vector orientation separately: D) nest in 180°: $y = 0.5x - 7.6$; $R^2 = 0.6$, $N = 35$ and E) nest in 90°: $y = 0.55x + 1.34$; $R^2 = 0.82$, $N = 64$ (one-way ANCOVA for slope homogeneity: $p = 0.46$). **G**, **H** The training situations with the oblique POL filter lead to linear regression functions: G) nest in 315°: $y = 0.5x + 3.08$; $R^2 = 0.7$, $N = 55$ and H) nest in 45°: $y = 0.43x - 6.27$; $R^2 = 0.56$, $N = 64$ (slopes do not deviate significantly, one-way ANCOVA: $p = 0.34$). *White arrows* in A and E point to intermediate homing directions of individual ants. **J** Three examples of typical homing courses on the open test field. **K** Sample of three zigzag homing paths after training with parallel e-vector orientation and a nest direction of 180° (R = release point). Taken from Lebhardt and Ronacher (2014a).

calculated as $y = 0.52x - 2.62$ with a correlation coefficient of $R^2 = 0.75$ ($N = 99$). The training situations with the oblique e-vector pattern (Fig. 4.3 G-I) yielded the linear regression function $y = 0.48x - 1.26$ and a correlation coefficient of $R^2 = 0.64$ ($N = 119$). In all cue conflict situations presented here, the heading directions scattered around a direction lying roughly half way between the two "pure" compass directions with a slope of approximately 0.5. The slopes of the six different training situations are not significantly different (after Bonferroni adjustment). The only significant difference ($p < 0.003$) found was between the slopes of the training situations with an orthogonal e-vector pattern and the nest in 90° (Fig. 4.3 A) and a parallel e-vector orientation and the nest in 90° (Fig. 4.3 E).

In Figure 4.4 A all data of the experiment with POL filter and direct view of the sun are combined (linear regression: $y = 0.47x - 2.09$, $R^2 = 0.66$, $N = 339$). This slope is highly significantly different from both slopes of 0 or 1, respectively (F test: $p < 0.0001$). For comparison, Figure 4.4 B depicts the homing directions after training under a POL filter but without direct view of the sun (see Chapter 3). In this experiment, the recorded heading directions normalized to the POL compass direction scattered around the horizontal line, i.e., the heading directions showed only a small deviation from the slope of 0 expected according to the POL compass ($y = 0.05x - 6.05$; $R^2 = 0.05$, $N = 162$) and were largely independent of the angular distance between the two compass directions.

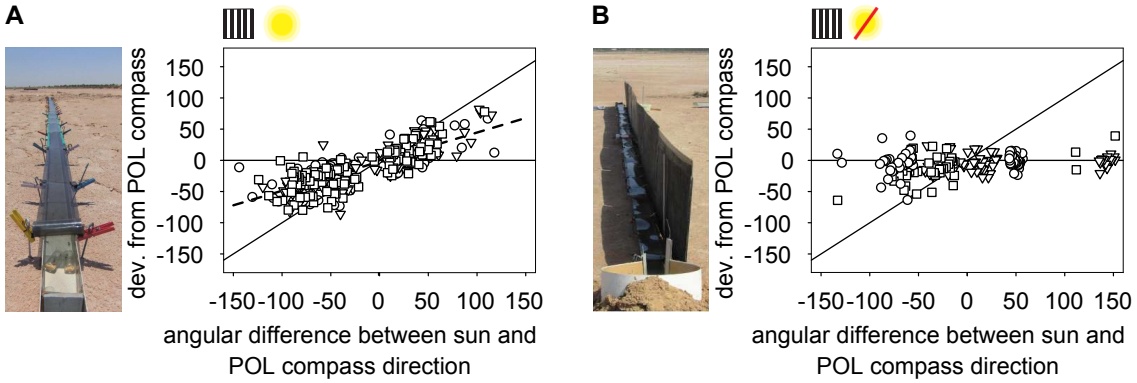

Fig. 4.4.: Comparison of heading directions relative to the POL compass direction in the cue conflict experiments (**A**), where the POL and the sun compass compete with each other and (**B**) control experiments without direct view of the sun (see Chapter 3, Fig. 3.2). For further description see Fig. 4.3. Reprinted from Lebhardt and Ronacher (2014a).

4.4.2. Manipulating the reliability of compass cues in the second cue conflict paradigm

A second approach aimed at making one of the compass cues less reliable. In the first version of this second cue conflict paradigm, I trained ants with a uniform e-vector pattern along the entire training distance while they were actually forced to change direction by 90° (inset on the left of Fig. 4.5 A). Thus, the ants experienced a constant POL direction, but the sun compass indicated a sudden change in the walking direction inconsistent with the POL cue. An ant experienced first a good agreement between the two compasses, which then changed to an inconsistency, or vice versa. The recorded homing directions show a very similar behavior of homing ants as observed in the same situation within a straight channel (compare Figs. 4.3 A and 4.5 A). The statistical analysis revealed no difference between the two experimental situations (Fig. 4.5 B: $y = 0.42x - 1.06$; $R^2 = 0.73$, $N = 45$ compared to $y = 0.4x - 2.24$; $R^2 = 0.6$ in the straight channel; one-way ANCOVA: $p = 0.684$). The reciprocal experiment with a change of the e-vector pattern in a straight channel system (90° turn of the e-vector orientation after half of the training distance; see sketch on the left of Fig. 4.5 C) is more difficult to interpret. Homing directions based on a uniform e-vector pattern are ambiguous due to the symmetry of the sky's polarization pattern. Therefore, the 90° turn of the POL filter orientation along the channel leads to a quadrimodal distribution of potential homing directions (for details of the argument see Chapter 3). Because of these four resulting POL compass directions very large conflicts between the POL compass and the sun compass direction cannot be achieved, the maximum theoretical angular distance is 45°. The results can again be described by a linear regression, $y = 0.51x - 3.08$ ($R^2 = 0.56$, $N = 53$; Fig. 4.5 D). A comparison of the slopes between this combined e-vector pattern with either uniform orthogonal or uniform parallel e-vector patterns revealed no significant difference ($p = 0.045$, one-way ANCOVA, with Dunnett's multiple comparisons test: $p = 0.133$ and $p = 0.998$, respectively). Taken together, the results confirm the outcome of the experiments described in Figure 4.3, indicating an equal contribution of the two compass systems, even if one of the two compasses was evidently unreliable, exhibiting a sudden change along a linear training excursion. Wystrach et al. (2013) report a backtracking behavior in ants: zero vector ants, i.e., ants without any path

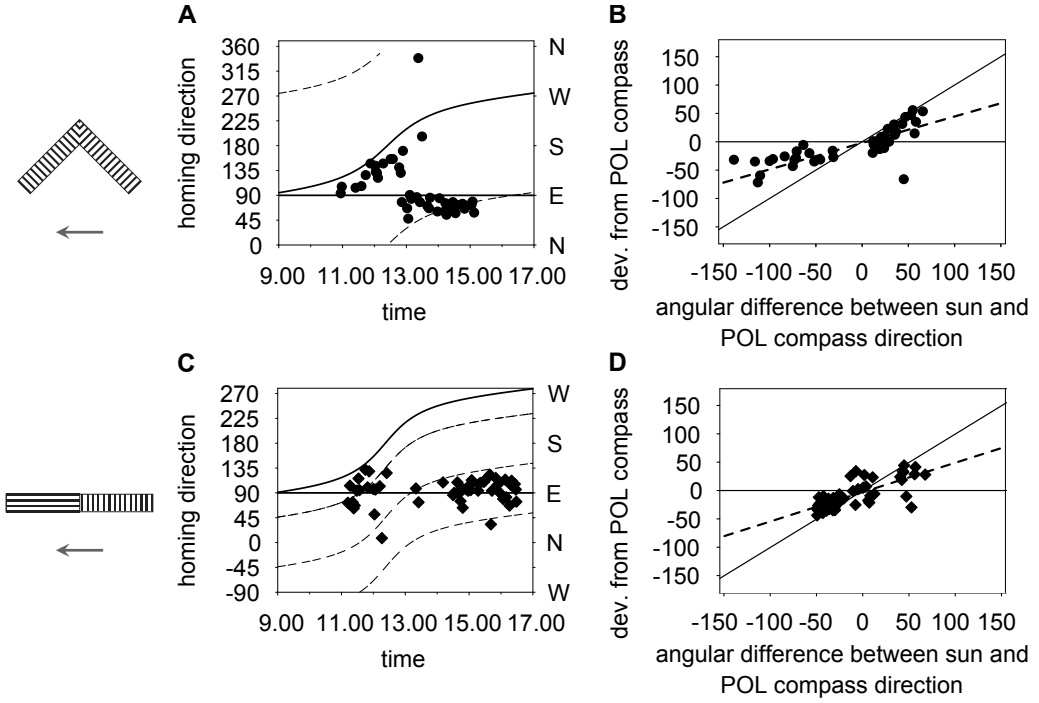

Fig. 4.5.: Ants' heading directions in cue conflict experiments with a directional change in either compass cue. The training situation is depicted in the sketches on the left (POL filter and *grey arrow* indicating the training direction). **A** Outcome of the experiment in a channel with a 90° bend and a constant e-vector pattern relative to the walking direction; **B** dependence of the heading directions ($N = 45$) normalized to the expected POL compass direction relative to the angular distance between sun and POL compass direction (as in Fig. 4 C). **C**, **D** Results of the experiment with a 90° turn of the POL filter along a straight channel. The data ($N = 53$) are plotted with respect to the most likely of all four POL compass directions, i.e., the POL direction with the shortest angular distance to the data which not necessarily is the one with the shortest angular distance to the sun compass direction. Therefore, some heading directions are plotted against an angular distance between the sun and the POL compass direction larger than 45° (for further details, see Fig. 4.3). Adapted from Lebhardt and Ronacher (2014a).

integration vector information that have been displaced, chose a direction opposite to the path segment that they had most recently traveled. However, in the experiment shown in Figure 4.5 C, there was no indication that the more recent compass direction had a stronger influence on the homing direction.

4.5. Discussion

The azimuthal position of the sun and the sky's pattern of polarized light provide the most prominent compass information in insects' path integration. In nature, these directional cues are physically tightly associated. In the experiments reported here, ants were confronted with contradictory compass information, i.e., a single e-vector pattern disconnected from the actual position of the sun. In this artificial situation, the ants determined their homeward direction as an intermediate course, instead of relying exclusively on either the sun or the POL cue (Figs. 4.3-4.4). The results of this cue conflict experiment indicated a roughly equal contribution of sun and POL compass in the computation of the home vector. Thus, the previously suggested dominance of the POL compass over the sun compass (Duelli and Wehner, 1973; Wehner and Müller, 2006) was not observed in the present experimental paradigm. The strong influence of the sun compass in the cue conflict experiments presented here becomes evident when we compare Figure 4.4 A and B. This kind of interaction between sun and POL compass in desert ants' path integration was retained even if one of the compass cues presented was obviously less reliable, by indicating a sudden change in direction, relative to the other (Fig. 4.5). There is, however, one important difference to the experimental set-up used by Wehner and Müller (2006). In their training situation, the ants could see a broad stripe of the celestial POL pattern, that is, an extended field combining many different e-vector directions. In contrast, in the present experiments, the ants saw a stripe with only a single e-vector orientation. This latter situation may have weakened the POL channel input and thereby strengthened the relative input of the sun compass to the path integration module. Interestingly, in bees and myrmicine ants, the sun appears to have a larger impact as compared to the POL pattern than in formicine ants like *Cataglyphis* (Duelli and Wehner (1973); see p 445 in Frisch (1965)). According to the symmetry and the resulting 180° ambiguity of POL information (Wehner, 1994), in principle, the ants could choose between two possible POL compass directions, e.g. solar meridian or antisolar meridian in case of training with the orthogonal e-vector. When combined with the sun compass direction in the cue conflict situation, this leads to four potential intermediate homing directions. But actually almost all of the tested ants exhibited a strong preference for homing courses calculated on the basis of the sun compass, indicating the actual nest direction, and the expected POL compass direction with the shortest angular distance (Fig. 4.3). Quite clearly, the ambiguity of the uniform e-vector pattern was reduced by the additional information from the sun's position, and possibly also the spectral composition of light in different parts of the sky.

The data were well described by linear regressions, and the slopes ranging from 0.37 to 0.55 indicate similar weights of sun and POL compass. There was only one significant difference between slopes in the experiments with uniform orthogonal and parallel e-vectors orientation (Fig. 4.3 A, E) which indicated a slight dominance of the POL compass when presented as an orthogonal e-vector pattern. This can be explained tentatively by the relative presence of orthogonal and parallel e-vectors in the entire POL pattern of the natural sky. Hence, a larger proportion of orthogonal e-vectors in the sky might have influenced the weighting in

favor of the POL compass, leading to a decreased slope. Note that the reported intermediate homing direction represents the homing courses of individual ants (highlighted by arrows in Fig. 4.3 A, E) and is not the result of calculating averages over individuals which might have adhered to either one or the other of both compass cues. Thus individual ants computed the homing directions as an average of the directions resulting from the POL compass and the sun compass. The homing paths were mainly performed as unitary, straight walks suggesting a direct comparison of the information provided by both compass systems. However, when ants were confronted with a large conflict at noon, when the sun is at high elevation and the sky's POL pattern is less reliable, some ants trained with a parallel e-vector orientation and the nest direction in 180° walked in zigzags towards the fictive nest position in the open test field (Fig. 4.3 K). In all other training situations or daytimes, this kind of behavior was very rarely observed, i.e., the ants behaved naturally and completed their homebound runs in rather straight paths (Fig. 4.3 J). A comparable zigzagging trajectory was observed and reported previously by Fent, in this case with an artificial parallel e-vector presented during homing (Fent, 1986).

The direct sunlight and the polarized scattered sunlight are detected by different parts of the eye and are most likely processed separately in further stages (Wehner and Müller, 2006). The present results indicate a direct interaction of sun and POL compass information. Hence, the hypothesis put forward by Wehner and Müller (2006) that in desert ant's path integration a combined value of sun and POL compass information might be determined which then can be recalled by either system is supported (this issue will be investigated in the next chapter). However, there exist several putative stages along the projection onto the central complex at which information from both compasses can be compared and consolidated. For instance, Pfeiffer et al. described neurons of the anterior optical tubercle of the locust brain (TuTu1) which responded to both specific e-vector orientations and light spots of different wavelength at particular azimuth positions (Pfeiffer et al., 2005; Pfeiffer and Homberg, 2007).

There are several recent reports indicating integration of different celestial and terrestrial directional cues which can lead to compromise directions in case of conflicting cues (e.g. Müller and Wehner (2007); Reid et al. (2011); Narendra et al. (2013); Kemfort and Towne (2013)). However, there are also counter examples indicating a strict hierarchy: in a conflict situation between celestial and idiothetic cues, the latter were completely ignored (Chapter 3). Another example is the dominance of the POL compass over the wind compass (Müller and Wehner, 2007).

In general, an intermediate direction calculated from two conflicting compass cues, would appear to be adaptive as it prevents individuals from choosing the wrong direction (see Cheng et al. (2007)). In case of a conflict between two approximately equally important directional cues, such as the sun and the POL pattern, however, the ant cannot decide which one is the more reliable. Thus, facing uncertainty, the ant will more likely find the actual nest position if it takes into account both reference directions with similar weights. However, the experimentally created situation here, a POL pattern extracted from the sun providing inconsistent directional information is extremely unlikely to occur in nature. It could tentatively be caused by a huge tree covering large parts of the sky, even though such kind of shielding structures rarely exist in the *C. fortis* habitat.

Apart from the two main celestial cues considered here, there are additional cues providing directional information, wind direction, spectral composition of skylight, light intensity distribution, landmark panoramas, and possibly even magnetic cues (Wehner, 1997; Müller and Wehner, 2007; Buehlmann et al., 2012; Narendra et al., 2013), which implies that the

animal could in principle be challenged by a diversity of conflicting directional information. Probably a mean direction is calculated when two cues are equally reliable.

5. Transfer of directional information between the polarization compass and the sun compass in desert ants

In the previous chapter we learned that desert ants compute their home vector by evaluating and weighting different compass cues; this requires a common input/output stage. If such a structure exists in the ant's brain that receives input from different cues, the question arises if it is also possible to recall such information by different compass systems. In this chapter, I address this question by performing experiments that selectively test the interaction between the sun and the polarization compass systems.

5.1. Summary

[1] Ants use several cues to determine their walking direction, two of the most important ones being the sun's azimuthal position and the polarization pattern of the sky. I tested whether an information transfer is possible from one compass system to the other, noting that both systems depend on different anatomical substrates. Since the sky's polarization pattern is detected by UV-photoreceptors located in the dorsal rim area (DRA), I used an orange Perspex filter that eliminated the UV part of the spectrum to prevent the use of the polarization compass. The use of the sun compass could be excluded by appropriate screens. Ants had learned a nest-feeder direction with the sun compass only and were later tested with the polarization compass, and vice versa. The results show that a transfer is possible in both directions.

5.2. Introduction

Desert ants of the genus *Cataglyphis* are champions of path integration (Müller and Wehner, 1988; Wehner and Srinivasan, 2003; Ronacher, 2008). This kind of navigation implies a vector computation of the distances traveled in certain directions, i.e., an integration of directional information and of the corresponding actual distance information. The necessary directional information can be derived from various celestial and terrestrial cues: the sky's polarization (=POL) pattern, the sun's azimuth, the spectral composition an intensity distribution of skylight (Wehner and Rossel, 1985; Fent, 1986; Wehner, 1994; 1997; Wehner and Labhart, 2006), wind (Wehner and Duelli (1971); see also Wolf and Wehner (2000); Müller and Wehner (2007)), and panoramic scenes including landmarks (Collett et al., 2001; Wehner, 2003; Graham and Cheng, 2009; Wystrach et al., 2011; Baddeley et al., 2012; Collett et al.,

[1] The results described in this chapter have been published in "Transfer of directional information between the polarization compass and the sun compass in desert ants", Lebhardt & Ronacher 2014b in J. Comp. Physiol. A (Contributions: Fleur Lebhardt: idea, performance of experiments, data analyses and presentation, manuscript writing; Bernhard Ronacher: manuscript writing, discussion)

2013). Under certain conditions wind or the panorama can influence path directions when experimentally disconnected from the celestial cues (Müller and Wehner, 2007; Graham and Cheng, 2009). However, the two celestial compass systems – POL and sun compasses – are the most relevant ones to infer the direction of a path segment (Wehner and Duelli (1971); Ronacher et al. (2006); Müller and Wehner (2007); Heß et al. (2009); see also Chapter 3). Therefore, in this chapter I will focus on these.

The sky's polarization pattern is detected by specialized ommatidia located in the dorsal rim area (DRA) and also by the ocelli (Wehner, 1982; Fent and Wehner, 1985). The ommatidia of the DRA house only a single photoreceptor type, which in *Cataglyphis* is sensitive in the UV part of the spectrum (Duelli and Wehner, 1973; Wehner, 1989; 1994; Labhart, 2000; Wehner and Labhart, 2006). Under most conditions, the sun's position is perceived by different parts of the eye. Thus, in the periphery both compass systems rely on different anatomical substrates (Wehner, 1997). Under natural conditions, the POL pattern is tightly linked to the sun's position (Wehner, 1997). In experiments that precluded the use of one of the two celestial compass systems, *Cataglyphis* ants nevertheless showed well-oriented homebound paths (Duelli and Wehner (1973); Wehner and Müller (2006); see also Chapter 3). Thus, sun and POL compasses, while acting together under natural conditions, may each be sufficient for navigation in the absence of the other cue. If ants are deprived from using both sun and POL compass cues they may still infer their homing direction, though less accurately, from the sky's spectral gradient (Wehner, 1997).

Remarkably, interocular transfer is possible for the celestial compass cues: ants trained to a feeder bearing a monocular eye cap found their way home when the eye cap was transferred to the other eye (Wehner and Müller, 1985). It is, however, still unknown if a transfer is possible from one compass system to the other: if a compass direction was learned exclusively with the POL compass, can the ant recall this direction on the basis of its sun compass alone – or vice versa? In a comprehensive account on the ant's polarization and spectral compass systems, Wehner (1997) tackled this question and based on preliminary data concluded that such an inter-compass transfer is possible. However, as this hypothesis was based on a rather small sample size, I present here an extensive study, in which I apply a new approach using a linear POL filter that allows to manipulate the POL compass cues independent of the sun's position (Chapter 3). To exclude the POL cues I used orange-colored Perspex that did not allow UV light to pass through, thus silencing the POL compass (Wehner, 1982; 1994). The data provide clear evidence that directional information obtained via the POL compass can be recalled by the sun compass, and vice versa.

5.3. Materials and methods

5.3.1. Training and test procedure

While running between the nest and the feeder, the ants were deprived from using either the POL compass or the sun compass (except for a distance of approx. 15 cm between the nest exit and the channel entrance). Individual ants were then captured at the feeder and released on a distant test field to perform their homebound run under a trolley that excluded the compass system that was available during training. The trolley was constructed following Duelli and Wehner (1973) and Fent (1986). It had a circular opening that allowed a view of the sky in an approx. 130° window (Fig. 2a in Fent 1986; see also photographs in Fig. 5.1). The opening was covered either with orange Perspex (to exclude the use of the POL

compass) or with UV-transparent Perspex that allowed a view of the celestial POL pattern (see Chapter 2); the direct view of the sun could be prevented by a movable circular screen (diameter 28-33°). Around the trolley a dark curtain was fixed that shielded the ant from wind (for further details see Wehner (1982); Fent (1986); Wehner (1994)). The trolley was moved by an assistant so that the ant was always in the center of the circular opening.

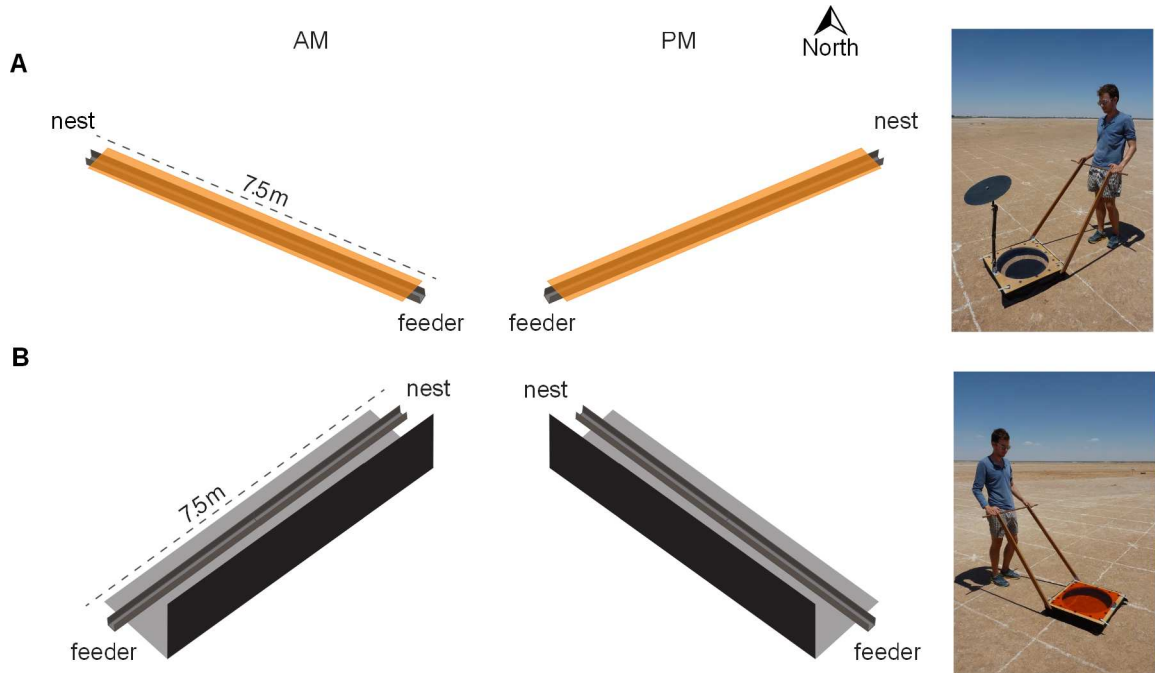

Fig. 5.1.: Scheme of the training channels. **A** Experimental Paradigm I (training without POL information). Channels were aligned differently in the morning (AM) and afternoon (PM) experiments to allow a view of the sun, such that nest directions were at 300° and 60°, respectively. **B** In the Paradigms II and III a linear POL filter reduced the available POL information to a single e-vector direction. The nest directions were at 45° and 315°, respectively, and direct view of the sun was prevented by a 50 cm high screen located alongside the channels. The photographs on the left show the experimental trolley used in the respective tests, for sun-only (top) and SKY POL test (bottom). Modified after Lebhardt and Ronacher (2014b).

5.3.2. Paradigm I: Training with sun compass information while excluding the POL compass cue

The POL compass can be knocked out by removing wavelengths below 410 nm (Duelli and Wehner, 1973). I trained ants under an orange Perspex sheet attached above the training channel that filtered all wavelengths below 530 nm. This filter also prevents the perception of spectral gradients, since only the long-wavelength photoreceptor is still functional. During the training, a nest-to-feeder orientation of the channel of 120° in the morning (AM) and of 240° in the afternoon (PM) was chosen to ensure that the ants had a direct view of the sun when shuttling in the training channel (Fig. 5.1 A, 0° corresponds to north). In the critical test, the ants performed their homebound run under the experimental trolley that was equipped with a UV light-transmitting Perspex allowing view of the sky's natural polarization pattern.

Tab. 5.1.: Details of the experimental paradigms. Reprinted from Lebhardt and Ronacher (2014b).

Paradigm	Training in Channel	Test		[Under trolley]	Figure
I	SUN	SKY POL	Transfer	[Y]	5.2 A
	SUN	SKY POL+SUN	Control	[No]	5.2 B
	SUN	SUN	Control	[Y]	5.2 C
II	POL(orthogonal)	SUN	Transfer	[Y]	5.3 A
	POL(orthogonal)	SKY POL	Control	[Y]	5.3 B
III	POL(parallel)	SUN	Transfer	[Y]	5.4 A
	POL(parallel)	SKY POL	Control	[Y]	5.4 B

5.3.3. Paradigm II and III: Excluding the sun compass cue while providing POL compass information during training

During training the direct view of the sun was prevented by thin wooden plates (50 cm height) erected along one side of the training channel. The best shadows were obtained when the channel was oriented perpendicular to the sun's position, i.e., towards 225° (AM) and 135° (PM) (Fig. 5.1 B). I further manipulated the polarization pattern visible to the ant by covering the training channels with a polarization filter that is transparent in the visible and the UV part of the spectrum. This filter provided uniform POL information along the entire training distance, consisting of a 60° broad overhead stripe with a single e-vector orientation (here either orthogonal or parallel to the ant's walking direction). Such POL compass information allows a good prediction of the respective homing directions when ants are later tested under open sky conditions (see Chapter 3). In the critical test the return run was performed under the trolley equipped with orange Perspex and with the sun visible to the ants. For the controls, the trolley was covered with UV-transparent Perspex allowing view of the sky's natural polarization pattern while the direct sunlight was blocked by the movable screen (see Table 5.1).

5.3.4. Data evaluation and statistical analysis

Trajectories of the homing ants were documented and the homing directions at 2, 3, and 4 m from the release point were determined. The data were then plotted either relative to the actual nest direction in case of the sun compass training or relative to the solar azimuth after training under the POL filter. The results are illustrated in circular diagrams and circular statistics were applied. The Rayleigh test was used to test against a random circular distribution and the one-sample t-test was used to determine whether the expected homing direction (either sun azimuth or nest direction) belonged to a confidence interval. I applied the Mardia-Watson-Wheeler test to test for differences between two distributions and used the Wilcoxon-Mann-Whitney test to compare the deviation from their respective means of two independent samples (see Batschelet (1981); Zar (1999)).

5.4. Results

5.4.1. Recall with the POL compass after sun compass training?

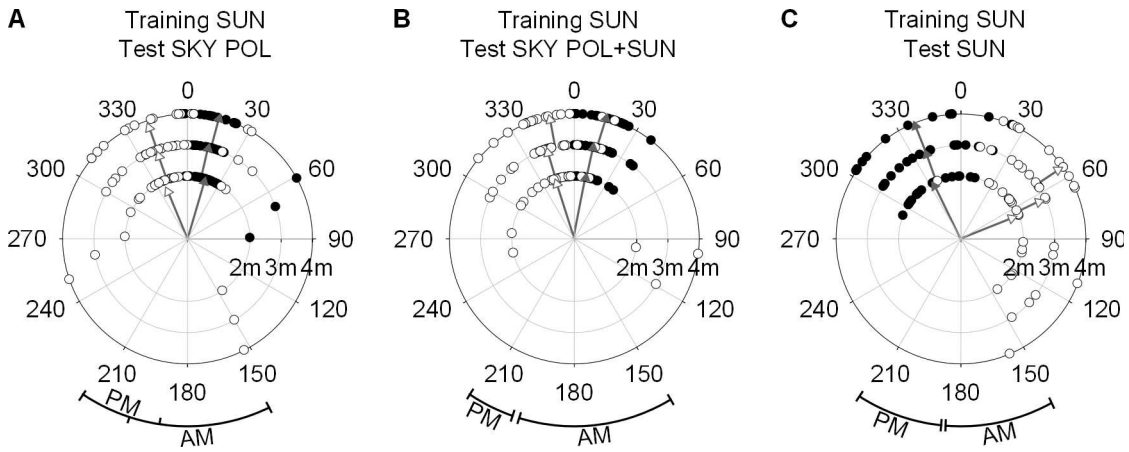

Fig. 5.2.: Results of Paradigm I: training with the sun as the only sky compass cue. **A** Critical test with POL only. **B** Control with sun and POL visible (without trolley), **C** control with only sun visible. 0° indicates nest direction; *open and closed symbols* correspond to AM and PM tests, respectively. *Arrows* indicate lengths of the mean vectors (r between 0.75 and 0.97 in A; $0.84 - 0.94$ in B; $0.78 - 0.92$ in C; all vectors indicate highly significant orientation, $p << 0.0001$ (Rayleigh test)). *Arcs below the diagram* indicate the ranges of the sun's azimuth during AM and PM tests. Samples of individual trajectories in the different test situations can be found in the Appendix A. Adapted from Lebhardt and Ronacher (2014b).

In the training Paradigm I (see Table 5.1), ants were trained to visit a feeder in a channel covered with orange Perspex that eliminated POL cues. To allow view of the sun, the feeder was located at 120° in the morning (viewed from the nest) and at 240° in the afternoon, yielding homing directions of 300° and 60°, respectively (Fig. 5.1 A). In the critical experiment, the ants were tested under a trolley that blocked a direct view of the sun but allowed UV light to pass through so that a large part of the sky's POL pattern was available for the POL compass. The homing paths were on average oriented towards the nest (0° in Fig. 5.2 A). There were significant deviations between the mean vectors in the morning and afternoon sessions (Mardia-Watson-Wheeler test: $p < 0.001$ for all distances; in the morning session, the 99% confidence intervals include 0° for 3 and 4 m, while in the afternoon the confidence intervals do not include the nest direction at all distances; N = 23 and 22 ants tested, respectively). However, the very same small deviations also occurred in a control experiment in which ants were again trained exclusively with the sun compass but then tested without the trolley, that is, with a full view of the sky (POL and sun compass cues (Fig. 5.2 B); N = 26 (AM) and 25 (PM)). The Mardia-Watson-Wheeler test indicates a good agreement between the mean vector directions in Figure 5.2 A, B (differences not significant: $p = 0.143 - 0.260$ for the AM tests at 2-4 m distance, and $0.098 - 0.90$ for the PM tests).

An additional control was performed: as before the ants were trained with only the sun compass, but in this case the return path was also performed with only sun compass cues available (under the trolley with orange Perspex; see Table 5.1). In this control the ants showed substantial deviations from the expected nest direction, in particular during the

AM tests (Fig. 5.2 C). However, the homing paths were clearly non-random (Rayleigh test: all $p << 0.001$, N = 17 (AM) and 19 (PM)), and the ants seemed to head in the direction of the nest rather than towards the sun's azimuth. The deviations from the nest direction in this control can be explained qualitatively by previous observations that the orange Perspex filter not only abolishes the POL cues but also color vision since only the long wavelength ("green") receptors are left functional. In this condition, the ants exhibited a strong phototactic response towards the brightest part of the sky even if the sun itself was occluded (Lanfranconi, 1982; Wehner, 1997). This positive phototaxis caused substantial deviations from the trained compass direction (up to 38°; pp. 165-169 in Wehner (1997)). In the control experiment (Fig. 5.2 C) the sun was mostly located at the northern side of the training channel during the morning (cf. Fig. 5.1); i.e., an ant returning to the nest experienced the brightest part of the sky on its right side. Correspondingly, during the test under the trolley the phototactic response would induce a deviation to the north, i.e., to the right side in Figure 5.2 C. During the afternoon tests the northern side of the channel was again brighter; hence a returning ant experienced a phototactic drive to its left side that competed with the compass response. This effect is also visible in Figure 5.2 C (filled symbols). In contrast, in the tests presented in Figure 5.2 A and B, the returning ants could rely on the celestial POL pattern and in this situation the phototactic response plays no role (Wehner, 1997).

When interpreting the heading directions depicted in Figure 5.2 A and B, a caveat has to be mentioned. An essential condition for this experiment was that the ants could see the sun while walking in the narrow training channel. Thus, the channel had to be aligned in a way that the ants walked towards a feeder which was located more or less in the sun's direction; conversely, the nest direction coincided roughly with the antisun meridian. For this reason, I cannot separate the nest direction from the antisun azimuth, and indeed if I normalize the data to the antisun azimuth this yields almost the same accuracy as normalization to the nest direction (lengths of mean vectors 0.771, 0.759, and 0.721 (antisun) versus 0.816, 0.789, and 0.754 (nest) in the morning session of Paradigm I Figure 5.2 A; and 0.789, 0.831, 0.864 versus 0.842, 0.875, 0.886 for Figure 5.2 B; for the afternoon the results of both normalizations yielded indistinguishable mean vector lengths). Nonetheless, based on evidence that ants exhibit strong phototaxis in some situations (Duelli and Wehner, 1973; Wehner and Müller, 1985; Wehner, 1997), it can be considered rather unlikely that in the training Paradigm I the ants had acquired a vector directed 180° away from the sun. On the contrary, in view of the phototaxis effects described above, the opposite effect (i.e., a bias towards the sun's azimuth) would be expected. Such a bias is clearly absent in Figure 5.2 A and B. In any case, the well-focused homing paths after a sun-only training and a SKY POL test (Fig. 5.2 A) show that the information derived during the training from the sun's azimuth was transferred and enabled a recall of the trained direction based on the POL compass. Thus, the results of Figure 5.2 A provide the crucial proof for a transfer from sun compass to POL compass.

5.4.2. Recall with the sun compass after training with the POL compass?

The reciprocal experiment differs from the first in that the training with a single e-vector direction does not allow an ant to pinpoint the nest direction. Instead, the expected homing direction shifts during the day along the sun's azimuth (Chapter 3). Hence, in these experiments I normalized the homing directions with respect to the sun's azimuth (0° in Figs. 5.3 and 5.4). If during training the ant experienced an orthogonal e-vector (Paradigm II), i.e.,

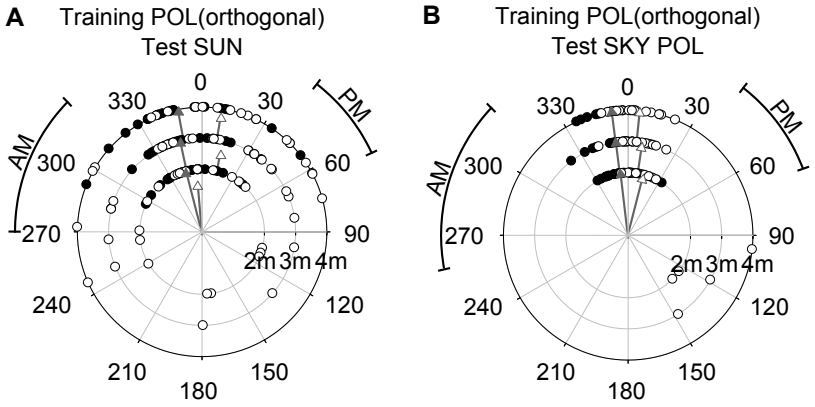

Fig. 5.3.: Results of Paradigm II: training with an orthogonal e-vector. **A** Critical test with the sun only, **B** control with the celestial POL pattern visible and shielded sun, i.e., compass condition similar to training. 0° indicates the sun azimuth; *open* and *closed symbols* correspond to AM and PM tests, respectively. The *arcs beside the diagrams* indicate the nest positions relative to the sun's azimuth; other conventions as in Fig. 5.2. Lengths of mean vectors $r = 0.457 - 0.680$ (AM) and $r = 0.905 - 0.928$ (PM) in A; $r = 0.83 - 0.98$ in B all values highly significant (Rayleigh test: $p = 0.004$ to $p < 0.0001$ for the AM data and all $p << 0.0001$ for the PM data in (A), all $p << 0.0001$ in (B)). Reprinted from Lebhardt and Ronacher (2014b).

perpendicular to its walking direction, this corresponds to a direction in the solar or antisolar meridian (Fent, 1986; see also Chapter 3). The results of the critical test are summarized in Figure 5.3 A. The ants were trained with the orthogonal POL filter without view of the sun (see Fig. 5.1 B; Table 5.1). On the test field they performed their homebound walk under the trolley equipped with orange Perspex, thus preventing the use of the POL compass. Although the scatter is relatively large, the ants showed a significant orientation towards the sun's azimuth (Fig. 5.3 A, Rayleigh test: $p = 0.004$ to $p < 0.0001$; the 99% confidence intervals include 0° for all AM data and for the 4 m PM data). In the control experiment (Fig. 5.3 B), the ants were trained in the same orthogonal e-vector paradigm in which they had no sight of the sun but an almost full view of the celestial POL pattern during their homebound run under the trolley. Again, the ants showed very precise orientation, with little scatter (the mean vector directions are not significantly different between Fig. 5.3 A and B, while the circular standard deviations are more than twice as large in A (mean difference 110%, significant in four out of six cases, $p = 0.009$ to $p < 0.001$; Wilcoxon-Mann-Whitney test for dispersion)). The data of Figure 5.3 A demonstrate that the ants can use directional information obtained with the POL compass in a test situation where only the sun compass is functional.

An analogous experiment was performed with a different orientation of the POL filter (Paradigm III). Now the e-vector direction in the training channel was parallel to the ant's walking direction. In that situation the ants expect their homing direction to lie perpendicular to the sun-antisun meridian (Fent (1986); see also Chapter 3). Indeed, in the control experiment (Fig. 5.4 B), the mean vector directions are close to the expected 90° and 270°, though with small but significant deviations towards the sun's azimuth (0°; AM 270°: $p < 0.01$ for 2 and 3 m data; 4 m n.s. (N = 11); PM all $p < 0.01$ for 90° data (N = 17-15), n.s. for 270° data). In the critical test the homing directions deviate more towards the sun's azimuth (Fig. 5.4 A; the respective distributions are significantly different from the control;

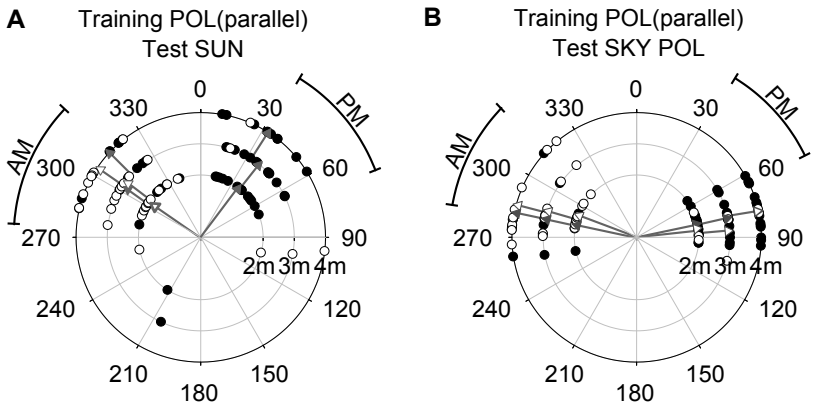

Fig. 5.4.: Results of Paradigm III: training with a parallel e-vector. **A** Critical test with sun only, **B** control with celestial POL pattern visible and shielded sun. 0° indicates the sun azimuth; *open* and *closed symbols* correspond to AM and PM tests, respectively. The *arcs beside the diagrams* indicate the nest positions relative to the sun's azimuth; other conventions as in Figure 5.2. The lengths of mean vectors were determined separately for the left and right halves of the diagrams except for the cases with less than five animals (AM 90° in (A) and (B) $r = 0.79 - 0.98$, PM 270° in (B) $r = 0.96 - 0.99$; all $p < 0.007$ (Rayleigh test)). Adapted from Lebhardt and Ronacher (2014b).

Mardia-Watson-Wheeler test: $p < 0.001$ for the PM and $p = 0.055$ to $p < 0.03$ for AM data). However, this result again is most likely due to the phototaxis effect mentioned above. In this paradigm, the ants should move at right angles to the sun meridian, and hence the phototaxis effect towards the brightest part of the sky would pull the ants towards the sun azimuth – which is what we see in Figure 5.4 A. The mean deviation from the control was 38° and 19° for the AM and PM data, respectively – lying in the same range as observed for the phototaxis effect by Wehner (Figs. 12, 13 in Wehner (1997)). Note that in the paradigm with the orthogonal POL filter (Paradigm II) the phototaxis effect would work in the same direction as the compass direction and therefore, was not evident in Figure 5.3 A.

5.5. Discussion

In the experiments presented in this chapter the ants had to cope with different combinations of celestial cues they experienced during the respective training and test situations. The data (Figures 5.2, 5.3, and 5.4) suggest that the ants can transfer directional information from the sun compass to the POL compass system, and vice versa.

5.5.1. Salience of different orientation cues

To substantiate the conclusion that directional information is transferable from one compass system to the other one must rule out other possible orientation cues. First, I consider the diverse cues known to be used by *Cataglyphis* to infer directional information (see Introduction of this chapter 5.2). All terrestrial cues – landmarks, panorama and wind (e.g. Wolf and Wehner (2000); Collett et al. (2001); Müller and Wehner (2007); Bregy et al. (2008); Graham and Cheng (2009); Zeil (2012); Collett et al. (2013)) – were excluded to a large degree by the experimental design. The landscape where the experiments were performed offered very few potential landmarks. In addition, during training the view was restricted

by the channel system, while during the tests under the trolley, landmarks were obscured by a curtain. During training in the channel the ants experienced some head or tail wind but in the test situation under the trolley they were shielded from wind. Hence, only celestial cues were available to infer walking directions: POL pattern, sun position and spectral or intensity gradients.

During training in Paradigms II and III the ants experienced only a modified POL pattern, i.e., an overhead stripe with a single e-vector orientation (either orthogonal or parallel to their walking direction). In a previous experiment, after the same type of training the ants performed well-oriented homing courses when tested with a free view of the sky (Chapter 3). This was confirmed here in the controls (Figs. 5.3 B, 5.4 B); the difference between the two experiments was that in the current design the trolley prevented the direct view of the sun. This type of experiment showed again that the POL (plus spectral) cues are sufficient to provide very good orientation.

5.5.2. The long-wavelength filter induces an additional phototaxis effect

In the sun-only training (Paradigm I) and in the sun-only tests (see Table 5.1) the orange Perspex eliminated not only the POL cues, but also prevented the perception of spectral gradients, since only the long-wavelength receptor type was left functional (Lanfranconi, 1982; Wehner and Müller, 2006). In this condition, the ants exhibited a strong phototactic response towards the brightest part of the sky even if the sun itself was occluded (Lanfranconi, 1982; Wehner, 1997). This positive phototaxis caused substantial deviations from the trained compass direction (up to 38°; Figs. 12, 13 in Wehner (1997)), and can explain the observed deviations from the expected homing directions in Paradigm I (Fig. 5.2 C) and Paradigm III (Fig. 5.4 A). However, since the orange filter affected not only the UV based POL compass, but also produced an unnatural perception of the sun, this could have influenced the salience of the sun compass. Nonetheless, I found clear evidence that the sun was used as a compass cue, even under the long-wavelength filter. Thus, even when there were restrictions on the available spectral information (or when the spectral information typically associated with the sun was distorted to a high degree), ants were able to orient with the sun compass. This conclusion corresponds with results of an earlier experiment reported by Wehner (Figs. 16, 17 in Wehner (1997)), while it is in contrast to Wehner and Müller (2006) who concluded that the natural spectral radiance distribution is essential for the compass.

Although the orange Perspex prevented the use of the POL compass and of spectral gradients, an intensity gradient across the sky still remained as a potential compass cue. Hence, theoretically the ants could have relied on the intensity gradient both under POL filter conditions during training as well as under the orange Perspex during the test, without the necessity of a transfer of directional information between sun compass and POL compass. This assumption, however, seems highly unlikely for the following reasons. During the AM POL filter training the nest direction was at 45° (Fig. 5.1 B) while the sun, representing the gravity center of the intensity gradient, wandered from 90° to 130°. The walking direction experienced during training thus was at -45° to -85° relative to the intensity gradient and the sun azimuth (see arcs in Figs. 5.3 A, 5.4 A). Relying on the intensity gradient alone, the ants should have chosen the same homing direction, irrespective of the different POL patterns experienced during training in Paradigm II and III. This was clearly not the case (compare Figs. 5.3 A, 5.4 A). In particular after orthogonal POL filter training, the homing paths of ants should deviate about 45°−85° from the sun azimuth, which is contradicted by the data of Figure 5.3 A. Finally, navigation based on the intensity gradient should have

led to a much larger scatter of homing directions (Wehner, 1997) than that observed in the experiments (see Figs. 5.2 A and 5.3 A (PM data) and Fig. 5.4 A).

The sky's polarization pattern as well as the pattern provided by a POL filter are symmetric and therefore, yield a 180° ambiguity resulting in a bimodal distribution of heading directions. Interestingly, this bimodality could be observed after training with the parallel oriented POL filter, but was absent for the orthogonal POL filter training (only one ant headed towards the antisolar direction) or the sun-only training which was followed by the test with only the sky's polarization pattern available. In the experiments described in Chapter 3, this bimodality was also absent in the paradigm with an orthogonal POL filter (see Fig. 3.2 A, B). Thus, it seems that the ants indeed can distinguish between the solar and the antisolar half of the sky (the latter is more polarized) and therefore, the ambiguity of the POL pattern is resolved (Fent, 1986). This leads to an unimodal distribution in the sun-only training situation as well as in the orthogonal POL filter training. Only after training under a parallel e-vector orientation relative to the walking direction, the directional information is ambiguous and the ants were not able to distinguish between the two possible homing directions directed perpendicular to the solar meridian.

5.5.3. Dominance of the POL compass?

According to Wehner and Müller (2006) the polarization compass of *Cataglyphis* completely dominates over the sun compass (Duelli and Wehner (1973); see also Müller and Wehner (2007)). However, in the experiments described in Chapter 4, which set the POL compass in conflict with the sun compass, the ants adhered to a compromise direction between sun and POL-based homing directions indicating a roughly equal contribution of the two compass systems. How can this result be reconciled with the postulated dominance of the POL compass system, and do the present results bear on this question?

The precision of homing directions in the present experiments may give additional hints to the salience of the two compass systems. First, comparing the results of Figure 5.2 A and B shows the impact of eliminating the sun as a compass cue. The circular standard deviations after sun-only training and SKY POL test (Fig. 5.2 A) were somewhat larger than when the sun was additionally visible during test (SKY POL+SUN, Fig. 5.2 B), although the differences were significant in only one out of six comparisons (two-sided F test: $p < 0.01$). In addition, some of the increased variances may be attributed to the test situation under the trolley – in the control tests with both the sun and POL pattern visible (Fig. 5.2 B) the ants moved freely after their release on the test field. Thus, elimination of the sun as a compass cue only marginally deteriorated the precision of orientation via the POL compass, if at all. The standard deviations in Figure 5.2 C cannot be compared directly to Figure 5.2 A, because of the influence of phototaxis on the compass direction (cf. Results section 5.4).

A direct comparison of the two compass systems can be made in Paradigm II, in which the ants could rely either on the sun (Fig. 5.3 A) or on the sky's POL pattern (Fig. 5.3 B) for their homing path. The circular standard deviations were on average more than twice as large if the homing was performed under the sun condition (see Results section 5.4). Although the significant increase in the variances under the sun condition may in part be attributable to the switch from one compass system to the other, the strength of the effect indicates that the sun is an inferior cue compared to the celestial POL pattern. Furthermore, removing the spectral information by the orange cut-off filter may have caused a further imbalance against the sun compass and in favor of the POL pathway. The standard deviations for the transfer experiments from POL compass to sun compass (Fig. 5.3 A) were

on average 57% larger than those for the transfer experiments from sun compass to POL compass (Fig. 5.2 A; the differences were significant in three out of six cases, one sided F test: $p < 0.01, < 0.005, < 0.001$). Taken together, these comparisons suggest a stronger weight for the POL compass. This conclusion is further supported by the observation that the phototaxis effect appeared to have an effect only when the sun compass was used and not in combination with the POL compass (compare Fig. 5.2 A and C; see also Wehner (1997)).

5.5.4. The main findings suggest a common final stage of compass direction processing

The results of Figures 5.2, 5.3, and 5.4 show that directional information obtained from the sun compass can be used to retrace a home vector, if only the POL compass is available, and vice versa. Hence, the results suggest that in the ant's brain an anatomical structure exists, before the motor output, into which both types of information – arriving via anatomically distinct pathways – are fed and can substitute each other. It is, however, not possible solely based on behavioral experiments to determine at which stage exactly a transfer or substitution of directional information takes place. Conceivably, the directional information obtained by either the POL compass or the sun compass could be forwarded via two separate pathways until they reach a common "path integration module" where they may substitute each other for the computation of the "home vector" without requiring any prior transfer of information between the two pathways. Alternatively, the information of two different compass systems may already be consolidated at an earlier, more peripheral stage, and then be further processed as a combined message in downstream centers. Indeed in locusts and monarch butterflies several neurons have been recorded at different stages of the polarization vision pathway that could play such an integrative role (the respective ganglia range from the optic lobe over the anterior optic tubercle to the central complex; Pfeiffer and Homberg (2007); Heinze and Reppert (2011); El Jundi et al. (2011); reviewed in El Jundi et al. (2014)). If both pathways feed into a common center, an exchange between sun and POL compasses as well as the resulting compromise directions in conflict experiments as observed in the results of Chapter 4 are easily explained. During training and test in the present experiments an ant had access to different reference signals, which are transmitted via two different anatomical substrates. The results of the experiments presented here provides an evidence that the compass information obtained by one system can be successfully recalled by the other, and that at some stage a transfer of directional information occurs.

I hypothesize that under normal conditions the POL compass may indeed be dominant since a large number of DRA-ommatidia are exclusively devoted to the processing of POL information. In addition, the ocelli contribute to this pathway (Fent and Wehner, 1985; Schwarz et al., 2011). In contrast, the sun is perceived by only one or a few ommatidia. Conceivably, the determination of an intensity or spectral gradient across the sky may yield smaller excitation values in downstream neurons because the ommatidia outside the DRA are not specifically tailored to such a task. In the cue conflict experiments described in Chapter 4 only a single e-vector direction was visible during training. Hence, fewer DRA ommatidia were optimally excited than would have been if the complete celestial POL pattern was visible, which may have reduced the strength of the POL input and favoured homing in a compromise direction. In the experiments yielding a dominance of the POL compass the ants could see the celestial POL pattern in a 90° stripe and thus, experienced a broad range of e-vector directions (Wehner and Müller, 2006). This may have increased the impact of

the POL compass relative to the sun compass.

A common integration stage might combine the input from the two compass pathways in a weighted fashion, with the weights depending on how many ommatidia are involved, and how strongly these are stimulated. By partial covering of the DRA it should be possible to reduce the input strength of the POL compass. Furthermore, one would expect a difference in homing precision between experiments performed under the orange filter and experiments in which only the DRA and ocelli are covered: in the latter, the sun should have a stronger influence compared to the former because the filter eliminates spectral cues.

6. The significance of different parts of the dorsal rim areas in the desert ant compound eyes

The previous chapters describe experiments where the perception of the celestial information used by *Cataglyphis fortis* for navigation was *non*-invasively manipulated. In contrast to that, in the following chapter the ants' compound eyes were occluded leaving open only specific parts of the dorsal rim area (DRA) in order to assess their significance for navigation.

6.1. Summary

Desert ants perceive polarized light via specialized ommatidia situated in the dorsal rim area (DRA) of their compound eyes and use this light as compass information for navigation. The polarized light analyzers are arranged along the upper dorsal rim of the compound eye in a distinct manner, representing the variety of e-vector orientations found in the polarization pattern of the natural sky. Here, the significance of the organization of the DRA was systematically investigated by occluding defined regions of the DRA (its frontal or caudal part), as well as the rest of the compound eye before releasing the ants to perform their homebound runs. In an additional series of experiments, ants which had a free DRA only in one eye were tested. Interestingly, the homing performances of ants with a considerably reduced number of available ommatidia largely depended on the time of the day, i.e., the relative position of the sun. Predominantly ants with either a free frontal or a caudal DRA were affected and could not use the polarization compass information for navigation, while ants with either an entire free right or left DRA behaved quite normally, however displayed a tendency to head towards a shifted homing direction.

6.2. Introduction

Cataglyphis fortis navigates through its featureless habitat by means of path integration. The relevant compass information is predominantly perceived visually from celestial cues (reviewed in Wehner et al. (1996); Wehner (1997)). The regional specialization within the compound eyes of insects is based on anatomical and physiological properties. A small number of highly specialized ommatidia located in the upper margin of the compound eye, the dorsal rim area (DRA), are able to detect polarized light. Thus, these DRA-ommatidia are suited to read the e-vector orientations of the polarization (POL) pattern in the natural sky and provide this information for navigation (reviewed in Wehner (1994); Wehner and Labhart (2006)).

The e-vector analyzers are maximally stimulated by linearly polarized light oriented parallel to the well-aligned microvilli of the photoreceptors, however each photoreceptor holds two orthogonally oriented microvillar orientations per rhabdom which are antagonistically

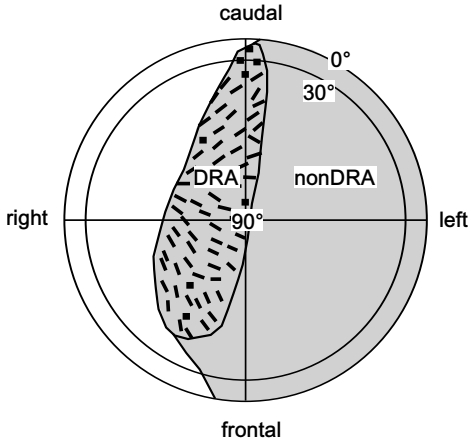

Fig. 6.1.: Hemisphere of the ants' dorsal visual field. *Grey colored area* represents the viewing direction of the left eye with the distribution of e-vector analyzers (*small black bars*) in the dorsal rim area (DRA) of *Cataglyphis bicolor*. Modified from Wehner (1982): Fig. 35

connected, thus increasing polarization sensitivity. As the transversal axes of the rhabdoms change their orientation in a fan-shaped fashion along the DRA, a large range of detectors with different e-vector orientations is present in each eye. These particularities have been first described for desert ants (Herrling, 1976; Räber, 1979; Labhart, 1986), but are typical for most insect DRAs (Labhart and Meyer, 1999). In previous studies, it has been shown that insects with occluded eyes and only a few number of DRA-ommatidia left open are still able to navigate accurately (bees: Wehner and Strasser (1985) and ants: Fent (1985)). In *Cataglyphis* which is equipped with a highly sophisticated polarization compass, however, not only the orientation of e-vector detectors changes within the DRA but also the number of rows of ommatidia specialized to detect polarized light. The asymmetric shape of the DRA represents a broader area of polarization detectors within the frontal part and a smaller but elongated profile in the caudal part of the DRA (Fig. 6.1). Such an asymmetric shape has also been reported in other insects, and only recently it has been shown in locusts that this shape is maintained during the neuronal projection towards the brain via the dorsal rim of the lamina and the medulla (Schmeling et al., 2015). However, hitherto little is known about the significance of this shape and previous studies focused on the functionality of the polarization analyzers and the necessary number of DRA-ommatidia involved for proper navigation. Thus, in the present chapter, a behavioral study will be presented with the aim of defining the significance of the unequal distribution of DRA-ommatidia directed to the frontal or caudal visual field as well as looking for a possible impact of a unilateral DRA on desert ant's orientation.

6.3. Materials and methods

6.3.1. Training and testing procedure

Desert ants were trained to walk to a feeder filled with biscuit crumbs at the end of a channel (length: 15 m, width: 30 cm, and height of sidewalls: 10 cm; Fig. 6.2 A). The channel provided the ants with an approx. 110° slit-like window of the natural sky while excluding potential landmarks and skyline cues. The channel was arranged in an East-West

alignment for Paradigm I and in a South-North orientation for Paradigm II. Individuals were marked using a three dot color code in order to register their exact number of visits at the feeder. After having completed at least three training runs, individuals were caught at the feeder and their compound eyes as well as their ocelli were painted with white light-tight color (paint or acrylic color). Depending on the experimental paradigm the DRA was either completely or partially left open. In Paradigm I, the ants' eyes were occluded except for the frontal (FRO) or the caudal (CAU) part of the DRA. In Paradigm II, ants with the DRA left open in one eye (LEFT or RIGHT) and a completely occluded second eye were tested. Additionally, appropriate control groups were separately set for each paradigm, namely: (1) animals that had their DRA open and the remaining part of the eye painted (DRA-control), (2) animals with completely occluded eyes (blind-control) and (3) untreated animals with two functional eyes (trolley-control). Less than one hour after the ants had been caught, they were individually released equipped with a biscuit crumb on a 20x20 square meter test field (mesh width of 1 m). There they performed their homebound runs under an experimental trolley (Fig. 6.2 B). The trolley had a circular overhead aperture providing a sky window of 110°, which was covered by a UV-transparent Perspex in order to prevent wind blowing into the trolley. Due to a movable screen (covering 27-30° of the natural sky, depending on the alignment) the ants' view of the sun was prevented while their homebound run was recorded.

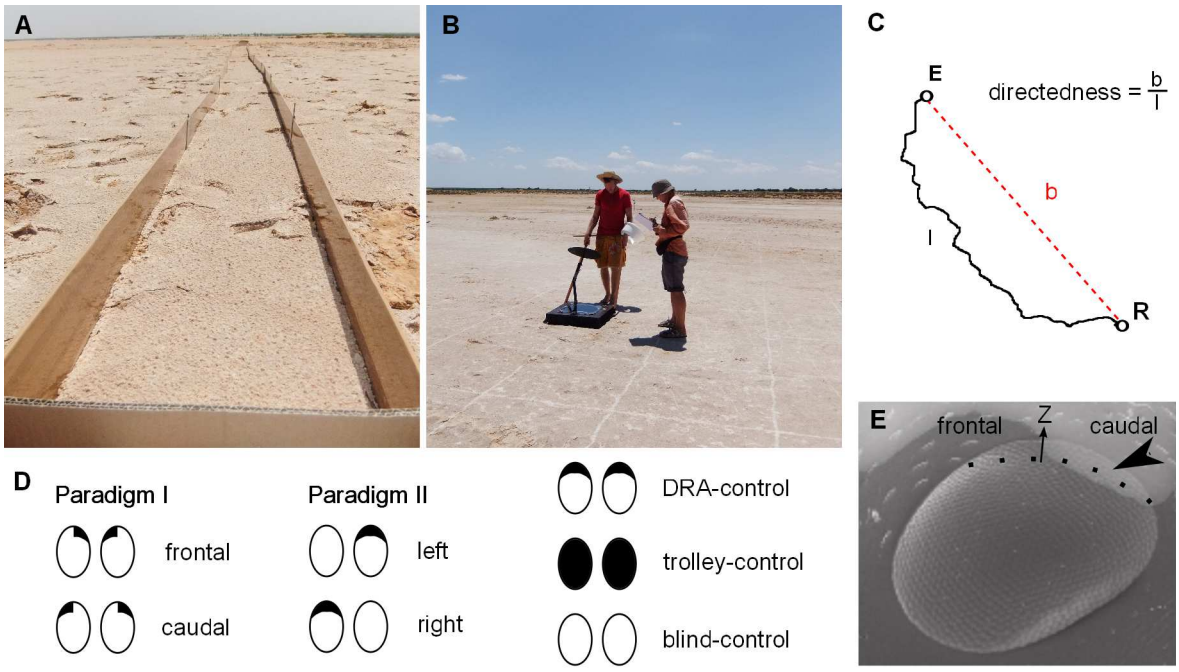

Fig. 6.2.: **A** Foto of the training channel (15 m long, approx. 30 cm wide). The ants walked in a lane on the desert floor which was restricted by wooden plates. **B** Experimental trolley with a sun shield used while recording the homebound run on the open test field. **C** Scheme to illustrate the determination of the directedness of an ant's walk (R = release point, E = end point, b = beeline, l = length of actual walk) **D** Different types of occluded eyes of ants tested in Paradigm I and II and the respective control groups, *the white parts were covered with paint.* **E** Scanning electron micrograph of a partially covered (left) *C. fortis* eye, the brighter parts had not been covered during the test (here the caudal part indicated by the *arrow head*). The *dotted line* marks the boundary between the dorsal rim area (above) and the rest of the eye. Z = zenith

6.3.2. Analysis of the compound eyes

After the test, the ant was caught and the quality of the painted compound eyes was later verified under a scanning electron microscope (SEM). The ants' heads were coated with gold sputter two times for approx. 60 sec and again for approx. 30 sec after having removed the eye cap (according to the double coating technique, described by Wehner (Wehner (1982), p. 90). Thus, the parts of the eye that had not been painted were more intensely gold-plated resulting in a brighter staining on the photomicrograph. The pictures were analyzed in order to define the number of ommatidia that were left open during testing. First, it was important to determine how well the area of ommatidia left open fitted the desired region (DRA) and second, how many additional non-DRA ommatidia had been uncovered and thus had free sight of the sky. The ants were classified according to the number of uncovered DRA-ommatidia in the less painted eye. Ants with less than 50% of the DRA-ommatidia (approx. 40 ommatidia) left open were grouped as ants with frontal (FRO) or caudal (CAU) DRAs depending on the location within the DRA and ants with more than 75% free DRA-ommatidia as DRA-control (Fent reported that 66% of the DRA already enable for accurate navigation (Fent, 1985)).

6.3.3. Analysis of the trajectories

The ants' homing courses recorded on protocol sheets during the test were later digitized using a WACOM graphic tablet and an appropriate MATLAB script. The ant's trajectory was analyzed as described here: (1) the ants' heading directions were measured in 1 m intervals from the release point and determined relative to the correct nest direction (homing direction; for details see paragraph 2.6 in Chapter 2), (2) the directedness of the trajectories was calculated as the quotient of the beeline (b, the straight line connecting the release point R with the end point E of the home vector, which is defined by the characteristic U-turn) and the actual length of the traveled route (l, see Fig. 6.2 C); the resulting value lies between 0 and 1 (the latter represents a completely straight walk), and (3) the distance from the release point to the point at which the ant began its search loops expecting the fictive nest, i.e., the beeline distance.

6.3.4. Data evaluation and statistics

In order to assess the impact of uncovered DRA- and nonDRA-ommatidia on the homing performance, the data was pre-analyzed in a multiple linear regression analysis; particularly with the intent to exclude a possible influence of nonDRA-ommatidia on the homing performance. The analysis was performed following Zuur et al. (2009) and the details are provided in the Appendix A.2. Afterwards further statistical analyses were performed, the One sample t-test to test whether the distributions of homing directions deviated significantly from the expected direction and the Mardia-Watson-Wheeler test to check for differences between different groups. Differences in circular dispersion between groups were tested using the Wallraff test of angular distances. To check for differences in mean tendencies (medians), the Kruskal-Wallis test was used followed by the Dunn's multiple comparison post hoc test. The statistical calculations were performed using R Studio (RStudio, 2012) and the AED-package (Zuur et al., 2009), as well as the circular statistics software Oriana 2.0 (Kovach Computing Services, Angelsey, Wales).

6.4. Results

6.4.1. Paradigm I: The impact of the asymmetric shape of the DRA

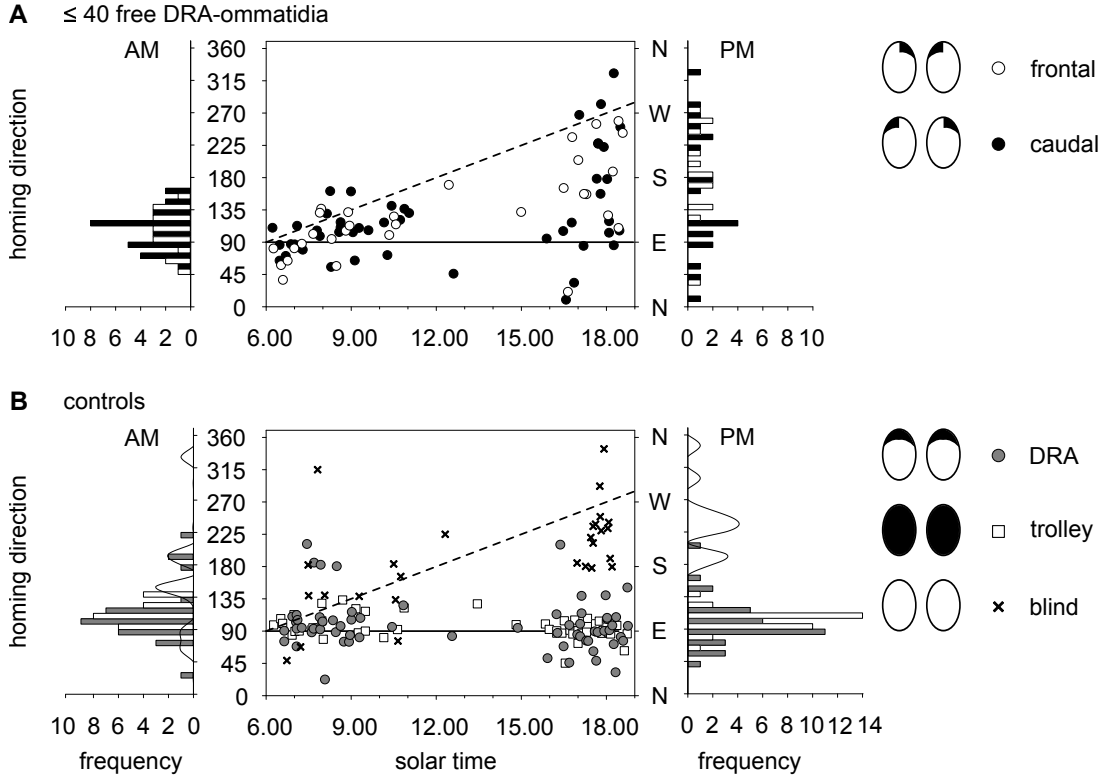

Fig. 6.3.: Homing directions (mean of heading angles at 1 to max. 5 m from the release point) of desert ants tested with partially occluded eyes at different times of the day are plotted relative to the earth coordinates. The *black horizontal line* at 90° represents the expected direction, i.e., the nest, while the *dashed line* illustrates the sun's course during the day. In **A**, heading directions of ants that had a maximum of 40 DRA-ommatidia left open either in the frontal part (*white circles*) or in the caudal part (*black circles*) are depicted. The horizontal histograms display the frequency of the respective homing directions for AM data on the left and for PM data on the right (bin width = 15°). **B** Homing directions of the control groups, ants with both DRAs completely uncovered (*grey circles*), of untreated animals (*white squares*) and of blind ants with entirely occluded eyes (*crosses*). The frequencies are depicted by grey (DRA-control) and white (trolley-control) bins, and the *grey spline line* (blind-control). Small insets on the right represent the type of occlusion

Daytime dependent homing directions After their training walks, ants were caught at the feeder and their eyes were partially occluded. Subsequently they were released on the test field and their homing courses were recorded. In Figure 6.3 A the heading directions (i.e., mean angles of the angles taken at 1 m steps from 1 to max. 5 m distance) of ants, with either the frontal (FRO, white circles) or the caudal (CAU, black circles) part of their DRA left open, are plotted relative to the earth's coordinates (North = 0° = 360°) and the solar time. Note that the data presented here in one graph was collected over a large period of time and not during just one or two days. The sun's course changes during the year and the resulting shift of the sun azimuth relative to the clock time becomes already noticeable within a few days during summer. Taking this into account and to accommodate for the

long experimental period, the data presented in this chapter are plotted relative to the solar time instead of the clock time (cf. diagrams of the previous chapters). The solar time is defined by the sun azimuth, i.e., an azimuth position of the sun at 90° corresponds to 6.00 h, at 180° to 12.00 h, and at 270° to 18.00 h. The straight horizontal line at 90° in Figure 6.3 A depicts the actual nest direction and the dashed line the movement of the sun during the day.

By observing this graph, it becomes obvious that the homing directions deviated quite drastically depending on the sun azimuth. During the morning tests (AM) the heading directions scattered around the nest direction, with mean angles (± circ. SD) of 95 ± 29° for ants with frontal (FRO: N = 17, mean of free DRA-ommatidia = 32) and 104 ± 27° for ants with caudal DRAs (CAU: N = 29, mean of free DRA-ommatidia = 28). However, the mean homing directions recorded during PM tests were at 152 ± 62° (FRO: N = 14, mean of free DRA-ommatidia = 30) and at 132 ± 96° (CAU: N = 21, mean of free DRA-ommatidia = 31). The scatter observed for ants with a free frontal or caudal DRA was significantly increased in the PM tests ($p = 0.03$ (FRO) and $p << 0.001$ (CAU); Wallraff test for dispersion), but did not differ between the groups tested at the same time ($p = 0.59$ (AM), $p = 0.16$ (PM)). Such large differences between AM and PM tests, observed in Figure 6.3 A, were not observed in the control groups of ants with the entire DRA free and the rest of the eye painted (DRA-control, grey circles, N = 27(AM), 32(PM)) or untreated ants (trolley-control, white squares, N = 22(AM), 31(PM); Fig. 6.3 B). Ants with no sight (completely occluded eyes and ocelli) again showed some discrepancy between AM and PM tests (blind-control, crosses, N = 11(AM), 16(PM)), their heading directions scattered quite randomly before 12.00 h and tended towards the south-west after 16.00 h solar time. Although the conclusion of different homing performances during AM and PM tests is here solely based on the homing directions, it indicates a general phenomenon that the ants behaved differently depending on the time of the day. Therefore, in the following paragraphs the data will be analyzed separately as AM and PM data.

Homing performances are impaired by a reduced number of DRA-ommatidia
Note, that Figure 6.3 represents preliminary results, as the heading directions of ants with different numbers of free DRA-ommatidia and - more importantly - an undefined additional number of free nonDRA-ommatidia are depicted all together. Both DRA- and nonDRA-ommatidia can provide compass information, although based on different skylight cues (polarized light and spectral gradient). Thus, to be able to make further predictions about the significance of particular parts of the DRA for accurate navigation, a possible additional influence of free nonDRA-ommatidia has to be excluded. This could be verified for all three homing performance parameters by a multiple regression analysis. Furthermore, the analyses revealed that only the number of uncovered DRA-ommatidia had a significant impact on the ants' homing performances ($p < 0.025$; details of the analysis are provided in the Appendix A.2, Tab. A.1 (upper part)). The assumption, that nonDRA-ommatidia had no relevant influence, is also true when comparing ants with only frontal or caudal DRAs (see Tab. A.1 (lower part) in the Appendix A.2). However, all regression models could only explain low percentages of the distributions ($R^2 = 0.05$ - 0.27) independent of the parameter considered, thus, as a consequence the following results have to be interpreted cautiously.

If and to what extent the homing performances of ants had been impaired due to the reduced number of free DRA-ommatidia or their location will be analyzed in the following. Figure 6.4 summarizes the orientation abilities of desert ants tested in paradigm I, assuming

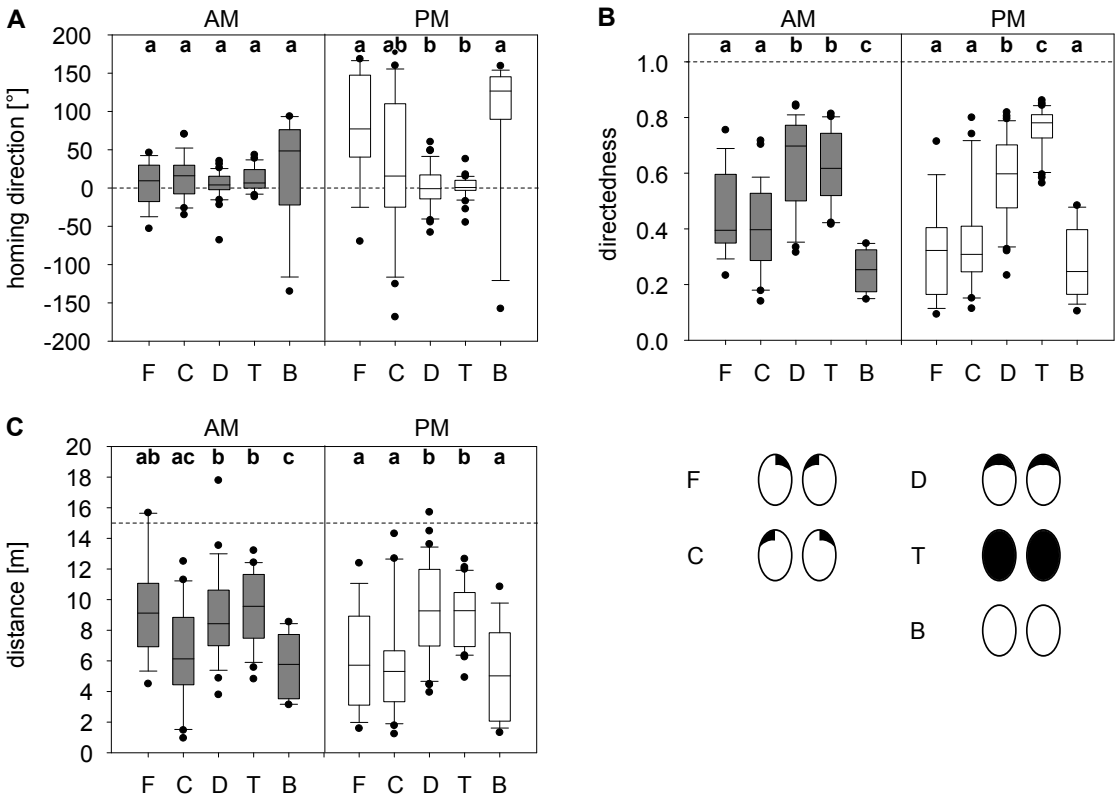

Fig. 6.4.: **A** Distributions of homing directions of ants with either a free frontal or caudal DRA (with a maximum of 40 DRA-ommatidia) and of the control groups (DRA-, trolley- and blind-control) represented as boxplots with medians, quantiles, whiskers and outliers during AM (*grey bars*) and PM (*white bars*) tests. **B-C** The respective boxplot representations for directedness and distance. F = ants with free DRA-ommatidia in the frontal part , C = ants with free caudally located DRA-ommatidia , D = DRA-control, T = trolley-control, and B = blind-control. The *dashed horizontal lines* reflect the respective optimal values. *Lowercase letters* indicate statistically significant differences among the groups. Insets depict the type of the eye cover

a non-relevant impact of nonDRA-ommatidia (see above). The three parameters for homing performance (homing direction, directedness, and distance) recorded for the different groups (FRO, CAU, and DRA-, trolley- and blind-controls) are presented as boxplots. The performances of the different groups tested at the same time of the day were compared applying the Kruskal Wallis test (followed by a Dunn's multiple comparison test) and differences between the AM and PM performances of the individual groups were tested by using the Mann-Whitney U-test[1]. Focusing on the AM tests and comparing the different groups with each other revealed no significant difference of heading directions, instead all groups scattered homogeneously around the expected value (= 0°). During PM tests, however, homing directions of ants with a free frontal DRA (FRO) deviated significantly from the DRA- and trolley-controls ($p < 0.01$). The same differences could be observed between the blind-control and the other controls ($p < 0.001$; Fig. 6.4 A), whereas heading directions of ants with free caudal DRAs (CAU) did not differ from the controls. The same tendencies can be reported for the homing directions of the respective groups recorded during AM or PM. Ants with a free frontal DRA as well as the blind-controls displayed significantly different heading directions depending on whether they were tested during AM or PM ($p < 0.01$), whereas for the other groups, there was no significant difference between AM and PM.

Referring to the directedness of the ants' trajectories recorded during AM tests (Fig. 6.4 B), ants with ommatidia left open in the frontal (FRO) or caudal (CAU) DRA performed significantly less straight walks than the DRA- or the trolley-control ($p < 0.01$). However, their paths were still significantly straighter than those of the blind-controls ($p < 0.05$). Thus, blind ants performed also significantly more tortuous walks than the other controls ($p < 0.001$). During PM, the directedness of the trajectories of ants with a frontal or caudal DRA did not differ any longer from the blind-controls and all three groups performed significantly worse than the control groups (DRA- and trolley-controls, $p < 0.001$); here, in addition, the DRA-control differed significantly from the trolley-control ($p < 0.05$). Differences in the different groups depending on the test time were significant for ants with free frontal DRAs with a reduced directedness during PM tests ($p < 0.05$). Untreated ants (trolley-control), however, performed significantly straighter walks when tested during PM ($p < 0.001$).

For the third parameter, the distances traveled (Fig. 6.4 C), the comparison between the groups tested during AM revealed that ants with free caudal DRAs (CAU) as well as blind ants walked significantly shorter distances compared to the DRA- and trolley-controls ($p < 0.05$). Ants with a free frontal DRA (FRO) did not differ from DRA- or trolley-controls and performed significantly longer walks compared to the blind-control ($p < 0.05$). This changed in the PM tests, where ants with a free frontal DRA (FRO) tended to cover relatively short distances comparable to those recorded for ants with caudal DRAs or the blind-control, resulting in significant differences between these three groups and the (DRA- and trolley-) controls ($p < 0.01$). Depending on the test time, significantly shorter distances were measured for ants with a free frontal DRA (FRO) during the respective PM tests ($p < 0.005$), the other groups traveled equally long distances independent of the time of the day.

Thus, the homing performance parameters seem to be predominantly influenced by the number of available DRA-ommatidia and only slightly by their location within the DRA, the differences were most notable between PM groups. During AM tests, however, ants with frontal DRAs seem to be less affected by the severe reduction of free DRA-ommatidia than

[1]These tests were used despite the unequal variances in the different groups; nevertheless, the results resembled statistically what is already detectable by eye

the ants with only caudal DRAs.

6.4.2. Paradigm II: Desert ant's orientation ability with a single DRA

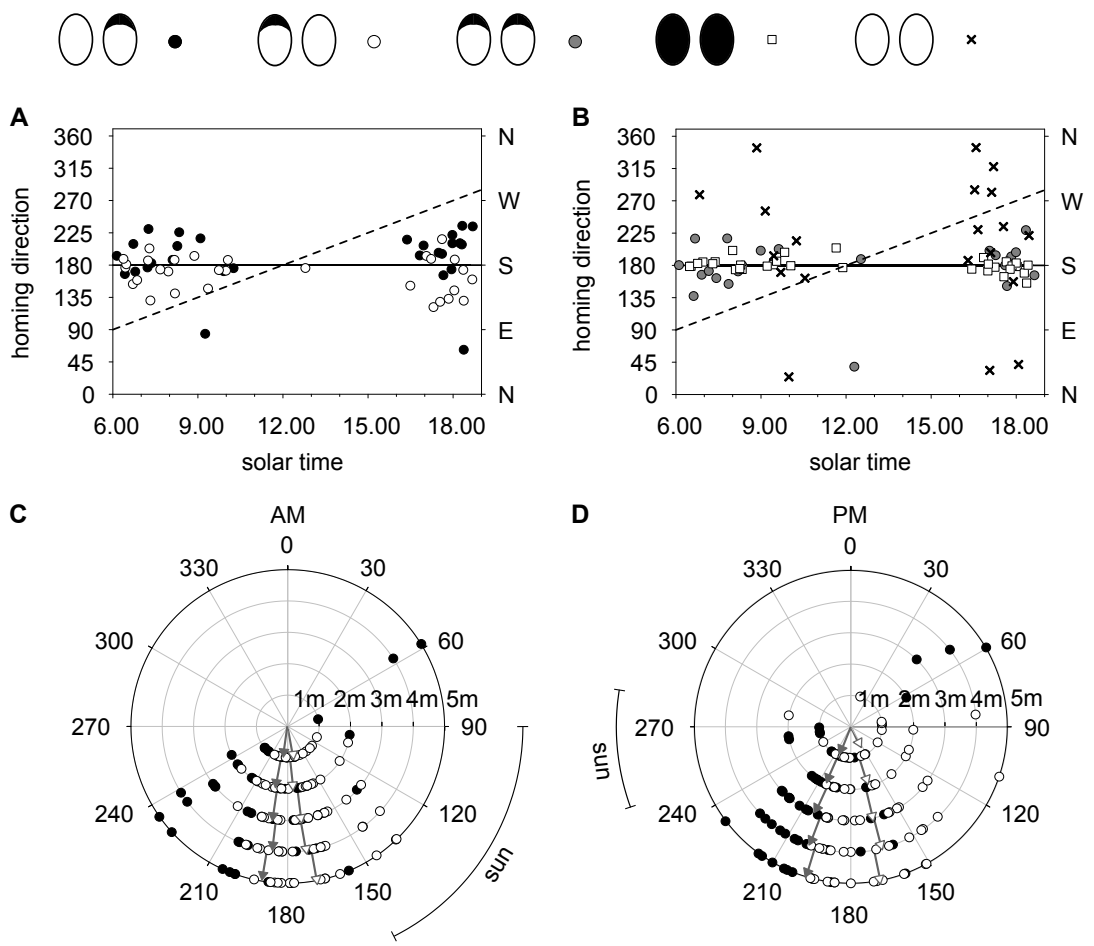

Fig. 6.5.: Homing directions across the day observed for ants with a free DRA in either their left or right eye (*black and white circles*, respectively; **A**) and the control groups (**B**). For details see Fig. 6.3; note that this time the expected direction lies at 180°. **C** and **D** Homing directions of monoDRA-ants during AM and PM tests plotted in circular diagrams. Length and direction of arrows indicate concentration of the heading directions around the mean vector of the sample. The *arcs besides the circular diagrams* depict the azimuth position of the sun during testing time. Small insets illustrate the manipulation of the ants' eyes

Ants with only one DRA tend to show systematic deviations from the correct nest direction Figure 6.5 A depicts the homing directions (means of 1-5 m) of ants with free DRA-ommatidia in only one eye – either the left (=LEFT, black circles) or the right (=RIGHT, white circles) eye – while the rest of that eye and the remaining contralateral eye were occluded. The recorded data scattered around the expected direction, with mean angles (± circ. SD) of 195 ± 35.3° and 167 ± 24.4° for ants with left DRAs (N = 28) or right DRAs (N = 30), respectively. Note, that for these experiments the nest direction was at 180°.

For a more precise description of the homing directions of ants with left or right DRAs,

the data are plotted in circular diagrams for AM and PM separately (Fig. 6.5 C and D, respectively). During PM tests (Fig. 6.5 D), ants with left DRAs tended to search for the nest at 202 ± 36.2° (N = 14) and ants with free right DRAs at 161 ± 28.9° (N = 13). Thus, both distributions (at 3 m) deviated significantly ($p < 0.05$) and for about 20° from the expected 180° - but in different directions (LEFT towards the right and RIGHT towards the left). Consequently, the mean heading directions (of 1-5 m) of ants with left of right DRAs also deviated significantly from each other in 4 out of 5 cases (Mardia-Watson-Wheeler test: $p \leq 0.05$). The same trend – but not significant – can be observed during AM tests (LEFT: 188 ± 33.1°, N = 14, and RIGHT: 171.9 ± 33.1°, N = 17; both not significantly different from 180°; Fig. 6.5 C). The controls (others than of Paradigm I), ants with the entire eye occluded except for the DRA of both eyes (DRA, grey circles), ants with completely occluded eyes (blind-control, crosses) and untreated ants tested under the trolley (trolley-control, white squares) are plotted in Figure 6.5 B. Mean homing directions for the DRA-control (182 ± 32.0°, N = 23) and the trolley-control (180 ± 9.3°, N = 32) coincided nicely with the expectation (One sample t-test: $p > 0.05$, AM and PM together), while blind-controls of ants that had no sight at all scattered largely (± 84.1°, N = 21) and deviated on average more than 60° from the correct nest direction (AM and PM tests together).

Directedness and distance of the ants' trajectories are not affected if only one DRA is available Before analyzing further differences in homing performances observed for the various groups, the multiple regression analysis was repeated to check for a possible influence of free DRA- and nonDRA-ommatidia (for detailed results see Appendix A.2). In an analogous manner to the previous analysis (see paragraph 6.4.1), AM and PM data were again separated. For the majority of the test conditions no significant impact of the number of free ommatidia or their location in either one or both eyes on the tested parameter could be determined. However, the homing directions and the distances recorded during PM tests depended not only on the type of occlusion but also to some degree on the number of free DRA- or nonDRA-ommatidia (Tab. A.2, Appendix A.2). Interestingly, the number of free DRA-ommatidia differed here between the groups. This result might be due to either unintentionally occluded DRA-ommatidia or more likely due to different sizes of ants which have different number of ommatidia. The significant models reached moderate R^2-values (0.36 and 0.44). The relatively low reliability and the possible influences of the number of (DRA- or nonDRA-) ommatidia apart from the type (free left or right DRA) for the mentioned parameters should be taken into account regarding the following results.

In order to assess the orientation abilities of ants possessing only one free DRA and to compare them to the control groups, the different homing performance parameters are illustrated as a general overview in Figure 6.6 (however, disregarding a possible impact of the number of free DRA- or nonDRA-ommatidia). The comparison of the heading directions recorded for the different groups tested at the same time of day revealed a significant deviation only during PM (Fig. 6.6 A), these were between ants with either left or right DRAs and also between the latter (RIGHT) and the blind-control ($p < 0.05$, Kruskal Wallis test followed by a Dunn's multiple comparison test). However, ants of the respective groups headed towards similar directions when tested during AM or during PM. The homing directions of the separate groups did not differ between the respective AM and PM tests, except for the heading directions of the trolley-controls, which differed – but only slightly – significantly between AM and PM tests ($p = 0.043$).

The directedness of the trajectories differed significantly during the AM tests between

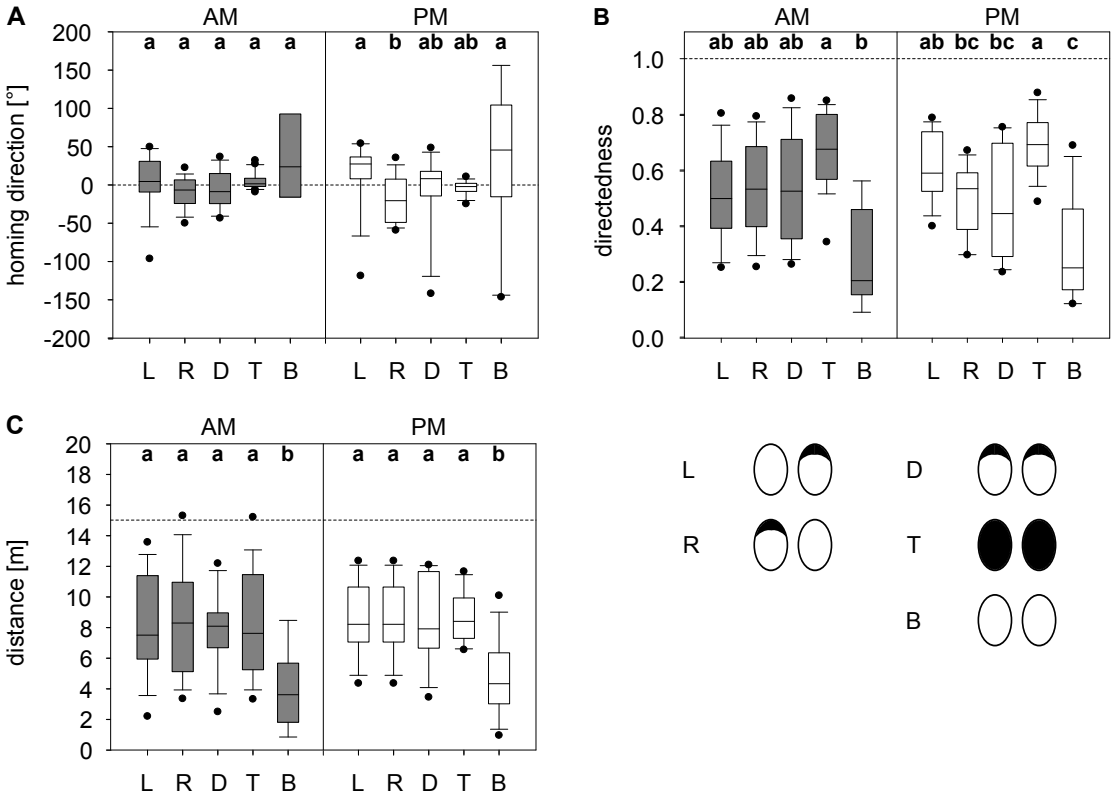

Fig. 6.6.: Comparison of **A** homing directions, **B** directedness of trajectories, **D** and distances of monocular ants and control groups represented as boxplots diagrams, for AM (*grey bars*) and PM (*white bars*). L = ants with free DRA only in the left eye (N = 14(AM), 14(PM)), R = ants with free DRA in the right eye (N = 17(AM), 13(PM)), D = DRA-control (N = 12(AM), 11(PM)), T = trolley-control (N = 18(AM), 14(PM)) and B = blind-control (N = 9(AM), 13(PM)). For further details see Fig. 6.4.

the trolley- and the blind-controls ($p < 0.001$). During PM tests, ants with only the right (RIGHT) or both DRAs (DRA-controls) and blind-controls performed significantly less straight walks than the trolley-controls ($p < 0.05$), whereas ants with a free DRA in their left eye (LEFT) and the trolley-controls performed significantly straighter walks than the blind-controls ($p < 0.01$). The respective trajectories did not differ for the individual groups when they were tested during AM or PM, except for ants with left DRAs which performed slightly significantly straighter paths when tested during PM ($p = 0.044$; Fig. 6.6 B). The distances measured for the different groups were equally long (of about 8 m) and only the blind-controls walked significantly shorter distances ($p < 0.05$; Fig. 6.6 C). This observation was the same for AM and PM tests and thus no inter-daytime differences could be reported.

6.4.3. Comparing homing performances of ants with partially covered DRAs and one-sided DRAs

According to the results presented in the previous paragraphs (6.4.1 and 6.4.2), one can already conclude that the number of free DRA-ommatidia in one eye consistently influenced the homing performances of desert ants. The location of the uncovered ommatidia within the DRA seems to be less important and depended to a certain degree on the time of the day (compare FRO and CAU in Fig. 6.4). However, it remains to be investigated how the ants' homing performances are affected by the distribution of free DRA-ommatidia among both eyes, i.e., if ants possessing a relative large contiguous area of free DRA-ommatidia are able to navigate more accurately than ants with two smaller areas of free DRA-ommatidia, one in each eye. Figure 6.7 allows to directly compare the homing performances of ants with the same total number of free DRA-ommatidia, which are situated either in only one eye (monoDRA-ants = ants with either a left or a right DRA) or in both eyes (partialDRA-ants = ants with free ommatidia in the frontal or caudal DRA). In order to meet the assumption of the same total number of free DRA-ommatidia, another subset of data than for the analysis presented in Paragraph 6.4.1 was used here. Ants with partially occluded DRAs had a total number of free DRA-ommatidia between 58 and 80, but a maximum of 45 in one eye, while monoDRA-ants had a total number of uncovered DRA-ommatidia between 60 and 75. During AM tests, ants with partially covered DRAs (FRO: N = 15 and CAU: N = 12) tended to perform only marginally worse in comparison with monoDRA-ants (LEFT: N = 14 and RIGHT: N = 17). Thus, their heading directions did not differ significantly during the respective AM test (Fig. 6.7 A). During PM tests presented in Figure 6.7 B, heading directions of ants with frontal DRAs (FRO: N = 13) differed significantly from those recorded for ants with a free right DRA (RIGHT: N = 13) and ants with caudal DRAs (CAU: N = 11) ($p < 0.05$; Kruskal Wallis test combined with a Dunn's multiple comparison post hoc test). The only significant difference found during AM tests were the considerably more torturous walks performed by ants with free caudal DRAs compared to the walks performed by ants with free right DRAs ($p < 0.05$; Fig. 6.7 C). Interestingly during PM tests (Fig. 6.7 D), ants with free ommatidia in the frontal DRA performed significantly worse than ants with either free left or right DRAs ($p < 0.05$), while ants with free caudally directed DRA-ommatidia only differed significantly from ants with free left DRAs ($p < 0.05$). During AM tests, the different groups covered similar distances, which did not deviated between the different types of occlusion. In the respective PM tests, ants with frontal or caudal DRAs covered significantly shorter distances compared to ants with free left DRAs ($p < 0.01$).

The most prominent differences between the homing performances recorded of monoDRA-

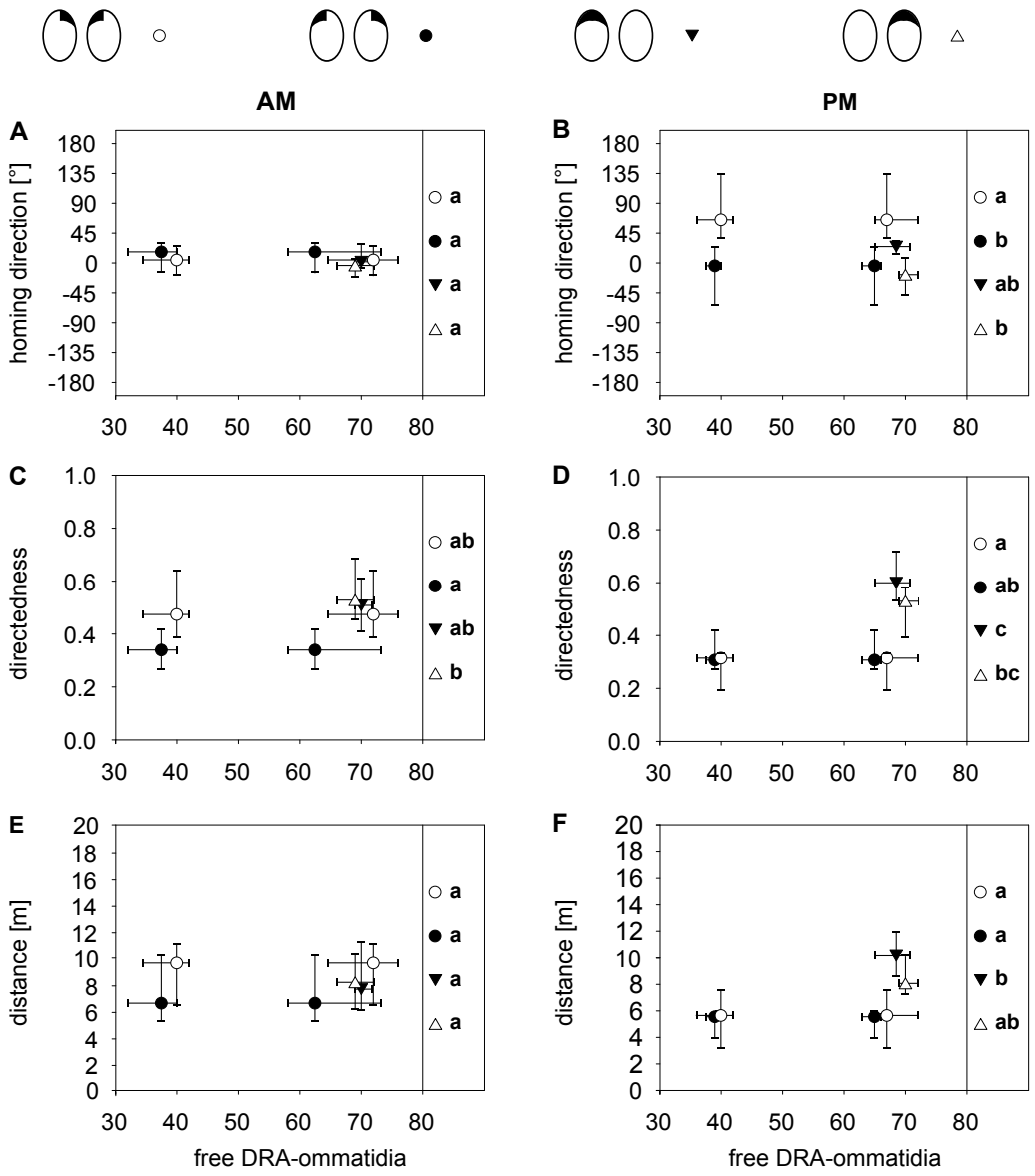

Fig. 6.7.: Comparison of homing performances of monoDRA- and partialDRA- ants with the same total number of free DRA-ommatidia. **A** Mean heading directions (*median and quartiles as whiskers*) relative to the respective nest directions plotted against the number of unpainted DRA-ommatidia. *Circles* represent ants with partially occluded DRAs (FRO = *white* (N = 15(AM), 13(PM)) and CAU = *black* (N = 12 (AM), 11(PM)), and the *triangles* the ants with one free DRA (LEFT = *black* (N = 14(AM), 14(PM)) and RIGHT = *white* (N = 17(AM), 13(PM)). Ants with partially occluded DRAs are depicted twice in the diagram either relative the number of DRA-ommatidia in the less occluded eye (∼40) or, alternatively, relative to the sum of free DRA-ommatidia in both eyes (∼70) – the respective values persist the same. The corresponding data for PM tests are illustrated in **B**. The AM and PM data for the remaining parameters of the homing behavior are illustrated in **C-F**. Small insets on the top depict the type of occlusion

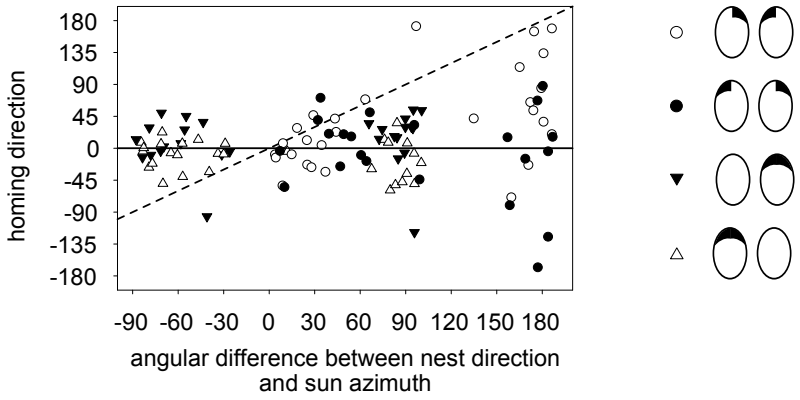

Fig. 6.8.: Observed heading directions normalized to the respective nest direction and plotted relative to the angle between the nest direction and the sun azimuth. *White and black circles* depict ants with frontal and caudal DRA and *black and white triangles* ants with left or right DRAs, respectively. The *straight horizontal line* represents the correct direction (nest) and the *dashed diagonal* the sun azimuth. Small insets on the right depict the type of occlusion

and partialDRA-ants occurred during PM tests. This might be due to the respective orientations of the training channels in Paradigm I and II, which caused the ants to search for the nest in different directions relative to the azimuth position of the sun. The angular difference between nest and solar meridian might indeed influence the ants' homing directions as ants determine their heading directions relative to the solar meridian. This issue will be addressed in the following sentences. Figure 6.8 displays the mean heading directions of monoDRA- (triangles) and partialDRA-ants (circles) normalized to the respective nest directions and plotted relative to the angle between the nest direction and the sun azimuth at test time. The expected direction is represented by the horizontal line and the sun azimuth is depicted by the dashed line. Obviously, a direct comparison between the tests with partialDRA- and monoDRA-ants turns out to be indeed difficult as the tests took place under different conditions with varying angles between sun azimuth and the respective nest directions. The angular distances ranged either between 0° and 65° during AM or between 160° and 190° (with a few exceptions) during PM in Paradigm I, but between 20° and 100° in Paradigm II. As already mentioned in the description of Figure 6.5 C and D, monoDRA-ants with a free right DRA deviated to the left from the nest in AM as well as in PM tests, whereas ants with a free left DRA deviated to the same degree to the right. In Figure 6.8, it becomes apparent, that these deviations are not a uniform trend but rather caused by an increased scattering coming along with an increasing angular distance between nest and sun azimuth. A similar observation can be done for heading directions of ants with partially occluded DRAs (FRO and CAU), they seem to be oriented more accurately during the morning tests, when the sun azimuth largely coincided with the nest direction and showed extremely large scattering during the afternoon, when the sun stood in the opposite direction. The tendencies are slightly different for ants with either frontal or caudal DRA-ommatidia left open (see also Fig. 6.7 B). Ants with a frontal DRA rather tended to head towards the South (positive deviations from the nest), while ants with a caudal DRA displayed a trend of heading directions towards the North (negative deviations from the correct nest direction). In any case, the heading directions of ants with partially uncovered DRAs and ants with a free DRA in one eye showed some dependence on the azimuth position of the sun. The homing performances

of ants tested under similar conditions (angular distances between sun position and nest of 0° to 100°) differed barely between the groups.

6.5. Discussion

The e-vector compass of *C. fortis* has been studied in detail by Wehner and colleagues (Wehner, 1982; 2003; Wehner and Labhart, 2006), and behavioral experiments on the functionality of the DRA have been performed in ants (Fent, 1986) and bees (Wehner and Strasser, 1985). In desert ants – which predominantly navigate visually – orientation is severely impaired by reducing the number of functional ommatidia, this has been reported in the aforementioned literature and is supported by the present experiments. Here, in addition, the significance of distinct parts of the DRA was investigated by occluding roughly half of the DRA-ommatidia (i.e., either the frontal or caudal parts in both eyes or the complete DRA of one eye) and the entire rest of the eye. The aim of the study was to determine the role of frontally or caudally located DRA-ommatidia for navigation and if a single intact DRA alone also is sufficient for accurate orientation. The homing performances of ants were characterized by three different parameters, (1) the homing direction, (2) the directedness, and (3) the distance covered. To cope with the large differences observed between the respective AM and PM tests, I will focus first on the comparison of the performances of the individual groups which were tested at the same time of the day, and then provide possible explanations for the daytime dependent deviations in the second part of the discussion.

6.5.1. Desert ants' orientation abilities with a reduced number of free DRA-ommatidia

In general, it was astonishing that manipulated ants still continued to carry food items to their nest even with the drastic occlusion of their eyes. Although such a behavior had been reported previously (Fent, 1985), the high motivation to reach the nest despite the large restriction of the visual field should be pointed out. This became most apparent when observing other ants with occluded eyes that were not tested but replaced to the nest after training. These individuals left the nest again only tentatively if at all and lingered preferably in close vicinity of their nest entrance.

By studying the homing performances of the ants that were displaced to the test field, I could investigate whether a reduced number of DRA-ommatidia or whether their particular location within the DRAs still allowed precise reading and correct interpretation of the sky's polarization pattern. First, the ant's ability to determine the correct heading angles via the detection of the celestial e-vector pattern with the remaining DRA-ommatidia will be examined – assuming that possible directional information detected by nonDRA-ommatidia had no relevant impact on the ants' navigation.

Ants with functional ommatidia in either the frontal or caudal part of the DRA were tested in Paradigm I. During the AM tests, the quite accurately oriented animals did not differ in their heading directions from the controls. However, during PM tests, a high variability of homing directions and, thus, a severely impaired orientation performance was obvious for the respective ants. Furthermore, impaired performances with respect to the directedness as well as the distance of their homing paths were observed during AM and PM tests. In this context, ants with a free caudal DRA performed significantly worse compared to the (DRA- and trolley-) controls during AM and PM tests, while ants with free frontal DRAs

only deviated during PM tests.

The directedness of the walks indicates how reliably the heading direction could be determined or if it was necessary to repeatedly reread the e-vector pattern and readjust during the journey, leading to more tortuous walks. Mainly ants with free caudal DRAs had difficulties to maintain a constant walking direction. This could be caused by the location of the uncovered DRA-ommatidia, i.e., ommatidia within the caudal part of the DRA might be less suited to determine a reliable heading direction relative to the solar meridian. Another possibility causing such tortuous paths could be an alternating use of both compass systems, POL and sun compasses, with different directional information, however both not sufficiently solid.

If the distances of the ants' journeys were interpreted as a measure of reliability of the directional information, i.e., the more reliable the information the longer the home vector would be followed, then one could infer the quality of the home vector information from the distances recorded in the tests. However, in the present study the ventral optic flow which contributes to the estimation of travel distances (Ronacher and Wehner, 1995) was affected due to the occlusion of the ventral ommatidia, and thus somewhat shorter distances are generally expected. Conform with the values determined for the directedness of the trajectories, again ants with a reduced number of DRA-ommatidia in both eyes also traveled shorter distances and thus showed less reliable homing performances, especially when possessing only caudal DRA-ommatidia – this applied for ants with frontal DRAs only in PM tests. These findings largely correspond with the findings for *C. bicolor* made by Fent (Fent, 1985), although here the occlusion was even more restricted and almost exclusively the DRA had been left open.

In Paradigm II, particularly interesting deviations from the expected homing direction could be observed for ants with either a free left or right DRA. These were more prominent during the PM tests, but could also be observed during AM tests. Ants with a free DRA in their left eye tended towards the right and ants with a free right DRA towards the left relative to the correct homing direction. Previous experiments reported that bees with only the DRA of one eye covered and the remaining parts of the eyes left open were well oriented towards the expected direction (Wehner and Strasser, 1985). Monocular ants, however, that were tested under comparable conditions, but with one entire eye open (and not only the DRA), also displayed deviations from the expected direction towards the seeing side (Wehner and Müller, 1985). Taking into account that the DRA faces the contralateral field of view, the monocular ants with only one DRA left open tested here also tended to head towards the seeing side. An alternative explanation of the systematic deviations observed in Figure 6.5 might be the following: ants with free DRA-ommatidia in the left eye determined the solar meridian more towards the right than it actually was, i.e., rotated clockwise. Consequently, heading directions were observed for which the angle between the nest and the azimuth position of the sun was overestimated during AM and underestimated during PM tests. The reciprocal case applied for ants with a free DRA in their right eye, they determined the solar meridian more to the left (i.e., rotated counterclockwise) resulting in deviations towards the left. Thus, ants with only one-sided DRAs were not able to determine the solar meridian accurately, i.e., the symmetry plane of the celestial e-vector pattern was not resolved correctly with the e-vector analyzers of just one eye. The recently discovered lower polarization sensitivity towards the medial part of the DRA in locusts might also contribute to the misinterpretation of the solar meridian (Schmeling et al., 2015). Anyway, comparable navigational errors have been reported in previous studies, when the presented POL pattern

differed between training and test (Müller, 1989). For the other two parameters of the homing performance, the directedness and the distance of the trajectory, similar performances could be observed for ants with only one DRA, irrespective of its location in the left or right eye or the test time, and the controls. Thus, ants with only one DRA were not further limited in their orientation abilities.

In both Paradigms, I and II, influences of additional directional information can not be excluded. Wind could provide such information as it is quite strong in the salt pan during the afternoon, yet, it should have been damped by the curtain around the trolley. More likely, especially for Paradigm I, is that the large discrepancy between heading directions recorded during AM or PM was caused by the different angular distances between the nest and the sun azimuth (Fig. 6.8). This aspect will be addressed in detail in the second part of the discussion.

A direct comparison between Paradigm I and II, i.e., between ants with the same total number of free DRA-ommatidia but located either in the frontal or caudal DRAs or exclusively in the left or right DRAs is only appropriate for AM tests, as an additional influence of directional information due to the angle between nest and sun can not be excluded. Ants tested under similar conditions (similar range of angles between nest and sun azimuth) only differed in the directedness of their trajectories. This difference could have been caused by the smaller number of free DRA-ommatidia and not only by their location within the caudal part (the median of free DRA-ommatidia for ants with free caudal DRA was at 62 and around 70 for the other groups). The respective heading directions in contrast differed barely and only a weak trend towards longer walks could be observed for ants with one-sided DRAs compared to ants with free frontal or caudal DRAs. Thus in contrast to the observations in bees (Wehner and Strasser, 1985), for *C. fortis* it does not seem to play a role if a given number of free DRA-ommatidia is confined to just one or two eyes.

Obviously, the parameters characterizing the homing performances were predominantly influenced by the number of free DRA-ommatidia and to a minor degree by the location within the DRAs. Thereby it seems that rather caudally located DRA-ommatidia provide less reliable information. However, largely similar homing performances could be achieved by ants with free frontal or caudal DRAs, if the information perceived by photoreceptors of different regions from the DRA is pooled and further projected via three POL neurons (as postulated by Labhart et al. (2001)). The most pronounced differences in the homing performances were detected here at large angular distances between the nest and the azimuth position of the sun, strongly suggesting additional influences of directional information obtained by the spectral or intensity gradient.

6.5.2. A potential impact of spectral cues (detected via free nonDRA-ommatidia)

Most differences in the homing performance parameters depending on the test time could be observed for ants with free frontal or caudal DRAs, while the respective controls, i.e., ants with two completely uncovered DRAs or untreated ants, did not display a different behavior when tested during AM or PM.

In Figure 6.8, it can be noticed that the spread of heading directions changed with the angular distance between the nest and the sun. A small angle, as it occurred during AM tests, allowed ants with a drastically reduced visual field (FRO and CAU) to navigate still accurately, while during PM with relatively large angular distances it was almost impossible for these ants to determine the correct homing angles. This can explain why such differences

were not observed for ants tested in Paradigm II. Here, during both test periods similar angular distances occurred (30-80° during AM and 65-100° during PM; cf. 0-60° during AM and 160-180° during PM in Paradigm I).

Ants might indeed have been navigating by the same orientation mechanisms during AM and PM tests. However, only during PM large angular distances between the nest direction and the azimuth position of the sun existed and created particular situations which caused an impairment of the homing performances. Such conflict situations emerge from different or contradicting directional information. In the present tests, these two types of information most likely derived from the polarization compass, at least as good as it could be determined by the remaining DRA-ommatidia, and from the information about the sun's position or rather about the spectral or intensity gradient in the sky, as the sun itself was shaded by a screen (27-30°, see Section 6.3). These gradients were not used as an actual compass, but more likely induced a phototactic response. Interestingly, the deviations from the correct nest direction recorded for ants with only one DRA could not be explained by an additional influence of phototaxis.

The necessary requirement to detect these gradients could be provided by the nonDRA-part that had been uncovered. The *C. fortis* DRA is not visually distinguishable from the rest of the eye, as it has been reported for other insects (e.g. crickets: Labhart (1980) and bees: Meyer and Labhart (1981)). Thus, an accurate occlusion of the desired parts of the eye was difficult and additional nonDRA-ommatidia had been left open. Although a significant influence of free nonDRA-ommatidia was excluded by the multiple regression analysis for the majority of the cases, the low determination coefficients of the models ($R^2 < 0.38$) reflect a high variability in the data. Additional information detected via the nonDRA-ommatidia might indeed have been processed into directional information. In a somehow comparable conflict situation, ants were confronted with two different directional information, a constant e-vector pattern (disconnected from the sun) and the azimuth position of the sun (presented in Chapter 4). However, under these conditions ants chose a uniform intermediate homing direction, in the present study, this was not observed neither for Paradigm I nor for Paradigm II. Moreover, the heading directions scattered almost randomly between the two directions of either the nest and the azimuth position of the sun. This could be due to the highly variable and particular individual combination of free ommatidia (within DRA and nonDRA). The weighting of the respective directional information, based on the POL compass or the spectral or intensity gradients, might depend on how many ommatidia represented the respective information. As already proposed in Chapter 5, the computation of the heading direction might have been different for the individual ants depending on the number of uncovered ommatidia in the DRA- and nonDRA-part of the eye and thus have led to different homing performances.

To summarize, the navigational abilities of *C. fortis* were affected by reducing the number of functional DRA-ommatidia in one eye and to a minor degree by their location within the DRA. The homing performances of ants with a one-sided DRA, however, were affected only in terms of systematic deviations of the mean homing directions relative to the expected direction, depending on the side of the occlusion. Ants with free ommatidia restricted to the frontal or caudal part of their eye might have tried to compensate their deficits by using additional directional information (apart from the POL compass). This strategy enabled them to navigate quite accurately at least when small angular distances between the correct homing direction and the sun azimuth occurred and, thus, less directional conflicts existed. However, the drastically impaired homing performances observed when the sun stood in the

opposite direction relative to the nest suggested that ommatidia located either in the frontal or caudal part of the DRA are insufficient to provide reliable POL compass information – at least when competing with further navigation strategies (e.g. phototaxis).

7. Conclusion

Desert ants of the genus *Cataglyphis* are excellent study objects to investigate insect navigation. Living in the desert demands sophisticated orientation abilities that allow a rapid and safe return to the nest after successful foraging. Within the ant's well-equipped navigational toolkit path integration represents the basic navigation strategy. Importantly, the information experienced by the ant during its trip can be selectively manipulated. Celestial cues consisting of the position of the sun, the polarized light as well as the spectral and intensity gradient provide relevant compass information to determine the walking direction (Wehner, 1994; 1997; 2003). This thesis gives new insights on how *C. fortis* uses the polarization compass by altering either (1) the polarization pattern using a linear polarization filter or (2) the perception of the polarization pattern by manipulating the relevant regions in the desert ant's eye.

By means of well-controlled behavioral experiments, this thesis could show that

1. The polarization compass dominates the celestial compass system in desert ants and,
2. it yields the most accurate directional information.
3. Sun and polarization compass information is processed jointly.

7.1. Manipulation of polarization compass information using a polarizing filter

How insects gain directional information from the polarization pattern can be explained by the template hypothesis first published for bees by Rossel and Wehner (1982; 1986). According to this hypothesis the insect uses an internal simplified template of the sky's polarization pattern to interpret its orientation relative to the actual polarization pattern. The best fit between the template and the actual pattern is achieved when the insect is aligned along the solar meridian. Fent tested this hypothesis for desert ants (Fent, 1986). In contrast to his experiments, in this thesis the ant's outbound – and not the inbound – run was manipulated. Besides the methodological advantage of this simplified and less error-prone testing procedure, a one-parameter training situation enables to control the acquisition of path-related information, while the manipulation of the inbound run addresses the recall of the information. The available celestial compass information during the outbound run was strictly reduced by a polarizing (POL) filter to a uniform e-vector pattern and the direct view of the sun was excluded by a barrier. This resulted in homing directions relative to the solar meridian under the open sky (Chapter 3). Experiencing a uniform pattern of e-vectors oriented orthogonally to the ant's walking direction was interpreted as moving along the solar meridian, while a pattern of e-vectors parallel to the walking direction simulated a movement perpendicular to the solar meridian. Interestingly, despite the ambiguous directional information provided by the exact symmetry of the POL filter, the ants exhibited preferred

heading directions. If the training was performed with an orthogonally oriented POL filter, the ants almost exclusively headed towards the sun. This supports Fent's assumption that an individual orthogonal e-vector is interpreted as lying on the antisolar meridian (Fent, 1986). In case of a parallel or oblique oriented POL filter, the heading preference was influenced by additional information from the spectral gradient, which was not excluded by the filter.

Summing up, filtered POL information is interpreted as directional information relative to the solar meridian. The accuracy of homing directions is comparable for training under the POL filter as well as under the natural sky. Thus, the POL filter offers a handy tool to manipulate polarization compass information independent from other directional cues.

7.2. Polarization compass information dominates over idiothetic information

By using the POL filter it was possible to provide two contradicting directional cues simultaneously (Chapter 3). Two different experimental designs were chosen to test how ants interpret directional information based on their polarization compass and their actual moving direction (idiothetic information). In the first experiment, the ants experienced a constant e-vector pattern, while they actually had to turn for 90° after half of the training distance. On their homebound run they completely ignored the idiothetic information and behaved as if they had walked in a straight channel. In the second experiment the ants experienced the reciprocal situation, they walked in a straight channel and this time sensed a change of the e-vector pattern. The observed homing directions were again exclusively determined by the POL information. An additional finding was that the POL filter segments were integrated linearly independent of their length or their position along the training distance.

The outcome of these experiments clearly shows that the polarization compass completely dominates over idiothetic information in the desert ant's navigation system.

7.3. Polarization compass and sun compass information is processed jointly

In the next series of experiments, the role of the polarization compass information was evaluated relative to another visual compass cue, the sun. The ants were allowed to additionally perceive direct sun light while walking under the polarizing (POL) filter. Although closely related in the natural sky, the ant interprets the pattern of polarized light and the position of the sun as separate compass cues which are detected via two separate areas in the eye (Fent, 1986; Wehner, 1997; Labhart and Meyer, 1999).

A combination of the POL filter information and conflicting directional information from the sun compass led to systematic deviations from the expected homing direction. The new heading direction was intermediate, indicating a contribution of both compass cues. This finding contradicts the statement of Wehner and Müller (2006), who concluded that "the polarization compass dominates over the sun compass to such an extent that, under the polarized sky present in the training situation, the sun compass is virtually ineffective".

Due to their experimental set-up, Wehner and Müller were able to create only small conflict situations of about 15-20° (between sun and polarization compass information). They modified the POL compass information by providing the ants with a restricted view of the natural sky during training. In this thesis (Chapter 4), the POL information was controlled

by the POL filter with a defined e-vector orientation and therefore independent of the actual position of the sun. This approach allowed much larger conflicts up to 90°. With such a range of conflicts the influence of both compass cues is more robust. The new finding of these experiments is that the sun influences the homing direction. As ants perceive separately both compass cues, combined neural processing can explain the phenomenon of the intermediate homing direction. Such kind of integration was shown by neurophysiological recordings in locusts and monarch butterflies (Pfeiffer and Homberg, 2007; Heinze and Reppert, 2011; El Jundi et al., 2011; 2014).

This hypothesis of combined processing sun and polarization compass information receives further support by the behavioral experiments reported in Chapter 5. These transfer experiments demonstrated the ant's ability to recall compass information with either system. Ants were trained with only one compass cue available, the sun, and later tested with the other cue, the polarization pattern and vice versa. The observed homing directions met the expectation from the training situation. That means directional information derived by the sun compass or the polarization compass was recalled by either compass system. It can be concluded that the sun and the polarization compass system can substitute each other under certain conditions (Chapter 5). Furthermore, control experiments showed that the orientation was less accurate if they had to rely on the sun compass only. Still, under natural conditions the ants preferred the polarization compass when available. This is consistent with previous experiments that reported the dominance of the polarization compass within the ant's celestial compass system under natural conditions (Wehner and Müller, 2006).

7.4. Number and combination of e-vector analyzers determine the functionality of the polarization compass

In the last chapter of this thesis the perception of the polarization pattern was affected by manipulating directly the ant's eye (Chapter 6). The eyes (and ocelli) were occluded, except for varying parts of the dorsal rim area (DRA) which is specialized in the detection of polarized light. The following manipulations were tested: binocular ants with either the frontal or the caudal parts of the DRAs left open and monocular ants with either a left or a right DRA left open.

Ants with either frontal or caudal DRAs had difficulties to maintain a constant walking direction and to determine the correct homing direction, especially when the sun azimuth did not coincide with the correct nest direction. The tortuousness of the paths as well as the miscalculation of the correct nest direction indicates a strongly reduced functionality of the polarization compass. The asymmetric shape of the DRA defined by a wider part of the frontal and a smaller elongated part of the caudal DRA had apparently no significant impact on the orientation performance. The functionality of the polarization compass is severely deteriorated if in either eye maximally half of the total number of DRA-ommatidia is left functional. Ants with only one functional DRA, either in the left or right eye, were able to perform their walking trajectories as straight as the controls. The combination of e-vector analyzers situated in a single DRA provides a consistent polarization pattern. However, the mean homing directions deviated systematically from the correct nest direction, ants with a left DRA deviated towards the right and vice versa. The partial POL pattern perceived might lead to systematic errors when determining the solar meridian.

7.5. Closing remarks

The present thesis suggests that the polarization compass provides the most accurate directional information and dominates the celestial compass system of the desert ant, *Cataglyphis fortis*. Ants rely exclusively on the polarization compass if they experience contradicting idiothetic information. Sun compass information, however, influences the polarization compass information indicating a combined neural processing of both signals. Apparently, this enables the ant to recall sun compass information by the polarization compass and vice versa. The functionality of the polarization compass depends on the number and combination of available e-vector analyzers in the DRA. By associating polarization compass information with other celestial features, *Cataglyphis fortis* is able to navigate efficiently and survive in the featureless and hostile desert.

A. Appendix

A.1. Trajectories observed in the experiments presented in Chapter 5

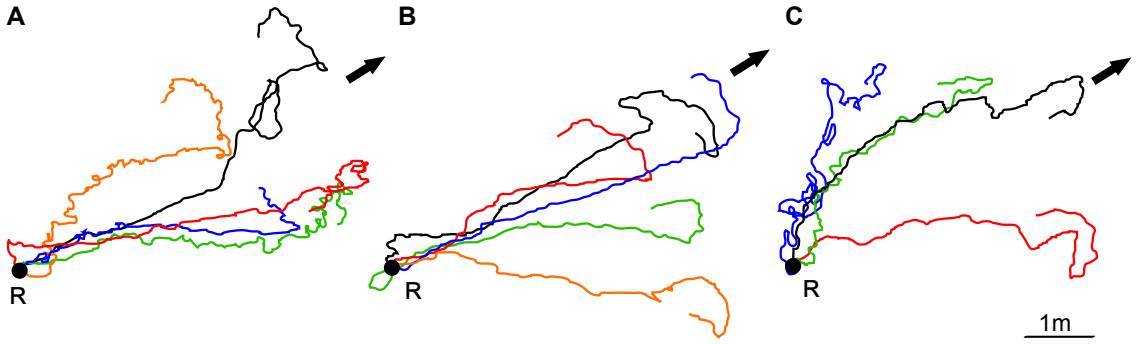

Fig. A.1.: Sample of trajectories of individual ants that had been trained according to Paradigm I under the orange Perspex and were later tested **A** under the natural sky but without view of the sun (cf. Fig. 5.2 A), **B** under the natural sky without view of the sun (cf. Fig. 5.2 B), or **C** under the orange Perspex (cf. Fig. 5.2 C). R = point of release, *black arrows* indicate correct nest direction

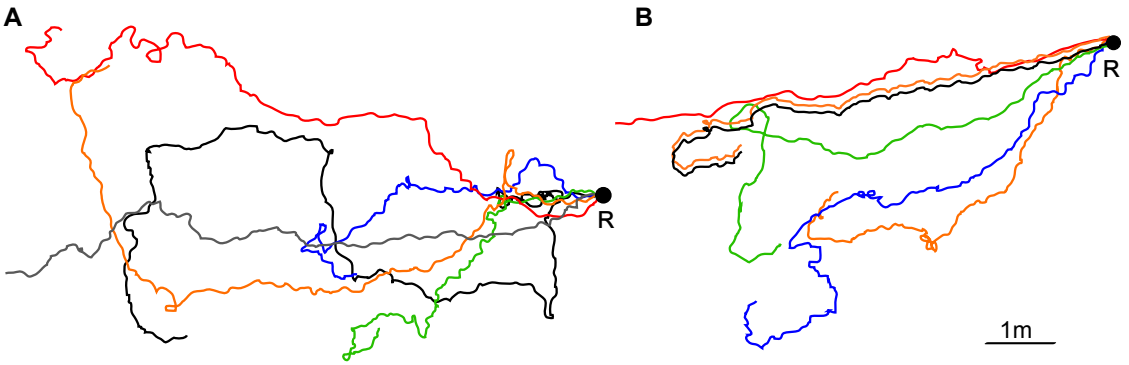

Fig. A.2.: Walking routes of ants that had walked under a POL filter oriented orthogonal to the ant's walking direction during training (Paradigm II) and were later tested **A** under an orange Perspex (cf. Fig. 5.3 A) or **B** under the natural sky but without view of the sun (cf. Fig. 5.3 B). R = point of release

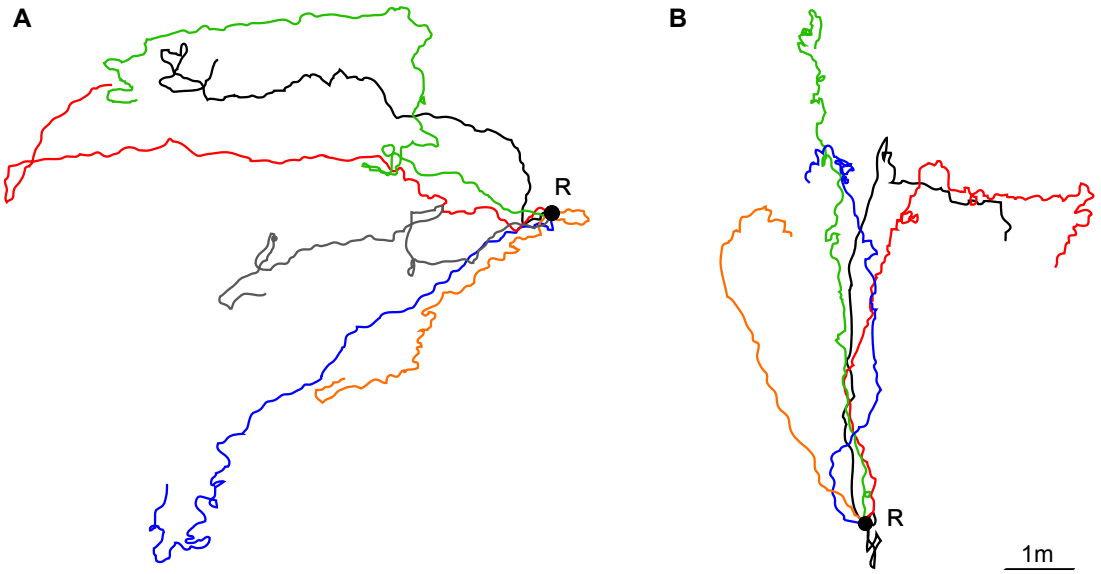

Fig. A.3.: Sample of walking paths of ants that had experienced an e-vector parallel to their walking direction (parallel POL filter; see Paradigm III) and were tested **A** under an orange Perspex (cf. Fig. 5.4 A) or **B** under the natural sky but without view of the sun (cf. Fig. 5.4 B). R = point of release

A.2. Defining the role of nonDRA-ommatidia via multiple regression analyses (Chapter 6)

Before being able to make further predictions about the significance of the different parts of the DRAs, other possible sources of directional information have to be excluded. However, this was not possible in the present study as some nonDRA-ommatidia providing additional compass information had been left open during the tests. To assess the impact of these uncovered nonDRA-ommatidia on the recorded homing performances, the "quality" of the eye covers, i.e., how many ommatidia in the DRA and nonDRA had been left open had to be investigated. Therefore, the exact number of ommatidia left open was counted for the DRA and nonDRA of each eye individually and the maximum number of DRA- and nonDRA-ommatidia were determined as reference values. In the next step significant influences of the respective ommatidia on the homing performances were investigated via a multiple regression analysis approach. For each of the parameters (1) homing direction (in this case the absolute deviation from the correct homing direction), (2) directedness, and (3) distance separate multiple regression models were defined.

The multiple linear regression analysis was performed following Zuur et al. (2009). After the data exploration to investigate possible outliers, collinearity of the independent variables (i.e., number of free DRA- and nonDRA-ommatidia) and their relationship with the response variable (see Figs. A.6, A.7 and A.8), a full model was formulated (including all variables and possible interactions). An optimal model then was selected via the AIC (Akaike information criteria) by dropping off least significant terms. By this means, the relative importance of the ommatidia that had been left open during the test was determined. An overview of the optimal models is provided for Paradigm I in Table A.1 (upper part: all data, and lower part: only ants with free frontal or caudal DRAs) and for Paradigm II in Table A.2.

Details of the multiple regression analysis: Paradigm I

The optimal models describing the relationships between the uncovered DRA- or nonDRA-ommatidia and the respective homing performance parameter of paradigm I revealed that the ants' performances seem to be independent of the number of free nonDRA-ommatidia; just the number of free DRA-ommatidia had and exclusive and significant impact (Tab. A.1, upper part). An additional analysis focused on possible effects of the number of free DRA- and non-DRA-ommatidia only between ants with frontal or caudal DRAs and here again no significant impact of nonDRA-ommatidia was found (Tab. A.1, lower part).

The data underlying the multiple regression analysis are depicted in Figure A.4. The analysis was initially performed with all animals that had partially covered eyes, i.e., ants with a number of free DRA-ommatidia between 40 and 60 designated as ants with free frontal or caudal DRAs. However for further analyses the groups were restricted to either a maximum of 40 DRA-ommatidia (FRO and CAU) or a minimum of 60 DRA-ommatidia (DRA-control) to emphasize differences of ants with either free frontal or caudal DRAs. The AM homing directions of ants with partially occluded eyes and variable parts of the DRA open (i.e., FRO, CAU, and DRA-control) are plotted as absolute deviations from the expected homing direction and relative to the number of free DRA-ommatidia (number within the less painted eye; Fig. A.4 A). The degree of the occlusion of the nonDRA-region is reflected by the size of the circles, i.e., the larger the circles the less nonDRA-ommatidia had free sight of the sky. As a reference, the means (± SE of the mean) of ants with no (blind-control, cross) or all ommatidia (trolley-control, white square) left open are inserted at the lower and upper end of the graph ($\mu = 3.73 \pm 0.23$ and $\mu = 2.07 \pm 0.20$, respectively). A slight trend of more accurate heading directions with an increasing number of free DRA-ommatidia is observable (slope = -0.01). The number of nonDRA-ommatidia had no influence; note, that the circles with different sizes are randomly distributed. The homing directions recorded for ants tested during PM were also independent of the number of free nonDRA-ommatidia, and showed an even stronger influence of the number of free DRA-ommatidia (slope = -0.04; reference values: 4.90 ± 0.09 (blind-control) and 1.81 ± 0.16 (trolley-control); Fig. A.4 B). Consistent with the improvement in heading towards the correct nest direction, the trajectories of ants with a larger number of free DRA-ommatidia were also straighter compared to those of ants with only few free DRA-ommatidia (Fig. A.4 C, D). The effect of the increasing number of free DRA-ommatidia seems to be the same during AM and PM tests (slope = 0.01) and again, according to the optimal models obtained for AM and PM tests, nonDRA-ommatidia had no significant impact on the directedness of the ants' trajectories. The control groups yielded mean values of 0.26 ± 0.02 (blind-control) and 0.62 ± 0.03 (trolley-control) during AM tests (Fig. A.4 C) and 0.28 ± 0.03 (blind-control) and 0.76 ± 0.01 (trolley-control) during PM tests (Fig. A.4 D). Free nonDRA-ommatidia had also no impact on the third homing performance parameter, the distances covered (Fig. A.4 E, F). Here again only free ommatidia of the DRA had a significant influence, which was stronger during PM tests (slope = 0.07, compared to 0.04 in the AM model). The blind-controls tended to cover distances of 5.7 ± 0.58 m (AM) or 5.15 ± 0.77 m (PM), while the trolley-controls on average started searching for the nest at distances around 9.42 ± 0.50 m (AM) or 8.99 ± 0.37 m (PM).

Thus, according to the main outcome of this analysis, an influence of free nonDRA-ommatidia could be excluded and the ant's homing performance seem to be predominantly driven by the number of available DRA-ommatidia ($p < 0.025$). However, all models described here, independent of the parameter considered, can only explain low percentages of

Tab. A.1.: Results of the multiple regression analysis, Paradigm I. Upper part shows the results of all data as shown in Fig. A.4 and the lower part only the data of ants with either frontal or caudal DRA occluded ("type" represents the type of occlusion, i.e., the frontal or caudal part of the DRA, as a categorical factor). The homing variable was transformed

condition (all data)	optimal model	coefficient of correlation (model)	estimated coefficients (if significant)
homing			
AM	$\sqrt[3]{\text{homing}} \sim DRA$	R^2=0.07; $p < 0.005$	DRA: -0.01; $p < 0.005$
PM	$\sqrt[3]{\text{homing}} \sim DRA$	R^2=0.25; $p << 0.001$	DRA: -0.03; $p << 0.001$
directedness			
AM	directedness$\sim DRA$	R^2=0.21; $p << 0.001$	DRA: 0.005; $p << 0.001$
PM	directedness$\sim DRA$	R^2=0.27; $p << 0.001$	DRA: 0.005; $p << 0.001$
distance			
AM	distance$\sim DRA$	R^2=0.05; $p < 0.03$	DRA: 0.04; $p < 0.03$
PM	distance$\sim DRA$	R^2=0.11; $p < 0.001$	DRA: 0.07; $p < 0.001$
condition (frontal, caudal)		coefficient of correlation (model)	estimated coefficients (if significant)
homing			
AM	$\sqrt[3]{\text{homing}} \sim 1$	–	–
PM	$\sqrt[3]{\text{homing}} \sim 1$	–	–
directedness			
AM	directedness$\sim DRA+nonDRA+type+DRA*nonDRA+DRA*type+nonDRA*type+DRA*nonDRA*type$	R^2=0.16; $p = 0.43$	–
PM	directedness$\sim DRA+nonDRA+type+DRA*nonDRA+DRA*type$	R^2=0.21; $p = 0.22$	–
distance			
AM	distance$\sim type$	R^2=0.17; $p < 0.01$	type: -2.81; $p < 0.01$
PM	distance$\sim DRA+nonDRA+type+DRA*nonDRA+DRA*type$	R^2=0.13; $p = 0.51$	–

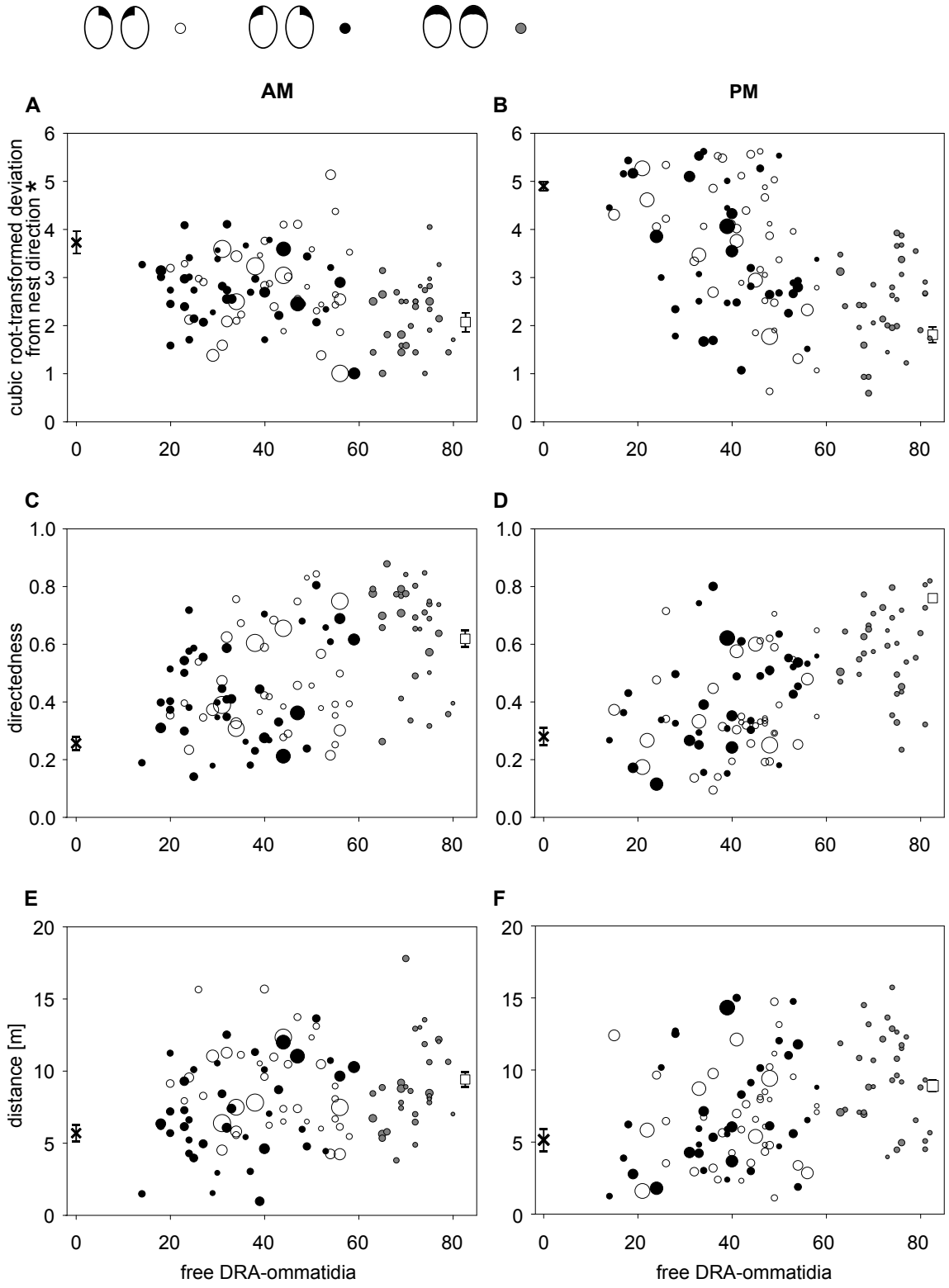
AM
PM
A
B
C
D
E
F
cubic root-transformed deviation from nest direction *
directedness
distance [m]
free DRA-ommatidia
free DRA-ommatidia

Fig. A.4.: Results of the multiple regression analyses. **A-B** Absolute deviations from the correct nest direction are plotted relative to the number of free DRA-ommatidia during AM (A) and PM (B) tests. The relationships between directedness or the distance and the number of uncovered DRA-ommatidia are depicted in **C-D** and **E-F**, respectively. *White circles* represent ants with a free frontal DRA, *black circles* ants with the caudal part of the DRA left open and *grey circles* stand for the DRA-controls. The *size of the circles* reflects the number of covered nonDRA-ommatidia, i.e., the larger the fewer ommatidia were left open. Reference values (means ± SE of the mean) of blind- and trolley-controls are added on the left and right end of the graphs, respectively. Insets represent the occlusion of the ants' eye. * = deviation from homing direction was (cubic root-)transformed in order to describe a linear relationship

the distributions (R^2 = 0.05 - 0.27) and, thus, the results have to be interpreted cautiously.

Details of the multiple regression analysis: Paradigm II

The multiple regression analysis was repeated to assess possible influences of free DRA- and nonDRA-ommatidia on the homing performances of ants with either left or right DRAs. In an analogous manner to the previous analysis for Paradigm I, AM and PM data was again separated (Fig. A.4). Interestingly, for Paradigm II only two parameters (the homing directions and the distances covered) under PM situation could be explained by a multiple regression model (see significant models in Tab. A.2). For the other conditions no adequate models could be determined, that means that in general the ants' behavior on the test field seemed to be largely independent of the quality (number of DRA or nonDRA-ommatidia) but also of the type of the occlusion (free DRA in the left or right eye or in both eyes). However, the homing of ants tested during PM were significantly influenced by the number of free DRA- and nonDRA-ommatidia, additionally to the type of occlusion as main effects (one or both eye, $p < 0.01$). But also depended on interactions between DRA and nonDRA-ommatidia, and between DRA-ommatidia and the type of occlusion ($p < 0.01$, Tab. A.2). Distances recorded during PM depended significantly on whether one or both DRAs were occluded (type, $p < 0.01$) and also on the interaction between the type of occlusion and the number of free DRA-ommatidia ($p < 0.02$). The impact of the number of DRA-ommatidia – although the entire DRA had been left open – might have been caused by testing ants of different sizes. Indeed, body size correlates with the number of ommatidia, and thus larger ants have more ommatidia (Wehner, 1982). The reference values for the homing directions obtained for the control groups are 71.01±22.28 (AM) and 82.19±16.24 (PM) for the blind-control and 6.02±1.71 (AM) and 6.81±1.82 (PM) for the trolley-control. The blind-control yielded values for directedness at 0.28±0.06 (AM) and 0.31±0.05 (PM) and the trolley-control at 0.68±0.03 (AM) and 0.70±0.03 (PM). Blind ants covered distances of 3.98±0.82 during AM and of 4.66±0.69 during PM tests. The distances covered by trolley-controls were 8.17±0.79 (AM) and 8.71±0.44 (PM).

To conclude, for the majority of the test conditions no significant impact of the number of free ommatidia or their location in either one or both eyes on the tested parameter could be determined. However two parameters could be explained by models which reached moderate R^2-values (0.36 and 0.44). The relatively low reliability and the possible influences of the number of (DRA- or nonDRA-)ommatidia apart from the type (free left or right DRA) should be taken into account regarding the results.

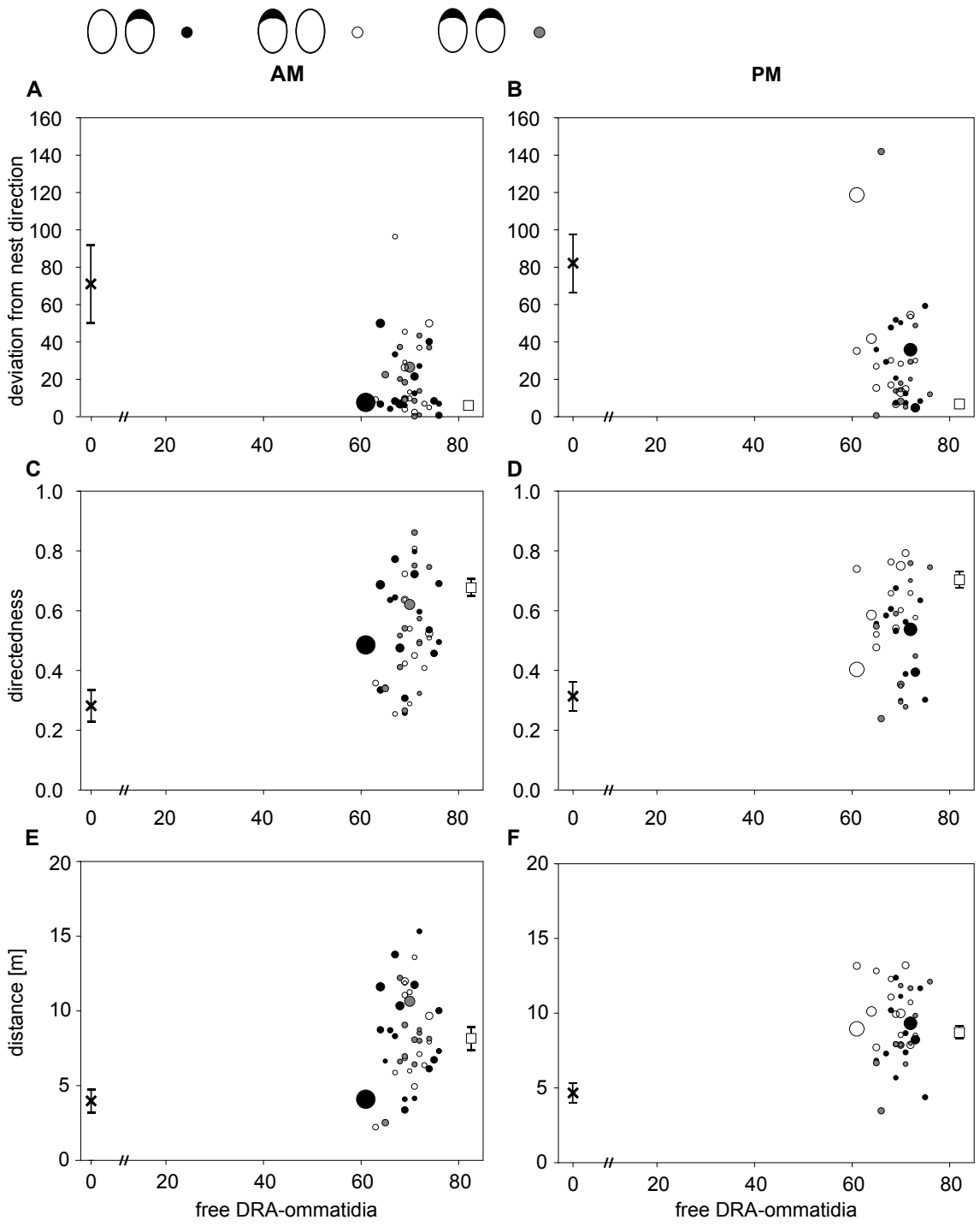

Fig. A.5.: Results of the multiple regression analyses. **A-B** Absolute deviations from the correct nest direction (after squared transformation) are plotted relative to the number of free DRA-ommatidia during AM (A) and PM (B) tests. The relationships between directedness or the distance and the number of uncovered DRA-ommatidia are depicted in **C-D** and **E-F**, respectively. *Black circles* represent ants with a free left DRA, *white circles* ants with a free right DRA left open and *grey circles* stand for the DRA-controls. * = deviation from homing direction was (square-)transformed in order to describe a linear relationship. For further details see Fig. A.4

Tab. A.2.: Results of the multiple regression analysis, Paradigm II. The type of occlusion, left or right or both DRA uncovered is represented by the categorical factor "type". The homing variable was transformed

condition	optimal model	coefficient of correlation (model)	estimated coefficients (if significant)
homing			
AM	$\text{homing}^2 \sim DRA + nonDRA + type + DRA * nonDRA + DRA * type + nonDRA * type + DRA * nonDRA * type$	R^2=0.36; $p = 0.15$	–
PM	$\text{homing}^2 \sim DRA + nonDRA + type + DRA * nonDRA + DRA * type$	R^2=0.44; $p < 0.01$	DRA: -1385; $p < 0.01$; nonDRA: -1152.21; $p < 0.01$ type(DRA): 98488; $p < 0.01$ DRA*nonDRA: 16.077; $p < 0.01$ DRA*type(DRA): -1376; $p < 0.01$
directedness			
AM	$\text{directedness} \sim DRA + nonDRA$	R^2=0.10; $p = 0.12$	–
PM	$\text{directedness} \sim DRA + nonDRA + type + DRA * nonDRA + DRA * type + nonDRA * type + DRA * nonDRA * type$	R^2=0.42; $p = 0.13$	–
distance			
AM	$\text{distance} \sim 1$	–	–
PM	$\text{distance} \sim DRA + nonDRA + type + DRA * nonDRA + DRA * type$	R^2=0.36; $p = 0.045$	type(DRA): -70.20; $p < 0.01$ DRA*type(DRA): 0.98; $p < 0.01$

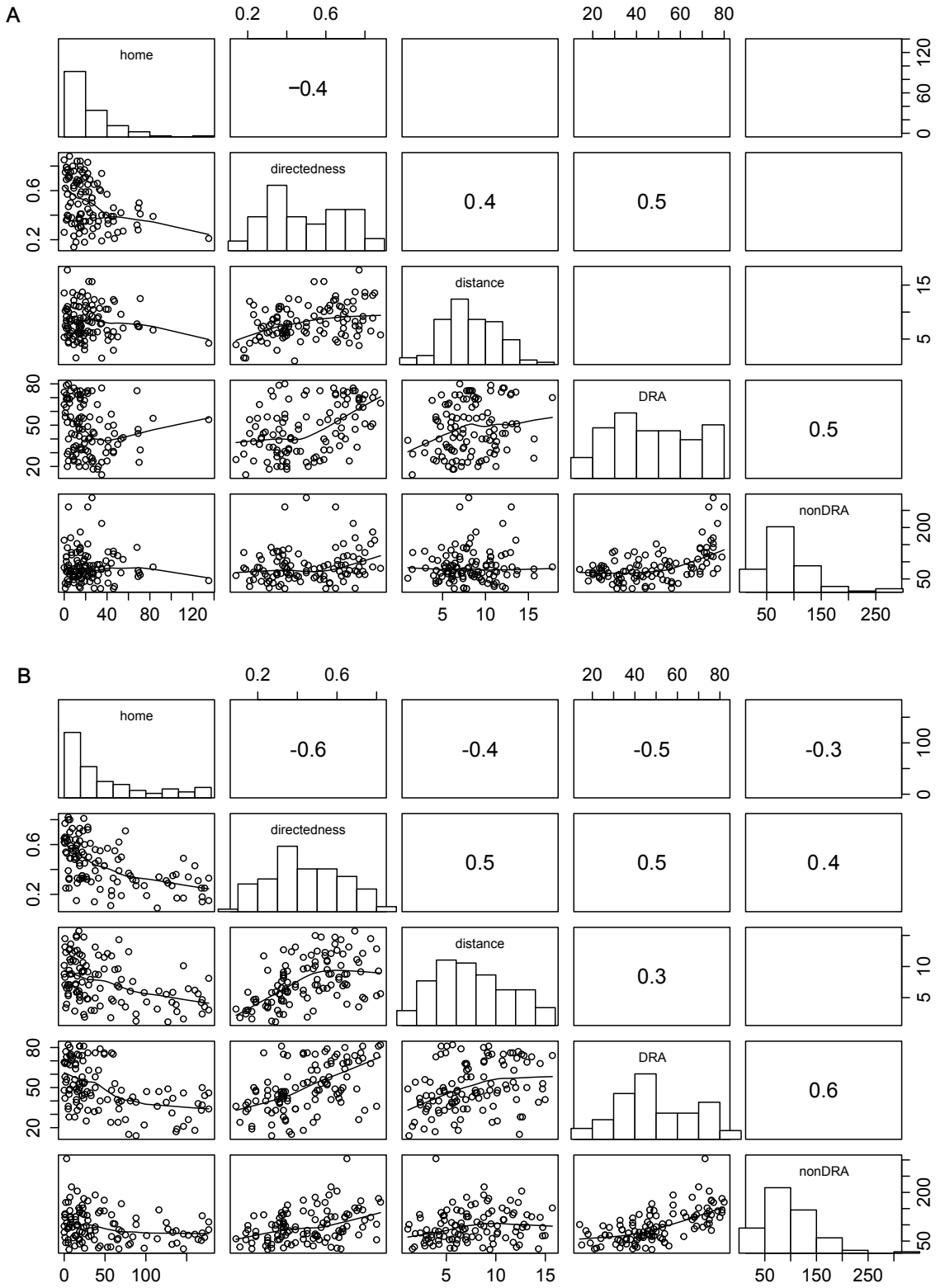

Fig. A.6.: Data exploration of Paradigm I: pairplots of all variables tested during AM (A) and PM (B). In the *diagonal panels* frequency histograms of the variables are depicted. The *upper panels* contain the pair-wise correlation coefficients (if larger than ±0.3) and the *lower panel* contain the scatterplots of the respective combinations.

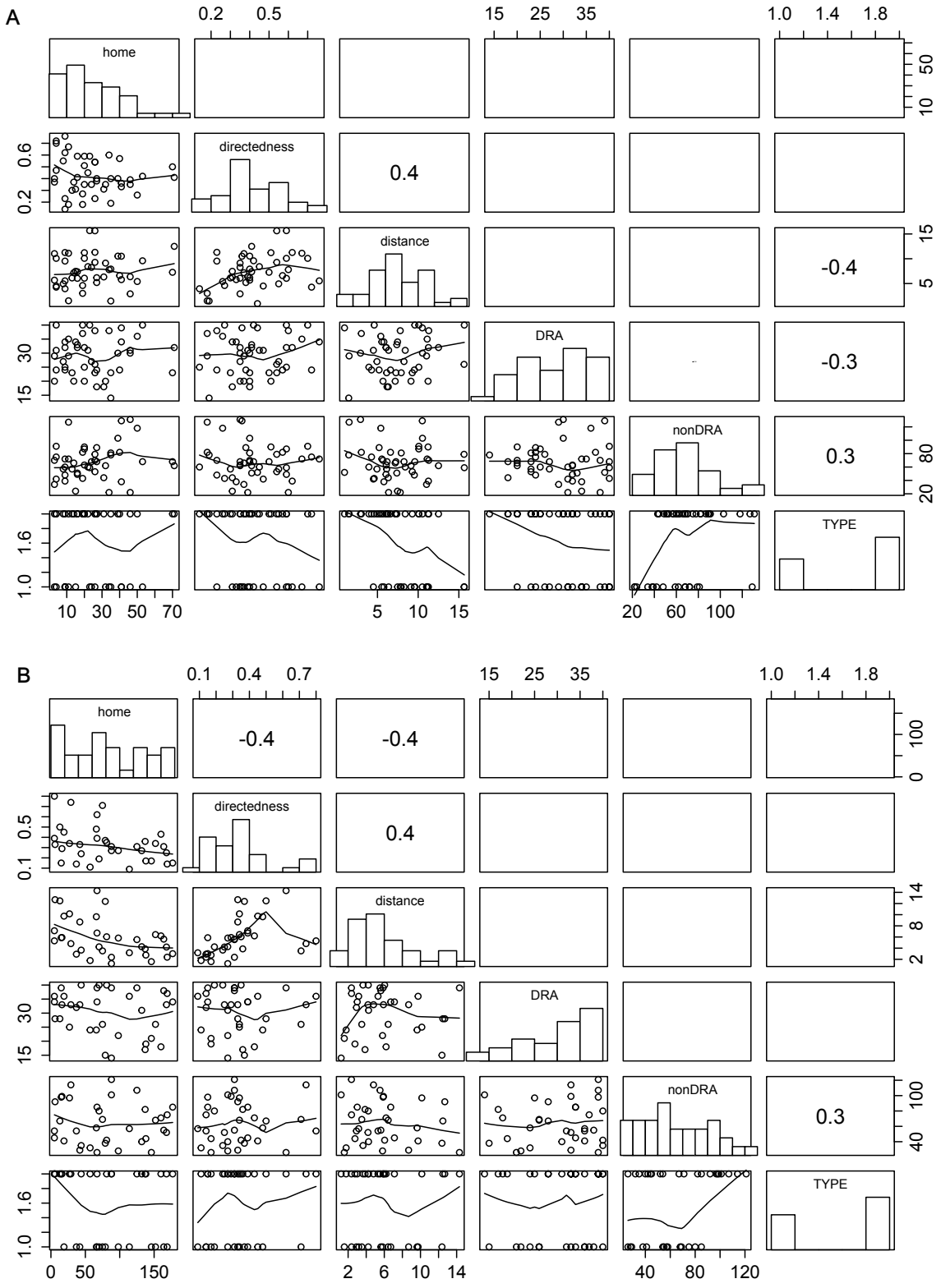

Fig. A.7.: Data exploration of Paradigm I, but here only ants with either free frontal or caudal DRAs: pairplots of all variables tested during AM (A) and PM (B). In the *diagonal panels* frequency histograms of the variables are depicted. The *upper panels* contain the pair-wise correlation coefficients (if larger than ±0.3) and the *lower panel* contain the scatterplots of the respective combinations. Type of occlusion (Type) 1=frontal, 2=caudal

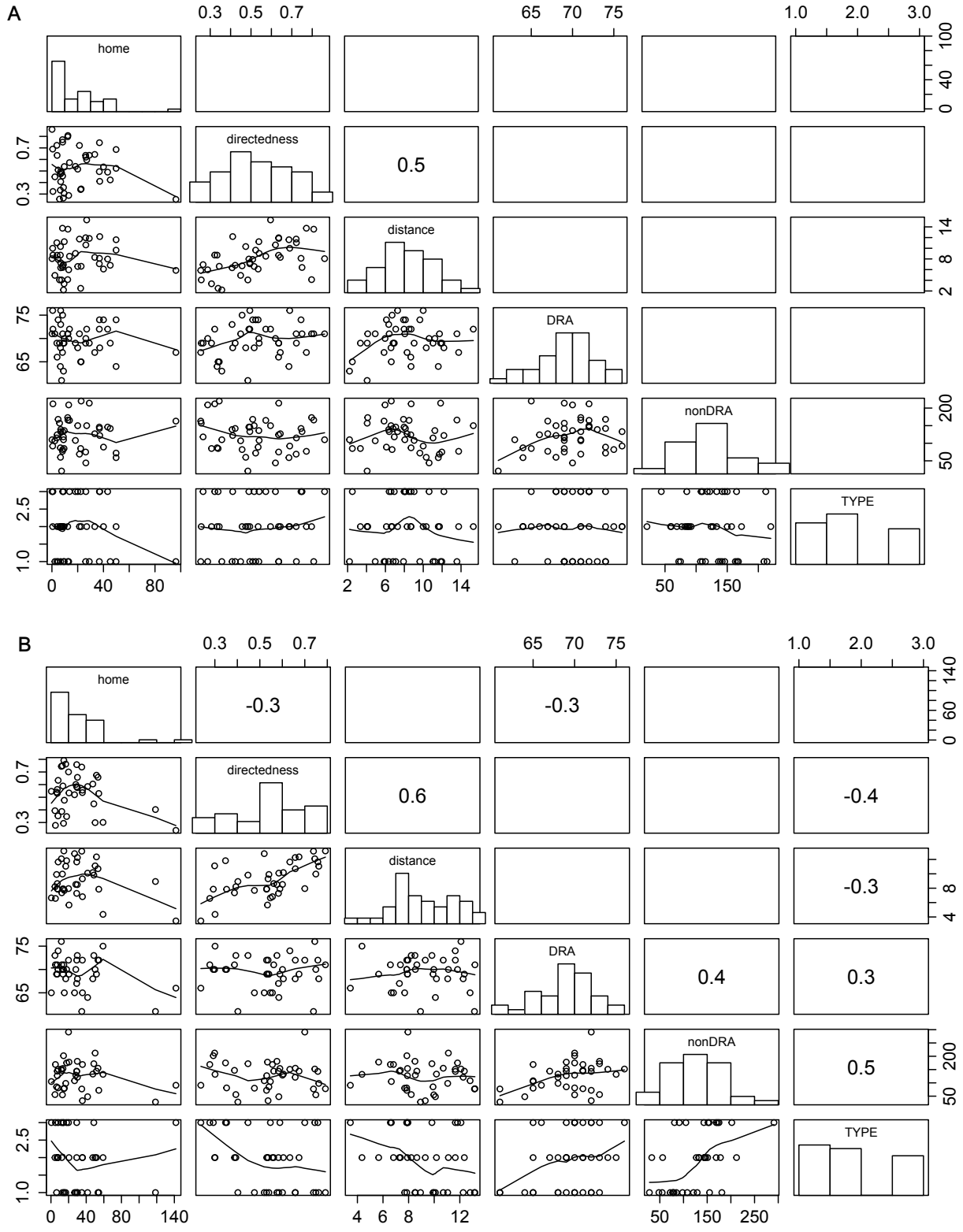

Fig. A.8.: Data exploration of Paradigm II. Pairplots of all variables tested during AM (A) and PM (B). In the *diagonal panels* frequency histograms of the variables are depicted. The *upper panels* contain the pair-wise correlation coefficients (if larger than ±0.3) and the *lower panel* contain the scatterplots of the respective combinations. Type of occlusion (Type) 1=left, 2=right, 3=DRA-control

Bibliography

Baddeley, B., Graham, P., Husbands, P. and Philippides, A. (2012). A model of ant route navigation driven by scene familiarity. PLoS Comput. Biol. *8*, e1002336.

Batschelet, E. (1981). Circular statistics in biology. Academic Press, London, New York, Toronto, Sydney, San Francisco.

Bregy, P., Sommer, S. and Wehner, R. (2008). Nest-mark orientation versus vector navigation in desert ants. J. Exp. Biol. *211*, 1868–1873.

Brower, L. (1996). Monarch butterfly orientation: missing pieces of a magnificent puzzle. J. Exp. Biol. *199*, 93 – 103.

Buehlmann, C., Hansson, B. S. and Knaden, M. (2012). Desert ants learn vibration and magnetic landmarks. PloS one *7*, e33117.

Cheng, K., Narendra, A. and Wehner, R. (2006). Behavioral ecology of odometric memories in desert ants: acquisition, retention, and integration. Behav. Ecol. *17*, 227–235.

Cheng, K., Shettleworth, S. J., Huttenlocher, J. and Rieser, J. J. (2007). Bayesian integration of spatial information. Psychol. Bull. *133*, 625.

Collett, M. (2010). How desert ants use a visual landmark for guidance along a habitual route. Proc. Natl. Acad. Sci. USA *107*, 11638–11643.

Collett, M. (2012). How navigational guidance systems are combined in a desert ant. Curr. Biol. *22*, 927–932.

Collett, M., Chittka, L. and Collett, T. S. (2013). Spatial memory in insect navigation. Curr. Biol. *23*, 789–800.

Collett, T. S. and Collett, M. (2000). Path integration in insects. Curr. Opin. Neurobiol. *10*, 757–762.

Collett, T. S., Collett, M. and Wehner, R. (2001). The guidance of desert ants by extended landmarks. J. Exp. Biol. *204*, 1635–1639.

Collett, T. S., Dillmann, E., Giger, A. and Wehner, R. (1992). Visual landmarks and route following in desert ants. J. Comp. Physiol. A *170*, 435–442.

Coulson, K. L., Dave, J. V. and Sekera, Z. (1960). Tables Related to Radiation Emerging from a Planetary Atmosphere with Rayleigh Scattering. University of California Press, Berkeley & Los Angeles.

Deneve, S. and Pouget, A. (2004). Bayesian multisensory integration and cross-modal spatial links. J. Physiol. - Paris *98*, 249–258.

Duelli, P. and Wehner, R. (1973). The spectral sensitivity of polarized light orientation in *Cataglyphis bicolor* (Formicidae, Hymenoptera). J. Comp. Physiol. A *86*, 37–53.

Durier, V. and Rivault, C. (1999). Path integration in cockroach larvae, Blattella germanica (L.)(insect: Dictyoptera): Direction and distance estimation. Animal Learning & Behavior *27*, 108–118.

El Jundi, B., Pfeiffer, K., Heinze, S. and Homberg, U. (2014). Integration of polarization and chromatic cues in the insect sky compass. J. Comp. Physiol. A *200*, 575–589.

El Jundi, B., Pfeiffer, K. and Homberg, U. (2011). A distinct layer of the medulla integrates sky compass signals in the brain of an insect. PloS one *6*, e27855.

Etienne, A. S. (1980). The orientation of the golden hamster to its nest-site after the elimination of various sensory cues. Experientia *36*, 1048–1050.

Fent, K. (1985). Himmelsorientierung bei der Wüstenameise *Cataglyphis bicolor*: Bedeutung von Komplexaugen und Ocellen. PhD thesis, Zentralstelle der Studentenschaft.

Fent, K. (1986). Polarized skylight orientation in the desert ant *Cataglyphis*. J. Comp. Physiol. A *158*, 145–150.

Fent, K. and Wehner, R. (1985). Ocelli: A celestial compass in the desert ant *Cataglyphis*. Science *228*, 192–194.

Field, L. H. and Matheson, T. (1998). Chordotonal organs of Insects. Adv. Insect Physiol. *27*, 1–204.

Frisch, K. v. (1949). Die Polarisation des Himmelslichtes als orientierender Faktor bei den Tänzen der Bienen. Cellular and Molecular Life Sciences *5*, 142–148.

Frisch, K. v. (1965). Tanzsprache und Orientierung der Bienen. Springer, Heidelberg, New York.

Gehring, W. J. and Wehner, R. (1995). Heat shock protein synthesis and thermotolerance in Cataglyphis, an ant from the Sahara desert. Proceedings of the National Academy of Sciences *92*, 2994–2998.

Grah, G., Wehner, R. and Ronacher, B. (2005). Path integration in a three-dimensional maze: ground distance estimation keeps desert ants *Cataglyphis fortis* on course. J. Exp. Biol. *208*, 4005–4011.

Graham, P. and Cheng, K. (2009). Ants use the panoramic skyline as a visual cue during navigation. Curr. Biol. *19*, R935–R937.

Hammer, Ø., Harper, D. and Ryan, P. (2001). PAST: Paleontological Statistics Software Package for education and data analysis. Palaeontolia Electronica 4 [Computer software].

Heinze, S. and Homberg, U. (2007). Maplike representation of celestial E-vector orientations in the brain of an insect. Science *315*, 995–997.

Heinze, S. and Reppert, S. M. (2011). Sun compass integration of skylight cues in migratory monarch butterflies. Neuron *69*, 345–358.

Herrling, P. (1976). Regional distribution of three ultrastructural retinula types in the retina of *Cataglyphis bicolor* Fabr. (Formicidae, Hymenoptera). Cell Tissue Res. *169*, 247–266.

Heß, D., Koch, J. and Ronacher, B. (2009). Desert ants do not rely on sky compass information for the perception of inclined path segments. J. Exp. Biol. *212*, 1528–1534.

Heusser, D. and Wehner, R. (2002). The visual centring response in desert ants, *Cataglyphis fortis*. J. Exp. Biol. *205*, 585–590.

Homberg, U., Heinze, S., Pfeiffer, K., Kinoshita, M. and El Jundi, B. (2011). Central neural coding of sky polarization in insects. Phil. Trans. R. Soc. B - Biol. Sci. *366*, 680–687.

Horváth, G. and Wehner, R. (1999). Skylight polarization as perceived by desert ants and measured by video polarimetry. J. Comp. Physiol. A *184*, 1–7.

Ivanenko, Y., Grasso, R., Israël, I. and Berthoz, A. (1997). The contribution of otoliths and semicircular canals to the perception of two-dimensional passive whole-body motion in humans. J. Physiol. *502*, 223–233.

Kearns, M. J., Warren, W. H., Duchon, A. P. and Tarr, M. J. (2002). Path integration from optic flow and body senses in a homing task. Perception *31*, 349–374.

Kemfort, J. R. and Towne, W. F. (2013). Honeybees can learn the relationship between the solar ephemeris and a newly experienced landscape: a confirmation. J. Exp. Biol. *216*, 3767–3771.

Labhart, T. (1980). Specialized photoreceptors at the dorsal rim of the honeybee's compound eye: polarizational and angular sensitivity. J. Comp. Physiol. *141*, 19–30.

Labhart, T. (1986). The electrophysiology of photoreceptors in different eye regions of the desert ant, *Cataglyphis bicolor*. J. Comp. Physiol. A *158*, 1–7.

Labhart, T. (1988). Polarization-opponent interneurons in the insect visual system. Nature *331*, 435–437.

Labhart, T. (2000). Polarization-sensitive interneurons in the optic lobe of the desert ant *Cataglyphis bicolor*. Naturwissenschaften *87*, 133–136.

Labhart, T. and Meyer, E. P. (1999). Detectors for polarized skylight in insects: a survey of ommatidial specializations in the dorsal rim area of the compound eye. Microsc. Res. Tech. *47*, 368–379.

Labhart, T. and Meyer, E. P. (2002). Neural mechanisms in insect navigation: polarization compass and odometer. Curr. Opin. Neurobiol. *12*, 707 – 714.

Labhart, T., Petzold, J. and Helbling, H. (2001). Spatial integration in polarization-sensitive interneurones of crickets: a survey of evidence, mechanisms and benefits. J. Exp. Biol. *204*, 2423–2430.

Lanfranconi, B. C. (1982). Kompassorientierung nach dem rotierenden Himmelsmuster bei der Wüstenameise *Cataglyphis bicolor*. PhD thesis, Zoologisches Institut der Universität Zürich.

Lebhardt, F., Koch, J. and Ronacher, B. (2012). The polarization compass dominates over idiothetic cues in path integration of desert ants. J. Exp. Biol. *215*, 526–535.

Lebhardt, F. and Ronacher, B. (2014a). Interactions of the polarization and the sun compass in path integration of desert ants. J. Comp. Physiol. A *200*, 711–720.

Lebhardt, F. and Ronacher, B. (2014b). Transfer of directional information between the polarization compass and the sun compass in desert ants. J. Comp. Physiol. A *201*, 599–608.

Markl, H. (1962). Borstenfelder an den Gelenken als Schweresinnesorgane bei Ameisen und anderen Hymenopteren. J. Comp. Physiol. A *45*, 475–569.

Merkle, T., Knaden, M. and Wehner, R. (2006). Uncertainty about nest position influences systematic search strategies in desert ants. J. Exp. Biol. *209*, 3545–3549.

Merkle, T. and Wehner, R. (2010). Desert ants use foraging distance to adapt the nest search to the uncertainty of the path integrator. Behav. Ecol. *21*, 349–355.

Meyer, E. P. and Labhart, T. (1981). Pore canals in the cornea of a functionally specialized area of the honey bee's compound eye. Cell Tissue Res. *216*, 491–501.

Mittelstaedt, H. (1996). Interaction of eye-, head-, and trunk-bound information in spatial perception and control. J. Vestibul. Res.-Equil. *7*, 283–302.

Mittelstaedt, H. and Mittelstaedt, M. L. (1973). Mechanismen der Orientierung ohne richtende Aussenreize. Fortschr. Zool. *21*, 46–58 b.

Mittelstaedt, M.-L. and Glasauer, S. (1991). Idiothetic navigation in gerbils and humans. Zool. Jb. Physiol *95*, 427–435.

Mittelstaedt, M.-L. and Mittelstaedt, H. (1996). The influence of otoliths and somatic graviceptors on angular velocity estimation. J. Vestib. Res. *6*, 355–366.

Moller, P. and Görner, P. (1994). Homing by path integration in the spider *Agelena labyrinthica* Clerck. J. Comp. Physiol. A *174*, 221–229.

Müller, M. (1989). Mechanismus der Wegintegration bei *Cataglyphis fortis* (Hymenoptera, Insecta). PhD thesis, Zoologisches Institut der Universität Zürich.

Müller, M. and Wehner, R. (1988). Path integration in desert ants, *Cataglyphis fortis*. Proc. Natl. Acad. Sci. USA *85*, 5287–5290.

Müller, M. and Wehner, R. (1994). The hidden spiral: systematic search and path integration in desert ants, *Cataglyphis fortis*. J. Comp. Physiol. A *175*, 525–530.

Müller, M. and Wehner, R. (2007). Wind and sky as compass cues in desert ant navigation. Naturwissenschaften *94*, 589–594.

Narendra, A., Gourmaud, S. and Zeil, J. (2013). Mapping the navigational knowledge of individually foraging ants, *Myrmecia croslandi*. Proc. R. Soc. B. - Biol. Sci. *280*, 20130683.

Nico, D., Israël, I. and Berthoz, A. (2002). Interaction of visual and idiothetic information in a path completion task. Exp. Brain Res. *146*, 379–382.

Pfeiffer, K. and Homberg, U. (2007). Coding of azimuthal directions via time-compensated combination of celestial compass cues. Curr. Biol. *17*, 960–965.

Pfeiffer, K., Kinoshita, M. and Homberg, U. (2005). Polarization-sensitive and light-sensitive neurons in two parallel pathways passing through the anterior optic tubercle in the locust brain. J. Neurophysiol. *94*, 3903–3915.

Räber, F. (1979). Retinatopographie und Sehfeldtopologie des Komplexauges von *Cataglyphis bicolor* Formicidae, Hymenoptera und einiger verwandter Formiciden-Arten. PhD thesis, Zoologisches Institut der Universität Zürich.

Reid, S. F., Narendra, A., Hemmi, J. M. and Zeil, J. (2011). Polarised skylight and the landmark panorama provide night-active bull ants with compass information during route following. J. Exp. Biol. *214*, 363–370.

Ronacher, B. (2008). Path integration as the basic navigation mechanism of the desert ant *Cataglyphis fortis* (Forel, 1902)(Hymenoptera: Formicidae). Myrmecological News *11*, 53–62.

Ronacher, B. and Wehner, R. (1995). Desert ants *Cataglyphis fortis* use self-induced optic flow to measure distances travelled. J. Comp. Physiol. A *177*, 21–27.

Ronacher, B., Westwig, E. and Wehner, R. (2006). Integrating two-dimensional paths: do desert ants process distance information in the absence of celestial compass cues? J. Exp. Biol. *209*, 3301–3308.

Rossel, S. and Wehner, R. (1982). The bee's map of the e-vector pattern in the sky. Proc. Natl. Acad. Sci. USA *79*, 4451–4455.

Rossel, S. and Wehner, R. (1984). How bees analyse the polarization patterns in the sky. J. Comp. Physiol. A *154*, 607–615.

Rossel, S. and Wehner, R. (1986). Polarization vision in bees. Nature *323*, 128–131.

RStudio (2012). RStudio: Integrated development environment for R (Version 0.96.122) [Computer software].

Sachs, L. (1999). Angewandte Statistik. Springer Verlag, Berlin, Heidelberg.

Sakura, M., Lambrinos, D. and Labhart, T. (2008). Polarized skylight navigation in insects: model and electrophysiology of e-vector coding by neurons in the central complex. J. Neurophysiol. *99*, 667–682.

Santschi, F. (1911). Observations et remarques critiques sur le mécanisme de l'orientation chez les fourmis. Albert Kündig.

Santschi, F. (1923). L'orientation sidérale des fourmis, et quelques considérations sur leurs différentes possibilités d'orientation. Impr. Réunies SA.

Schmeling, F., Tegtmeier, J., Kinoshita, M. and Homberg, U. (2015). Photoreceptor projections and receptive fields in the dorsal rim area and main retina of the locust eye. J. Comp. Physiol. A *201*, 427–440.

Schwarz, S., Albert, L., Wystrach, A. and Cheng, K. (2011). Ocelli contribute to the encoding of celestial compass information in the Australian desert ant *Melophorus bagoti*. J. Exp. Biol. *214*, 901–906.

Séguinot, V., Maurer, R. and Etienne, A. S. (1993). Dead reckoning in a small mammal: the evaluation of distance. J. Comp. Physiol. A *173*, 103–113.

Seidl, T. and Wehner, R. (2006). Visual and tactile learning of ground structures in desert ants. J. Exp. Biol. *209*, 3336–3344.

Seyfarth, E.-A., Hergenröder, R., Ebbes, H. and Barth, F. G. (1982). Idiothetic orientation of a wandering spider: compensation of detours and estimates of goal distance. Behav. Ecol. Sociobiol. *11*, 139–148.

Sommer, S. and Wehner, R. (2005). Vector navigation in desert ants, *Cataglyphis fortis*: celestial compass cues are essential for the proper use of distance information. Naturwissenschaften *92*, 468–471.

Sommer, S. and Wehner, R. (2012). Leg allometry in ants: Extreme long-leggedness in thermophilic species. Arthropod structure & development *41*, 71–77.

Steck, K., Hansson, B. S. and Knaden, M. (2009). Smells like home: Desert ants, *Cataglyphis fortis*, use olfactory landmarks to pinpoint the nest. Front. Zool. *6*.

Thiélin-Bescond, M. and Beugnon, G. (2005). Vision-independent odometry in the ant *Cataglyphis cursor*. Naturwissenschaften *92*, 193–197.

Wahl, V., Pfeffer, S. E. and Wittlinger, M. (2015). Walking and running in the desert ant *Cataglyphis fortis*. J. Comp. Physiol. A *201*, 645–656.

Wallace, D. G., Martin, M. M. and Winter, S. S. (2008). Fractionating dead reckoning: role of the compass, odometer, logbook, and home base establishment in spatial orientation. Naturwissenschaften *95*, 1011–1026.

Wang, X., Gao, J. and Fan, Z. (2014). Empirical corroboration of an earlier theoretical resolution to the UV paradox of insect polarized skylight orientation. Naturwissenschaften *101*, 95–103.

Wehner, R. (1968). Optische Orientierungsmechanismen im Heimkehrverhalten von *Cataglyphis bicolor* (Formicidae, Hymenoptera). Rev. Suisse Zool. *75*, 1076–1085.

Wehner, R. (1982). Himmelsnavigation bei Insekten. Neurophysiologie und Verhalten. Neujahrsbl. Naturforsch. Ges. Zürich *184*, 1–132.

Wehner, R. (1983). Taxonomie, Funktionsmorphologie und Zoogeographie der saharischen Wüstenameise *Cataglyphis fortis* (Forel 1902). Senck. Biol. *64*, 89–132.

Wehner, R. (1989). Neurobiology of polarization vision. Trends Neurosci. *12*, 353–359.

Wehner, R. (1994). The polarization-vision project: championing organismic biology. In Neural basis of behavioural adaptations, (Schildberger, K. and Elsner, N., eds), Fortschritte der Zoologie pp. 103–143. Gustav Fischer Verlag Stuttgart.

Wehner, R. (1997). The ant's celestial compass system: spectral and polarization channels. In Orientation and Communication in Arthropods, (Lehrer, M., ed.), pp. 145–185. Birkhäuser Basel.

Wehner, R. (2003). Desert ant navigation: how miniature brains solve complex tasks. J. Comp. Physiol. A *189*, 579–588.

Wehner, R. and Duelli, P. (1971). The spatial orientation of desert ants, *Cataglyphis bicolor*, before sunrise and after sunset. Experientia *27*, 1364–1366.

Wehner, R., Gallizzi, K., Frei, C. and Vesely, M. (2002). Calibration processes in desert ant navigation: vector courses and systematic search. J. Comp. Physiol. A *188*, 683–693.

Wehner, R. and Labhart, T. (2006). Polarization vision. In Invertebrate Vision, (Warrant, E. and Nilsson, D. E., eds), pp. 291–347. Cambridge University Press Cambridge.

Wehner, R., Michel, B. and Antonsen, P. (1996). Visual navigation in insects: coupling of egocentric and geocentric information. J. Exp. Biol. *199*, 129 – 140.

Wehner, R. and Müller, M. (1985). Does interocular transfer occur in visual navigation by ants? Nature *315*, 228–229.

Wehner, R. and Müller, M. (1993). How do ants acquire their celestial ephemeris function? Naturwissenschaften *80*, 331–333.

Wehner, R. and Müller, M. (2006). The significance of direct sunlight and polarized skylight in the ant's celestial system of navigation. Proc. Natl. Acad. Sci. USA *103*, 12575–12579.

Wehner, R. and Räber, F. (1979). Visual spatial memory in desert ants, *Cataglyphis bicolor* (Hymenoptera: Formicidae). Experientia *35*, 1569–1571.

Wehner, R. and Rossel, S. (1985). The bee's celestial compass: a case study in behavioural neurobiology. Fortschr. Zool. *31*, 11–53.

Wehner, R. and Srinivasan, M. V. (1981). Searching behaviour of desert ants, genus *Cataglyphis* (Formicidae, Hymenoptera). J. Comp. Physiol. A *142*, 315–338.

Wehner, R. and Srinivasan, M. V. (2003). Path integration in Insects. In The neurobiology of spatial behaviour, (Jeffery, K. J., ed.), pp. 9–33. Oxford University Press Oxford.

Wehner, R. and Strasser, S. (1985). The POL area of the honey bee's eye: behavioural evidence. Physiol. Entomol. *10*, 337–349.

Wehner, R. and Wehner, S. (1990). Insect navigation: use of maps or Ariadne's thread? Ethology Ecology & Evolution *2*, 27–48.

Wintergerst, S. and Ronacher, B. (2012). Discrimination of inclined path segments by the desert ant *Cataglyphis fortis*. J. Comp. Physiol. A *198*, 363–373.

Wittlinger, M., Wehner, R. and Wolf, H. (2006). The ant odometer: stepping on stilts and stumps. Science *312*, 1965–1967.

Wittlinger, M., Wehner, R. and Wolf, H. (2007a). The desert ant odometer: a stride integrator that accounts for stride length and walking speed. J. Exp. Biol. *210*, 198–207.

Wittlinger, M., Wolf, H. and Wehner, R. (2007b). Hair plate mechanoreceptors associated with body segments are not necessary for three-dimensional path integration in desert ants, *Cataglyphis fortis*. J. Exp. Biol. *210*, 375–382.

Wohlgemuth, S., Ronacher, B. and Wehner, R. (2001). Ant odometry in the third dimension. Nature *411*, 795–798.

Wohlgemuth, S., Ronacher, B. and Wehner, R. (2002). Distance estimation in the third dimension in desert ants. J. Comp. Physiol. A *188*, 273–281.

Wolf, H. and Wehner, R. (2000). Pinpointing food sources: olfactory and anemotactic orientation in desert ants, *Cataglyphis fortis*. J. Exp. Biol. *203*, 857–868.

Wystrach, A., Beugnon, G. and Cheng, K. (2011). Landmarks or panorama: what do navigating ants attend for guidance? Front. Zool. *8*, 21 – 21.

Wystrach, A., Schwarz, S., Baniel, A. and Cheng, K. (2013). Backtracking behaviour in lost ants: an additional strategy in their navigational toolkit. Proc. R. Soc. B. - Biol. Sci. *280*, 20131677.

Zar, J. (1999). Biostatistical Analysis. 4th edition, Prentice Hall.

Zeil, J. (2012). Visual homing: an insect perspective. Curr. Opin. Neurobiol. *22*, 285 – 293.

Zuur, A., Ieno, E., Walker, N., Saveliev, A. and Smith, G. (2009). Mixed Effects Models and Extensions in Ecology with R. Statistics for Biology and Health, Springer Verlag.

Danksagung

Mein besonderer Dank gilt Prof. Bernhard Ronacher für die Betreuung dieser Doktorarbeit. Mit Deiner Faszination für die Navigationskünste der Wüstenameisen hast Du mich angesteckt. Die gemeinsamen Diskussionen und Interpretationen meiner Daten und Ergebnisse haben wesentlich zur Entstehung dieser Arbeit beigetragen. Für Deine anhaltende Unterstützung, die Einarbeitung in die Freilandforschung in Tunesien und das Vertrauen das Projektteam selbstständig vor Ort zu leiten möchte ich Dir herzlich danken.

Prof. Rüdiger Wehner danke ich für all die interessanten und fruchtbaren Diskussionen, die einen bedeutenden Anteil an den in dieser Arbeit präsentierten Ergebnissen hatten. Es war mir eine große Ehre mit Ihnen als Koryphäe auf dem Gebiet der Insektennavigation zu arbeiten und von Ihnen zu lernen. Nicht zuletzt möchte ich mich bei Ihnen für die Begutachtung der Arbeit bedanken.

Des Weiteren gilt mein Dank Prof. Harald Wolf für die Begutachtung der Doktorarbeit und die Kooperation unserer Arbeitsgruppen in Tunesien.

Je voudrais bien remercier la République tunisienne pour me donner l'opportunité de faire de recherches dans ses belles terres. Tous les habitants de Mahares toujours ont été très gentils avec nous. Particulièrement, Slim et sa famille nous a souhaité toujours la bienvenue avec son grandiose hospitalité dès le début. Avec sa compréhension technique il a assuré la fonctionnalité de notre voiture. Merci aussi à Monsieur Hechmi pour nous organiser un logement à Mahares.

Cornelia, vielen lieben Dank für Deine Freundschaft, ohne Dich wäre die Zeit auf dem Salzsee nur halb so schön gewesen. Die langen, sehr unterhaltsamen und fruchtbaren Gespräche mit Dir bei über 40°C in Tunesien oder bei milderen Temperaturen in Mitteleuropa werde ich genauso wenig vergessen, wie den Schluck eisgekühlten Wassers, den Du mir nach meinem ersten Tag auf dem Salzsee angeboten hast.

Ein weiteres großes Dankeschön geht an alle meine Helfer im Feld: Coline, Matthijs, Pauline, Linn, Darja, Timo, Julia und Joshua. Ihr habt euren "Sommerurlaub" mit mir bei brütender Hitze auf dem Salzsee verbracht. Ich danke Euch für eure tolle Unterstützung und Ausdauer auf dem Feld. Sabine, es war mir eine Freude mit Dir zu arbeiten, Du warst mir vor allem bei der ersten Fahrt eine unschätzbar große Hilfe und Unterstützung. Auch bei Julja möchte ich mich besonders bedanken: die Konzeption ihrer Diplomarbeit hat mir einen schnellen und erfolgreichen Start in die Doktorarbeit ermöglicht.

Bei den Mitgliedern der Arbeitsgruppen aus Ulm, Jena und Würzburg möchte ich mich für die gemeinsame Zeit in Tunesien, die fachlichen Diskussionen genauso wie für die geselligen Grillabende auf den verschiedenen Dachterrassen bedanken. Insbesondere danke ich Siggi und Matthias für die große Hilfe und Unterstützung bei der Vorbereitung der ersten Tunesien-Reise.

Allen aktuellen und ehemaligen Mitgliedern meiner Arbeitsgruppe danke ich für die tolle Zeit. Euer Interesse an meinem etwas exotischen Thema, sowie eure Unterstützung und

Hilfsbereitschaft waren eine große Hilfe. Die gemeinsamen Kaffeepausen waren ein fixer Bestandteil während der Zeit meiner Doktorarbeit. Florian möchte ich für die Unterstützung bei der Digitalisierung und Auswertung der Läufe sowie die großzügige und langfristige Leihgabe seines Grafik Tablets danken. Michael danke ich für seine freundliche Beratung bei Statistikfragen.

Anne und Sabine, danke für Eure langjährige Freundschaft, unsere gemeinsamen Erlebnisse haben meinen Eindruck von Berlin geprägt.

Stef, vielen lieben Dank, dass schon früh aus fachlichen Diskussionen eine gute Freundschaft wurde und auch für den regelmäßigen sportlichen und kulturellen Ausgleich.

Ich danke all denjenigen, die mich bei der Fertigstellung dieser Arbeit hilfreich unterstützt haben: Tobias, Anne, Sabine, Stef, Cornelia und Jorge.

Jorge, muchísimas gracias por estar ahí para mi, confiar en mi y apoyarme siempre.

Meiner liebevollen Familie danke ich von Herzen für den steten Rückhalt und Ihren unerschütterlichen Glauben an mich.

Selbständigkeitserklärung

Ich erkläre, dass ich die vorliegende Arbeit selbständig und nur unter Verwendung der angegebenen Literatur und Hilfsmittel angefertigt habe. Die Dissertation ist in keinem früheren Promotionsverfahren angenommen oder als ungenügend beurteilt worden. Die dem angestrebten Verfahren zugrundeliegende Promotionsordnung erkenne ich an.

Berlin, _____ _____

Fleur Lebhardt